

FLUID INCLUSION AND OXYGEN ISOTOPE STUDIES OF  
HIGH-GRADE QUARTZ-SCHEELITE VEINS, CANTUNG  
MINE, NORTHWEST TERRITORIES, CANADA: PRODUCTS  
OF A LATE-STAGE MAGMATIC-HYDROTHERMAL EVENT

---

A Thesis presented to the Faculty of the Graduate School  
University of Missouri-Columbia

---

In Partial Fulfillment  
of the Requirements for the Degree

Masters of Science

---

by  
JASON YUVAN

Dr. Kevin L. Shelton, Thesis Supervisor

MAY 2006

The undersigned, appointed by the Dean of the Graduate School, have  
examined the thesis entitled:

FLUID INCLUSION AND OXYGEN ISOTOPE STUDIES OF  
HIGH-GRADE QUARTZ-SCHEELITE VEINS, CANTUNG  
MINE, NORTHWEST TERRITORIES, CANADA: PRODUCTS  
OF A LATE-STAGE MAGMATIC-HYDROTHERMAL EVENT

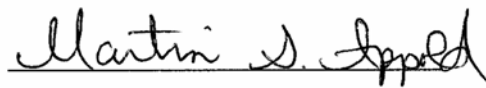
Presented by Jason Yuwan

a candidate for the degree of Master of Science

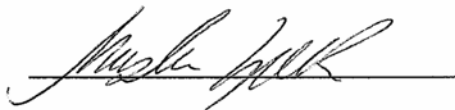
And hereby certify that in their opinion it is worthy of acceptance.

A handwritten signature in cursive script, reading "Kevin L. Shelton", written over a horizontal line.

Kevin L. Shelton

A handwritten signature in cursive script, reading "Martin S. Appold", written over a horizontal line.

Martin S. Appold

A handwritten signature in cursive script, reading "Angela K. Speck", written over a horizontal line.

Angela K. Speck

## ACKNOWLEDGEMENTS

I thank Dr. Kevin Shelton for his guidance and support during completion of this thesis. I also thank Hendrik Falck and the Mineral and Energy Resource Assessment (MERA) of Natural Resources Canada for assistance in the field and in the lab. I thank Dr. Kevin Shelton, Dr. Martin Appold, and Dr. Angela Speck for serving on my thesis committee. I also thank Bridget, my family, and fellow graduate students for encouragement throughout this entire process.

I acknowledge financial support from the Society of Economic Geologists Canada Foundation, the Geological Survey of Canada (GSC), and the University of Missouri Research Council (to Kevin Shelton). I thank Cantung geologist, Dave Tenney, for assistance in the field. Finally, I thank the UMC Department of Geological Sciences for financial support including the W.A. Tarr fund, Fred Strothmann Scholarship, and other scholarships received during my graduate studies.

# TABLE OF CONTENTS

ACKNOWLEDGEMENTS.....	iii
LIST OF FIGURES.....	viii
LIST OF TABLES.....	x
ABSTRACT.....	xi
CHAPTER 1: INTRODUCTION AND OBJECTIVES OF THE STUDY	
History.....	1
Rationale for Study.....	3
Questions Addressed.....	4
References.....	5
CHAPTER 2: TRACE METAL, FLUID INCLUSION, AND OXYGEN ISOTOPE STUDIES OF HIGH-GRADE QUARTZ- SCHEELITE VEINS AT THE CANTUNG MINE, NORTHWEST TERRITORIES, CANADA: A LATE STAGE MAGMATIC- HYDROTHERMAL EVENT	
Introduction.....	7
Geology.....	9
Description of Skarn Orebodies.....	10

E-Zone Orebody.....	10
Open Pit Orebody.....	11
Igneous Rocks.....	11
Mine Stock.....	11
Aplite Dikes.....	13
Quartz Veins.....	14
High-Grade Quartz-Scheelite Veins from the Open Pit Orebody.....	14
Quartz Veins from the Underground E-Zone orebody.....	14
Vein Attitudes.....	19
Vein Alteration.....	19
Trace Metal Analysis.....	22
Interpretation of Trace Metals.....	23
Previous Geochemical Studies.....	25
Fluid Inclusion Studies.....	26
Occurrence and Compositional Types of Fluid Inclusions.....	26
H <sub>2</sub> O-CO <sub>2</sub> -NaCl±CH <sub>4</sub> Inclusions.....	26
Aqueous Brine Inclusions.....	27
Heating and Freezing Data.....	30
H <sub>2</sub> O-CO <sub>2</sub> -NaCl±CH <sub>4</sub> Inclusions.....	30

Aqueous Brine Inclusions.....	32
Interpretation of Fluid Inclusion Data.....	34
P-T Considerations.....	37
Relevance of the Aqueous Brine Inclusions.....	41
Comparison to Other Scheelite Skarn and Vein Deposits.....	41
Quartz-Scheelite Vein Deposition at Cantung.....	42
Oxygen Isotope Studies.....	42
Isotope Results.....	43
Oxygen Isotope Thermometry.....	43
Calculated $\delta^{18}\text{O}_{\text{water}}$ Values.....	45
Summary.....	46
Comparison to Other Distal Skarn Systems.....	47
Distal Skarns.....	47
Veins in Distal Skarns.....	47
Conceptual Model for Cantung.....	48
Distal Vein Deposits of the Cantung Region.....	48
Intrusion-Related Gold Deposits.....	49
Reconnaissance Fluid Inclusion Studies of Outlying Deposits.....	49
Reinterpretation of the HY Gold Prospect.....	50

Implications for Exploration.....	51
References.....	53
 CHAPTER 3: CONCLUSIONS	
Conclusions.....	59
 APPENDIX	
I.    Sample Descriptions.....	61
II.   Cantung Fluid Inclusion Data.....	65
III.  Fluid Inclusion Data from Other Locations.....	75
IV.   Raw Trace Metal Data.....	77
V.    Raw Structural Data.....	79
VI.   Other Charts and Graphs.....	82
VII.  Reconnaissance Fluid Inclusion Studies.....	86
Rifle Range Creek.....	86
Lened.....	87
Zantung Creek.....	88
HY Gold Prospect.....	88
VIII. The Use of Scheelite Florescence in the Field.....	91
References.....	93

## LIST OF FIGURES

Figure		Page
1.	Location of Cantung mine within the Northwest Territories, Canada	2
2.	Cross section showing the location of E-Zone and Open Pit orebodies and host rocks at Cantung	8
3.	Geologic map of the Open Pit orebody	12
4.	Underground picture of an aplite dike extending into massive garnet and pyroxene with abundant scheelite	15
5.	Underground picture of aplite dike extending vertically into a quartz vein	16
6.	Picture of typical Open Pit quartz-scheelite vein	17
7.	Doubly polished thin section of Open Pit quartz-scheelite vein	18
8.	Rose diagram of orientations of (a) quartz-scheelite veins (b) other features at Cantung	20
9.	Thin section pictures of (a) dark and (b) light green alteration surrounding Open Pit quartz-scheelite vein	21
10.	Trace metal plots for Open Pit quartz-scheelite veins	24
11.	Photos of (a) Primary H <sub>2</sub> O-CO <sub>2</sub> -NaCl±CH <sub>4</sub> inclusions in scheelite. (b) Secondary aqueous brine inclusions	28
12.	Frequency diagram of T <sub>mCO2</sub> values for H <sub>2</sub> O-CO <sub>2</sub> -NaCl±CH <sub>4</sub> inclusions	31
13.	Histogram for T <sub>h</sub> values for (a) H <sub>2</sub> O-CO <sub>2</sub> -NaCl±CH <sub>4</sub> and (b) aqueous brine inclusions	33
14.	(a) T <sub>mCO2</sub> versus T <sub>hCO2</sub> values (b) T <sub>h</sub> versus salinity values for H <sub>2</sub> O-CO <sub>2</sub> -NaCl±CH <sub>4</sub> inclusions	35
15.	T <sub>h</sub> versus XCO <sub>2</sub> +CH <sub>4</sub> graph	38
16.	Representative isochores from primary H <sub>2</sub> O-CO <sub>2</sub> -NaCl±CH <sub>4</sub> inclusions in scheelite	40



17.	Additional trace metal plots for high-grade quartz-scheelite veins from the Open Pit orebody. (a) Cu (ppm) versus Bi (ppm). (b) Ag (ppm) versus Bi (ppm)	82
18.	Salinity versus $T_h$ values for aqueous brine inclusions from all samples at Cantung	83
19.	Salinity versus $X_{CO_2 + CH_4}$ values for aqueous brine inclusions and $H_2O-CO_2-NaCl \pm CH_4$ from all samples at Cantung	84
20.	Representative isochores calculated from secondary aqueous brine fluid inclusions	85
21.	Polished thin section of quartz vein with scheelite from the HY gold prospect	89
22.	Improvised dark room used to observe scheelite	92

## LIST OF TABLES

Table	Page
1. List of oxygen isotope data for quartz, scheelite, and aplite dikes, including calculated quartz-scheelite temperatures and $\delta^{18}\text{O}_{\text{water}}$ values in equilibrium with minerals and rocks	44

FLUID INCLUSION AND OXYGEN ISOTOPE STUDIES OF  
HIGH-GRADE QUARTZ-SCHEELITE VEINS AT THE  
CANTUNG MINE, NORTHWEST TERRITORIES, CANADA:  
PRODUCTS OF A LATE-STAGE MAGMATIC-  
HYDROTHERMAL EVENT

Jason G. Yuwan

Dr. Kevin L. Shelton

Thesis Supervisor

---

Abstract

High-grade quartz-scheelite veins (up to 3.7 wt. %  $\text{WO}_3$ ) in the Open Pit orebody of the Cantung mine, Tungsten, NWT occur 300 m vertically above a Cambrian limestone-Cretaceous monzogranite contact along which the E-Zone orebody, a world-class tungsten skarn, is developed. The trend of the 80 m wide quartz-scheelite vein swarm is nearly parallel to the strike and dip of a near-vertical aplite dike along the edge of the Open Pit. Adjacent to these quartz-scheelite veins, dark green alteration selvages overprint earlier light green skarn alteration, indicating that the high-grade quartz-scheelite veins are not part of the early skarn-forming event, but represent a distinct, later event.

Oxygen isotope data from quartz-scheelite pairs yield equilibrium temperatures of 430° to 595°C. These temperatures indicate that the quartz-scheelite veins are related to a deep magmatic-hydrothermal system and are likely a distal expression of a protracted skarn-forming event, perhaps related to aplite dike emplacement. Quartz-scheelite veins did not form in a shallower, cooler, hydrothermal system during uplift.

Primary ore fluids in quartz-scheelite veins from the Open Pit orebody, in skarn-related quartz veins from the E-Zone skarn orebody, and in aplite dikes are grossly similar  $\text{H}_2\text{O}-\text{CO}_2-\text{NaCl}\pm\text{CH}_4$  fluids. However, two distinct end-member fluids have been documented: aplite-related fluids and skarn-related fluids. Fluids in high-grade quartz-scheelite veins contain components of both end-member fluids. Fluids in veins from the Open Pit orebody contain an aplite-related fluid end-member even when occurring up to 70 meters from the nearest exposed aplite dike. Thus, quartz-scheelite veins and aplite dikes in the Open Pit orebody may have a genetic relationship in addition to their structural relationship.

I envision a conceptual model for the Cantung hydrothermal system in which ore-grade tungsten deposits formed where fluids emerged from the granite and encountered rocks favorable for skarn development (e.g. cleaner 'Ore Limestone' versus cherty 'Swiss Cheese Limestone'). Due to the folded geometry of the sedimentary sequence in other areas along the granite contact, fluids emerging from the granite encountered strata less favorable to skarn development (i.e. argillite). Where these less favorable units were breached by fracture systems, potential skarn-forming fluids (and aplite dikes) gained access to host rocks more conducive to ore development vertically distal to the granite contact. The presence of magmatic ore fluids distal to intrusions is intriguing and has significant implications for mineral resource assessment in the region.

# CHAPTER 1: INTRODUCTION

## History

The Cantung mine, Tungsten, Northwest Territories, Canada (Fig. 1), is an unusually large (4 Mt of ore) and high-grade ( $> 1.6$  wt. %  $\text{WO}_3$ ) tungsten skarn deposit (Hart and Lewis, 2003). Two skarn orebodies are developed in a package of folded and overturned Proterozoic to Cambrian metasedimentary rocks above a Cretaceous ( $\sim 98.2$  Ma) monzogranite (Mathieson and Clark, 1984; Bowman et al., 1985; Marshall et al., 2003; Rasmussen et al., 2006).

Discovered in 1954, the Cantung area was explored originally for copper (Crawford, 1963). In 1958, the area was bought by Mackenzie Syndicate who restaked the deposit for tungsten. Diamond drilling exploration from 1959 until 1961 indicated 1,176,000 tons of ore at 2.47 wt. %  $\text{WO}_3$ , one million tons of which could be mined by open pit methods. By 1962, the mine was acquired by its current owner, North American Tungsten Corporation Ltd., which built a mill and town site that year. By 1973, North American Tungsten Corporation Ltd. recovered 1,343,370 tons of ore averaging 1.64 wt. %  $\text{WO}_3$  from the Open Pit orebody. Exploration in 1971 discovered the E-Zone orebody approximately 600 m north and 300 m below the Open Pit orebody. Underground production began in 1974 and by 1977, 498,000 tons of ore had been extracted (Hodgson, 2000). Reserves were calculated at 5,221,640 tons of ore averaging 1.54 wt. %  $\text{WO}_3$ . The mine closed in May 1986 due to low metal prices and was subsequently placed into care and maintenance. Cantung was the western world's largest tungsten producer during its operation from 1962 to 1985.

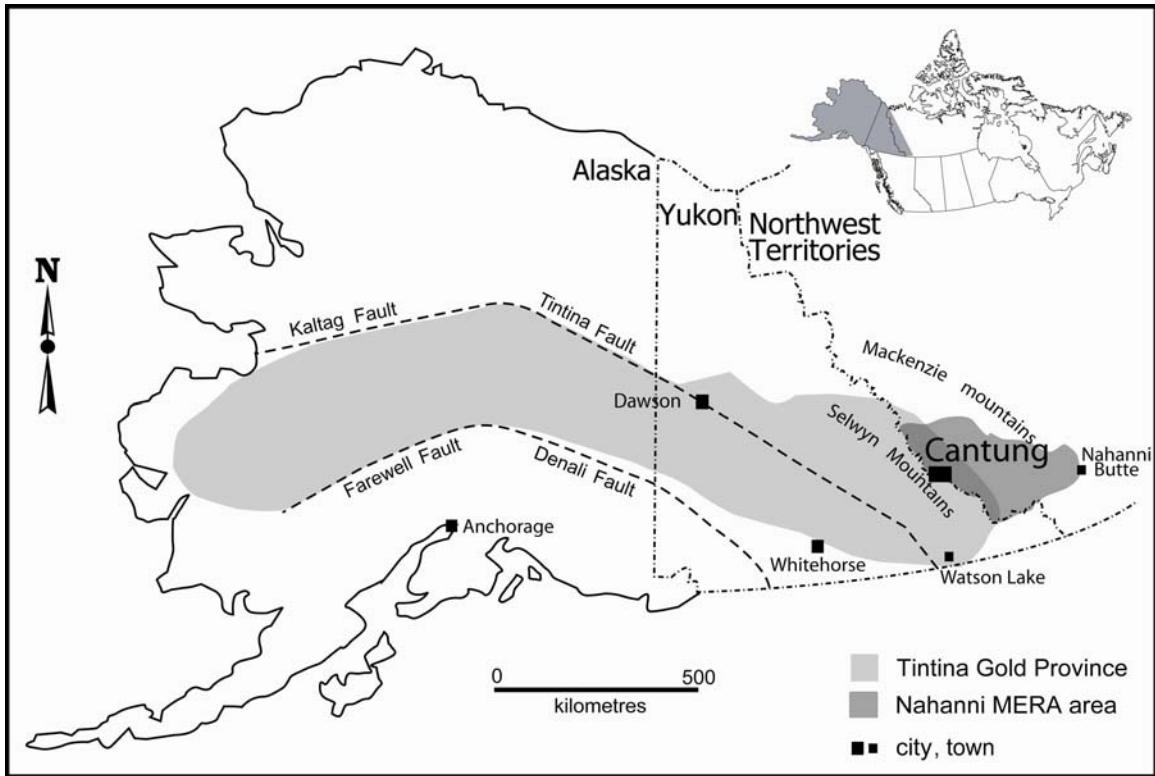


Figure 1. Location of the Cantung mine, Northwest Territories, Canada. Modified after Mortensen et al. (2000) and Rasmussen et al. (2006).

The mine reopened for two years in 2001. It reopened again in 2004, thanks to rising tungsten prices. Remaining reserves are estimated at 771,000 tons of ore grading 1.75 wt. %  $\text{WO}_3$  (Yukon Geological Survey, 2005).

## **Rationale for Study**

The initiation and completion of this project complements the area's Mineral and Energy Resource Assessment (MERA) process (Yuvan et al., 2006). MERA was founded in 1980 to take an "inventory of non-renewable natural resource potential of areas in the Yukon and Northwest Territories prior to their establishment as new national parks" (MERA Homepage, 2006). The Cantung mine is located within the Nahanni MERA study area (Fig. 1).

Two skarn orebodies in the Cantung mine have been exploited for tungsten, the E-Zone and Open Pit orebodies. High-grade quartz-scheelite ( $\text{CaWO}_4$ ) veins and aplite dikes crosscut the Open Pit orebody. Aplite dikes that crosscut the E-Zone orebody can be seen grading into (1) massive garnet and pyroxene with abundant scheelite and (2) quartz-scheelite veins similar to those in the Open Pit orebody. Quartz-scheelite veins from the Open Pit orebody and aplite dikes from both orebodies share a common structural attitude. The origin of these late-stage, high-grade quartz-scheelite veins from the Open Pit orebody and their genetic relationship to aplite dikes is poorly understood.

Geochemical studies of high-grade quartz-scheelite veins and their relationship to aplite dikes test the possibility that the veins may represent distal products of a protracted magmatic-hydrothermal event. If this idea proves true at Cantung, there are important implications for recognizing similar distal, granite-related deposits regionally. Distal exploration targets need not be manifested as massive skarns, but could take on various

forms depending on the geometry and chemistry of host lithologies. Vein and replacement-type deposits in metasedimentary rocks of the Tungsten region frequently have been assumed to represent older ore-forming events. Their origins should be re-evaluated, as some of them could instead represent distal, granite-related deposits.

This study utilizes trace metal analysis, fluid inclusion microthermometry, and oxygen isotope geochemistry to investigate the genesis of high-grade quartz-scheelite veins and their relationship to the skarn-forming magmatic-hydrothermal system at Cantung.

## **Questions Addressed**

Specific research questions addressed in this study include:

1. Did the quartz-scheelite veins form at similar high temperatures and pressures as the skarn ores? Or, do they represent a cooler, shallower hydrothermal system that developed after uplift of the area?
2. Did late skarn-forming fluids form the quartz-scheelite veins or do the veins represent a unique fluid chemistry?
3. Do the quartz-scheelite veins that share a common structural attitude with aplite dikes also share a genetic relationship with them?
4. What are the implications for regional resource assessment if the veins represent a distal expression of a protracted magmatic-hydrothermal skarn-forming event?



## References

- Bowman, J.R., Covert, J.J., Clark, A.H., and Mathieson, G.A., 1985, The CanTung E Zone scheelite skarn orebody, Tungsten, Northwest Territories: Oxygen, hydrogen, and carbon isotope studies: *ECONOMIC GEOLOGY*, v. 80, p. 1872-1895.
- Crawford, W.J.P., 1963, Geology of the Canada Tungsten mine S.W. District of Mackenzie Canada: Unpublished M.S. thesis, University of Washington, Seattle, 79 pp.
- Hart, C.J.R., and Lewis, L.L., 2003, Yukon's tungsten advantage: Placemat for Whitehorse Geoscience Forum, 1 pp.
- Hodgson, C.J., 2000, Exploration potential at the Cantung Mine, District of Mackenzie, NWT: Andean Engineering, Cantung Internal Files, 26 pp.
- Marshall, D., Falck, H., Mann, B., Kirkham, G., and Mortensen, J., 2003, Geothermometry and fluid inclusion studies of the E-Zone biotite skarn, CanTung mine, Tungsten, NWT: Abstracts of the 31<sup>st</sup> Yellowknife Geoscience Forum, p. 60.
- Mathieson, G.A., and Clark, A.H., 1984, The CanTung E-Zone scheelite skarn orebody, Tungsten, Northwest Territories: A revised genetic model: *ECONOMIC GEOLOGY*, v. 79, p. 883-901.
- MERA Homepage, 2006, [http://www.nrcan.gc.ca/mms/poli/mera\\_e.htm](http://www.nrcan.gc.ca/mms/poli/mera_e.htm).
- Mortensen, J.K., Hart, C.J.R., Murphy, D.C., and Heffernan, S., 2000, Temporal evolution of Early and mid-Cretaceous magmatism in the Tintina Gold Belt: *in* Jambor, J., ed., *The Tintina Gold Belt: Concepts, Exploration, and Discoveries: British Columbia and Yukon Chamber of Mines, Special Volume 2*, p. 49-57.
- Rasmussen, K.L., Mortensen, J.K., and Falck, H., 2006, Geochronological and lithochemical studies of intrusive rocks in the Nahanni region, southwestern Northwest Territories and southeastern Yukon: *in* Emond, D.S., Bradshaw, G.D., Lewis, L.L., and Weston, L.H., eds., *Yukon Exploration and Geology 2005: Yukon Geological Survey, Whitehorse*, p. 287-298.
- Yukon Geological Survey, 2005, Canada's Yukon tungsten: Yukon Geological Survey Brochure, 4 pp.

Yuvan, J.G., Shelton, K.L., and Falck, H., 2006, Geochemical investigations of high-grade quartz-scheelite veins of the Cantung mine, NWT: *in* Falck, H., and Wright, D., eds., Mineral and energy resource assessment of the South Nahanni Watershed under consideration for the expansion of Nahanni National Park Reserve, Northwest Territories: 40 pp.

## **CHAPTER 2: TRACE METAL, FLUID INCLUSION, AND OXYGEN ISOTOPE STUDIES OF HIGH-GRADE QUARTZ-SCHEELITE VEINS AT THE CANTUNG MINE, NORTHWEST TERRITORIES, CANADA: A LATE-STAGE MAGMATIC-HYDROTHERMAL EVENT**

### **Introduction**

The Cantung mine, Tungsten, Northwest Territories, Canada (Fig. 1) is an unusually large (4 million tonnes of ore) and high-grade (1.6 wt. %  $\text{WO}_3$ ) tungsten skarn deposit (Yukon Geological Survey, 2005) developed in folded and overturned Cambrian limestones above a Cretaceous monzogranite (Mathieson and Clark, 1984; Bowman et al., 1985). Two skarn orebodies have been exploited in the mine, the E-Zone and Open Pit orebodies. The E-Zone orebody occurs at the monzogranite-limestone contact, and the Open Pit orebody is located approximately 300 m vertically above the E-Zone orebody (Fig. 2). Due to the folded geometry of the sedimentary rocks, the two skarn orebodies were deposited in the same stratigraphic units.

An 80 m wide *en echelon* swarm of high-grade quartz-scheelite veins crosscuts the Open Pit orebody. These veins contain up to 3.7 wt. %  $\text{WO}_3$ . Adjacent to these quartz-scheelite veins, dark green alteration selvages overprint earlier light green skarn alteration. This overprint implies that the high-grade quartz-scheelite veins are not part of the early skarn-forming event, but represent a distinct, later event (Yuvan et al., 2005).

In the underground E-Zone skarn orebody, near-vertical aplite dikes that crosscut skarn ore infrequently grade into quartz veins similar to the high-grade quartz-scheelite veins found in the Open Pit orebody. Other aplite dikes in the E-Zone orebody are observed to extend upward into massive garnet and pyroxene with abundant scheelite

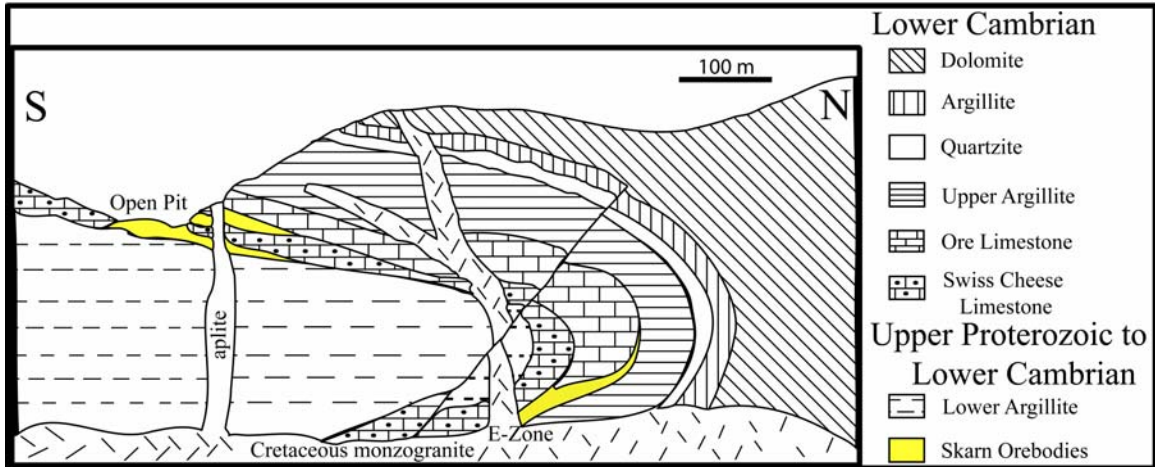


Figure 2. Idealized cross section of the E-Zone and Open Pit orebodies at Cantung modified after Cummings and Bruce (1977). A Cretaceous monzogranite intruded a sequence of folded and overturned Proterozoic to Cambrian metasedimentary rocks. The E-Zone and Open Pit orebodies are separated vertically by approximately 300 m, although they are developed in the same stratigraphic units.

(Yuvan et al., 2004). Aplite dikes that crosscut both orebodies share a common structural attitude with quartz-scheelite veins from the Open Pit orebody, suggesting a possible genetic relationship.

Questions this study addresses are: (1) Did the quartz-scheelite veins form at similar high temperatures and pressures as the skarn ores? Or, do they represent a cooler, shallower hydrothermal system that developed after uplift of the area? (2) Did late skarn-forming fluids form the quartz-scheelite veins or do the veins represent a unique fluid chemistry? (3) Do the quartz-scheelite veins that share a common structural attitude with aplite dikes also share a genetic relationship with them? (4) What are the implications for regional resource assessment if the veins represent a distal expression of a protracted magmatic-hydrothermal skarn-forming event?

## **Geology**

The Cantung mine is located within a polymetallic W-Au province of the Northwest Territories near the Yukon border (Brown, 1961; Lang et al., 2000; Baker et al., 2005). Proterozoic and Cambrian metasedimentary rocks that host ore deposits in the Cantung area include, from oldest to youngest, the Lower Argillite, the Swiss Cheese Limestone, the Ore Limestone, and the Upper Argillite (Fig. 2).

The Upper Proterozoic Lower Argillite is light-brown to dark gray and fine-grained (Zaw, 1976). It is infrequently fractured and crosscut by aplite dikes and quartz veins in the Cantung mine area.

The Lower Cambrian Swiss Cheese Limestone contains massive, boudinaged or nodular calcareous pods and lenses, composed of microcrystalline calcite, intercalated with siltstone (Blusson, 1967; Rasmussen, 2004). The siltstone is composed of

cryptocrystalline clay minerals, carbonates, and quartz (Crawford, 1963). The Swiss Cheese Limestone has been metamorphosed to a mineable calc-silicate/siliceous skarn unit and has also been termed the “Chert” (Cathro, 1969). In other areas where it is not converted to a skarn, the different weathering rates between the limestone and siltstone result in the unit’s porous (“swiss cheese”) nature.

The Ore Limestone is composed of anhedral, finely crystalline calcite. It is vaguely laminated with dark and light gray to white layers. It is a relatively clean limestone receptive to skarn development.

The Upper Argillite is brown to gray and interbedded with thin, impure carbonate, mudstone, and sandstone lenses. Carbonate lenses are converted to calc-silicate skarns (Dick and Hodgson, 1982).

The Upper and Lower Argillites appear to act as confining units for ore fluid flow. Where breached by faults and fractures, fluids gain access to more reactive units higher in the section. The Swiss Cheese and Ore Limestones host ore at the contact with the Mine Stock (E-Zone orebody) and approximately 300 m vertically above the contact (Open Pit orebody).

### **Description of Skarn Orebodies**

*E-Zone Orebody:* The underground E-Zone skarn orebody is hosted in the Ore Limestone at the Mine Stock-Ore Limestone contact. It occurs on the flat to gently dipping east limb of an overturned anticline and has a tabular cross section (Blusson, 1967). The E-Zone skarn orebody is approximately 40 to 200 m wide, 450 m in length, and originally contained 4.2 Mt of ore averaging 1.6 wt. %  $WO_3$  (Zaw, 1976; Mathieson

and Clark, 1984). Current mineable reserves are 771,000 tons of ore averaging 1.75 wt. % WO<sub>3</sub> (Yukon Geological Survey, 2005).

Four mineral assemblages were documented in the skarn orebodies and were interpreted as facies by Dick (1980) and Dick and Hodgson (1982): garnet-pyroxene, pyroxene-pyrrhotite, amphibole-pyrrhotite, and biotite-pyrrhotite. Scheelite is present in all four assemblages, but its abundance increases with increasing pyrrhotite content.

*Open Pit Orebody:* The Open Pit orebody is located approximately 300 m above the E-Zone orebody (Figs. 2 and 3). It is hosted in the base of the Ore Limestone and in the upper Swiss Cheese Limestone, where calcareous lenses were converted preferentially to skarn. Main ore-bearing skarn zones are tabular in shape and approximately 200 m long, 90 m wide, and up to 25 m thick. Because the orebody is within 120 m of a fault that predates ore formation, Zaw (1976) hypothesized that this fault acted as a conduit for migrating ore fluids. Hodgson (2000), however, stated that a nearby aplite dike could also be responsible for the influx of ore fluids. In the Open Pit orebody, scheelite-bearing skarn is dominated by anhydrous garnet-pyroxene mineral assemblage. An 80 m wide *en echelon* swarm of high-grade quartz-scheelite veins crosscuts the Open Pit orebody along a 025 trend (Fig. 3).

## **Igneous Rocks**

*Mine Stock:* The Mine Stock is a monzogranite, consisting of quartz, plagioclase, K-feldspar, and biotite (Rasmussen, 2004). It is an “S”-type granitoid and conforms to Ishihara’s (1977) “ilmenite-series” (Mathieson and Clark, 1984; Christiansen and Keith, 1996). Dating of the Mine Stock by Rasmussen et al. (2006) yielded a U-Pb age of

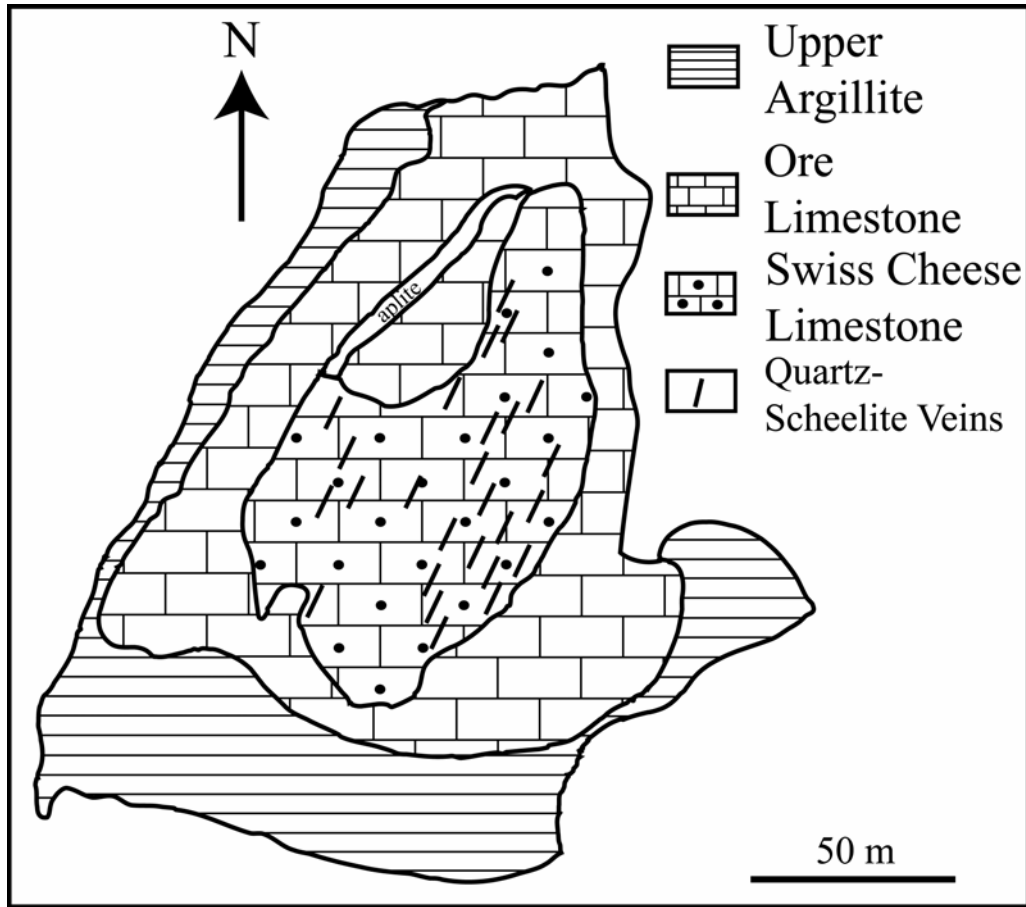


Figure 3. Geologic map of the Open Pit orebody at Cantung showing the *en echelon* pattern and trend of the vein swarm. Note that the trends of the aplite dike and quartz-scheelite veins are nearly parallel.



approximately  $98.2 \pm 0.4$  Ma. Igneous biotite yielded a  $^{40}\text{Ar}$ - $^{39}\text{Ar}$  cooling age of  $95.1 \pm 0.4$  Ma. The difference in ages was interpreted to indicate slow cooling of the Mine Stock over a time interval of up to 3 m.y. This is sufficient time to develop an extensive magmatic-hydrothermal system capable of depositing the world class tungsten skarn at Cantung and later vein deposits during the waning stages of a protracted magmatic-hydrothermal skarn-forming event.

*Aplite Dikes:* Aplite dikes, present as both pre- and post-skarn intrusions, crosscut the Mine Stock and the Open Pit and E-Zone skarn orebodies (Bowman et al., 1985; Rasmussen, 2004). Aplite dikes crosscutting the E-Zone orebody are < 2 cm to 1 m wide and are concentrated around the Mine Stock's margins. In the Open Pit orebody, dikes are 2 to 5 m wide with wall rock alteration selvages extending 10 to 20 cm from vein margins (Rasmussen, 2004).

In the E-Zone and Open Pit orebodies, aplite dikes are similar mineralogically and geochemically. Aplite dikes contain phenocrysts of quartz, plagioclase, K-feldspar, tourmaline, and biotite, but quartz and tourmaline are the only phenocrysts that have not been altered and which retain sharp grain margins. Potassic, sericitic, calcic, and albitic alteration styles have all been observed within the aplite dikes (Rasmussen, 2004).

The dikes display two interesting features relative to ore. Firstly, aplite dikes from the E-Zone orebody can be seen crosscutting skarn and extending into massive garnet and pyroxene with abundant scheelite (Yuvan et al., 2004; Fig. 4). These dikes could have leached tungsten from deeper in the skarn orebody and concentrated tungsten at higher levels. Alternatively, the dikes could be bringing in a new, unique source of tungsten. No matter which explanation is correct, these aplite dikes are responsible for

localized higher concentrations of tungsten, increasing the economic feasibility of mining the ore. Secondly, some aplite dikes from the E-Zone orebody can be seen grading vertically into quartz-scheelite veins (Fig. 5). These E-Zone quartz veins are similar in mineralogy to the high-grade quartz-scheelite veins crosscutting the Open Pit orebody and suggest a possible genetic link to aplite intrusion.

## **Quartz Veins**

*High-Grade Quartz-Scheelite Veins from the Open Pit Orebody:* Quartz-scheelite veins from the Open Pit orebody are 10 cm to 1 m wide (Fig. 6). They are typically unzoned or crudely zoned and contain massive, white quartz and lesser amounts of clear quartz especially where adjacent to scheelite (Fig. 7).

Scheelite is up to 2 cm in diameter. It is white to light orange in hand specimen and fluoresces blue under ultraviolet light. Scheelite is found as isolated, fractured, euhedral to subhedral grains or as crystal clusters in the central parts of veins or adjacent to wall rock contacts. Blocky, white alkali feldspar grains are present infrequently. Sulfides, dominantly pyrrhotite and minor chalcopyrite, occur in pods and in late veinlets cutting massive quartz (Fig. 6).

Infrequently, quartz-scheelite veins from the Open Pit orebody contain biotite-rich masses with abundant fine-grained scheelite. The biotite-rich masses are similar mineralogically to biotite-pyrrhotite assemblages in the underground E-Zone skarn orebody and may indicate that the Open Pit veins are distal products of the subjacent magmatic skarn-forming event.

*Quartz Veins from the Underground E-Zone Skarn Orebody:* Two types of quartz veins were found in the underground E-Zone orebody. One type of vein contains quartz, alkali

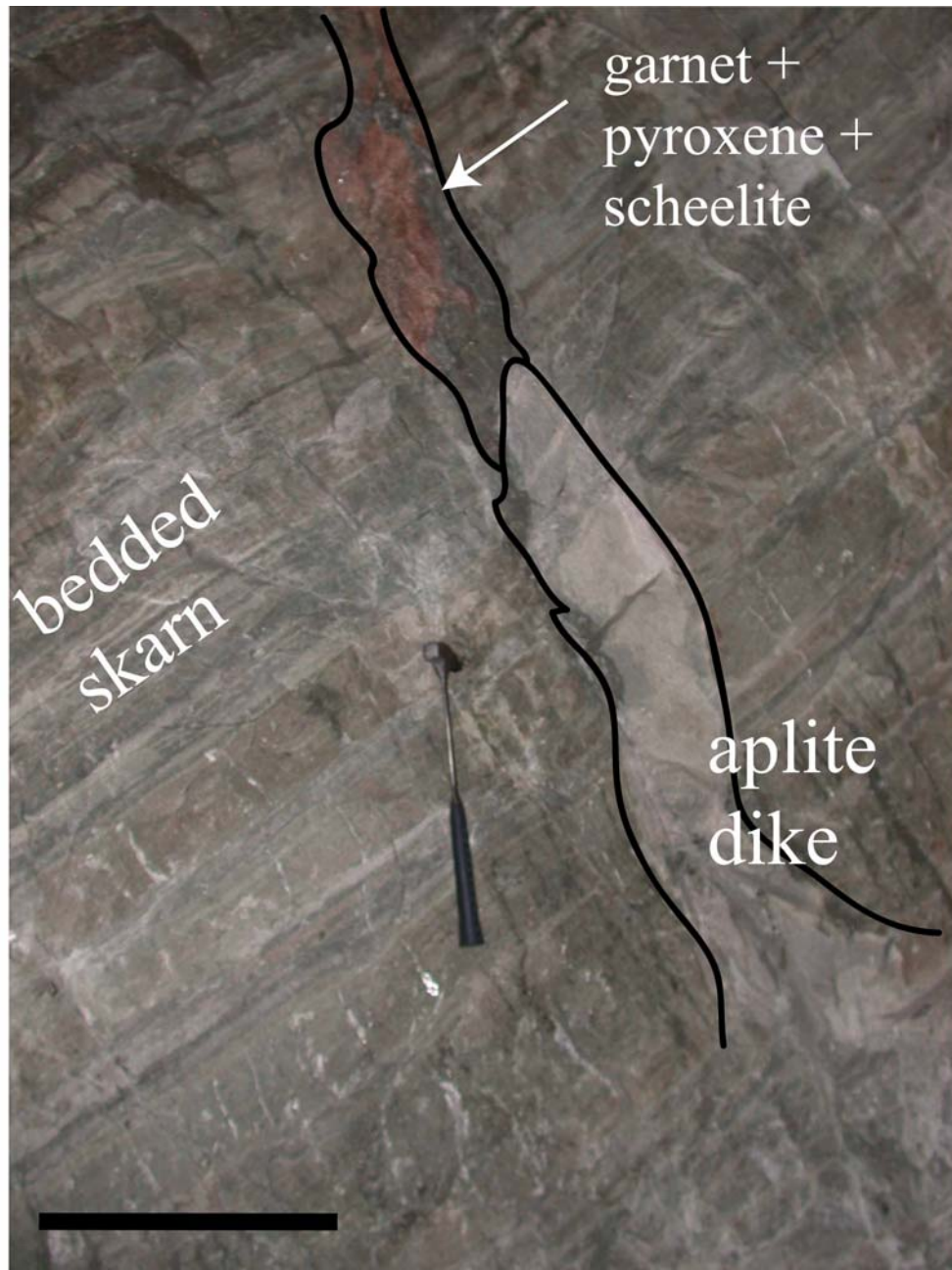


Figure 4. Aplite dike crosscutting E-Zone skarn orebody from the 3850 drift. The aplite pinches out and extends upward into massive pyroxene and garnet with abundant scheelite. Scale bar is 50 cm.

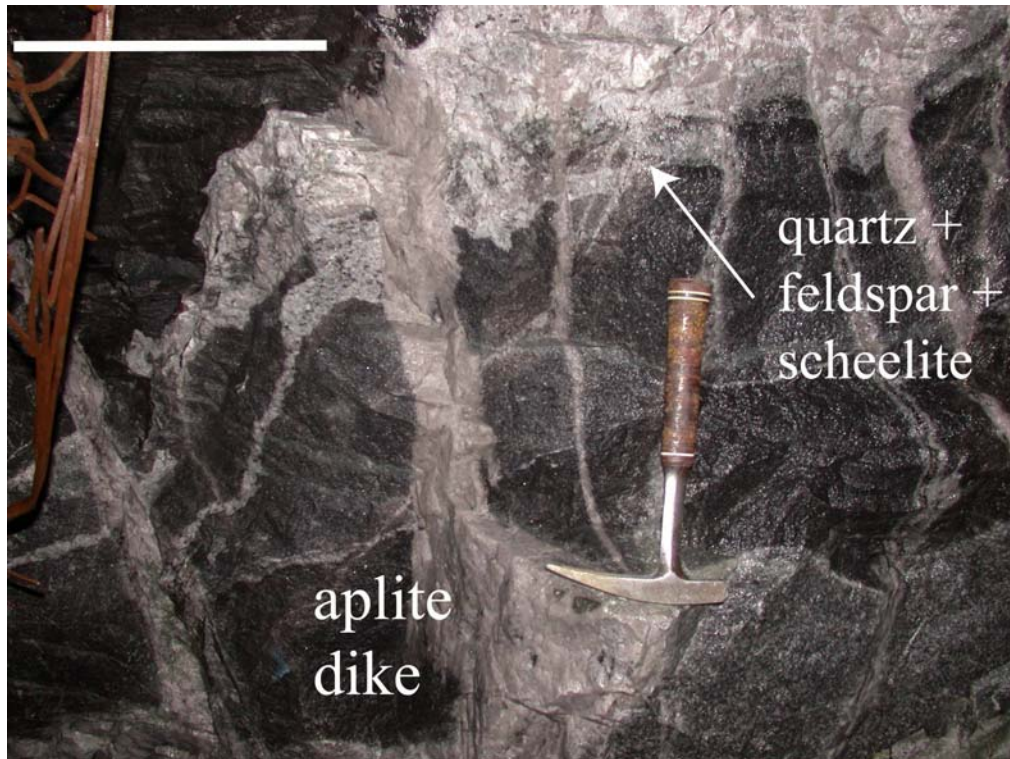


Figure 5. Aplite dikes grading vertically into quartz-scheelite vein in the E-Zone orebody near the Four Corners area of the 4100 level. These veins are similar to the high-grade quartz-scheelite veins in the Open Pit orebody. Scale bar is 30 cm.





Figure 6. Quartz-scheelite vein in the Open Pit orebody within diopsidic skarn. Note the presence of dark green alteration adjacent to the vein that overprints earlier light green skarn alteration. Rust-colored veinlet near the vein center is pyrrhotite rich. Scale bar is 10 cm.

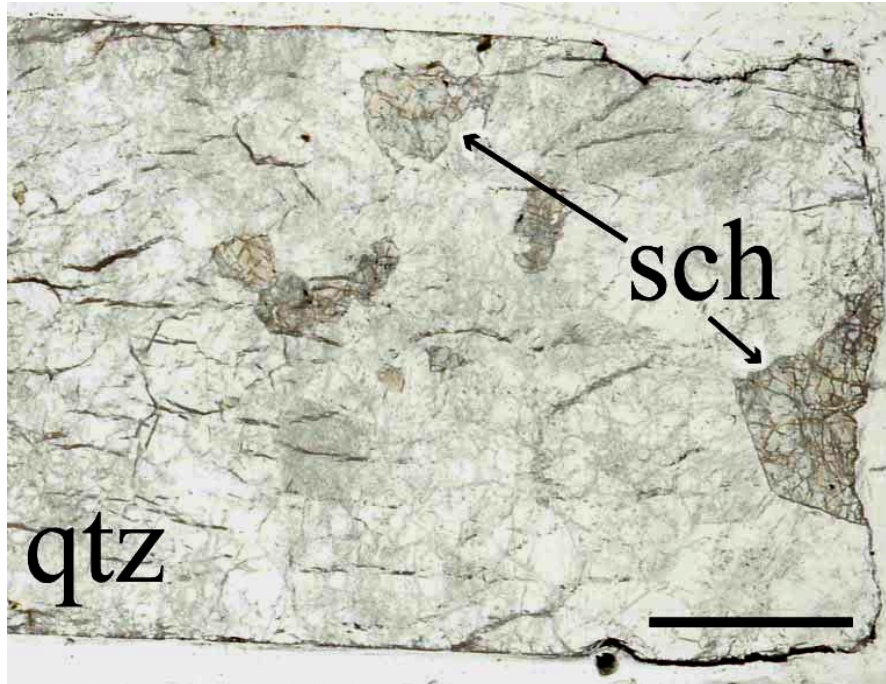


Figure 7. Doubly polished thin section of high-grade quartz-scheelite vein HF03-17 from the Open Pit orebody. Note the highly fractured nature of the vein. Dark lineations in quartz are healed fractures containing abundant secondary aqueous brine inclusions.

Scale bar is 1 cm. Abbreviations: sch = scheelite; qtz = quartz.

feldspar, pyrrhotite, and scheelite, and has biotite-rich alteration selvages, similar to alteration associated with skarn ore. This vein type appears to be related directly to skarn formation. A second type of quartz vein appears to be related genetically to aplite dikes. Vertical aplite dikes can be seen extending upward into quartz veins mineralogically similar to quartz-scheelite veins from the Open Pit orebody (Fig. 5).

*Vein Attitudes:* High-grade quartz-scheelite veins from the Open Pit orebody are steeply dipping ( $\sim 90^\circ$ ) and have strikes between 000 and 080, with most near 030 (Fig. 8a). The overall trend of the 80 m wide *en echelon* vein swarm is approximately 025 (Fig. 3).

Aplite dikes, faults, fractures, and sulfide veinlets from the E-Zone and Open Pit orebodies also have strikes that cluster near 030 (Fig. 8b). If quartz-scheelite vein-forming fluids and aplite magmas utilized the same structural pathways, it is also possible that they may have shared a common genetic relationship (similar to that observed in the underground E-Zone skarn orebody, Fig. 5).

*Vein Alteration:* High-grade quartz-scheelite veins from the Open Pit orebody have dark green alteration selvages up to 15 cm wide. This alteration overprints light green alteration associated with development of the earlier Open Pit skarn (Fig. 6). The dark green alteration adjacent to the veins consists of finer-grained diopside, quartz, opaque minerals, and lesser chlorite (Fig. 9a). Earlier, light green skarn alteration consists of coarser-grained diopside, quartz, K-feldspar, and calcite with minor epidote, chlorite, and garnet (Fig. 9b).

The overprinting nature of the vein-related alteration indicates that the high-grade quartz-scheelite veins represent a later event distinct from the early skarn-forming event (Yuvan et al., 2005).

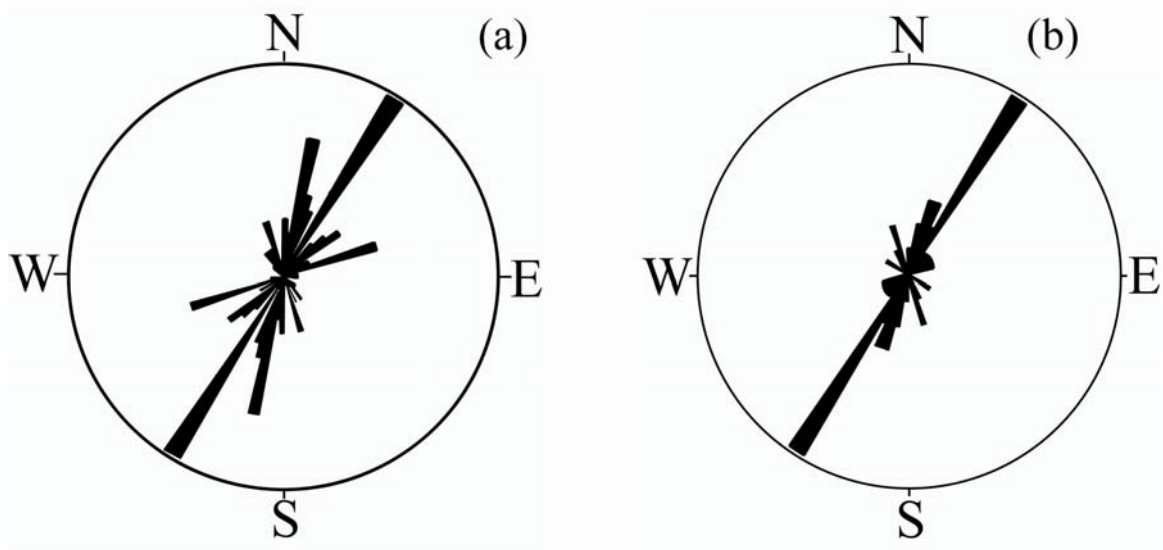


Figure 8. Equal area rose diagrams. (a) Strikes of quartz-scheelite veins from the Open Pit orebody. Outer circle is 19 % of the data. Strikes cluster around 030. (b) Trends of aplite dikes, fractures, faults, and sulfide veinlets within quartz veins from the E-Zone and Open Pit orebodies. Outer Circle is 29 % of the data. These features also cluster around 030, similar to the strikes of high-grade quartz-scheelite veins in the Open Pit orebody. Diagrams made using Stereowin program of Allmendinger (2002).



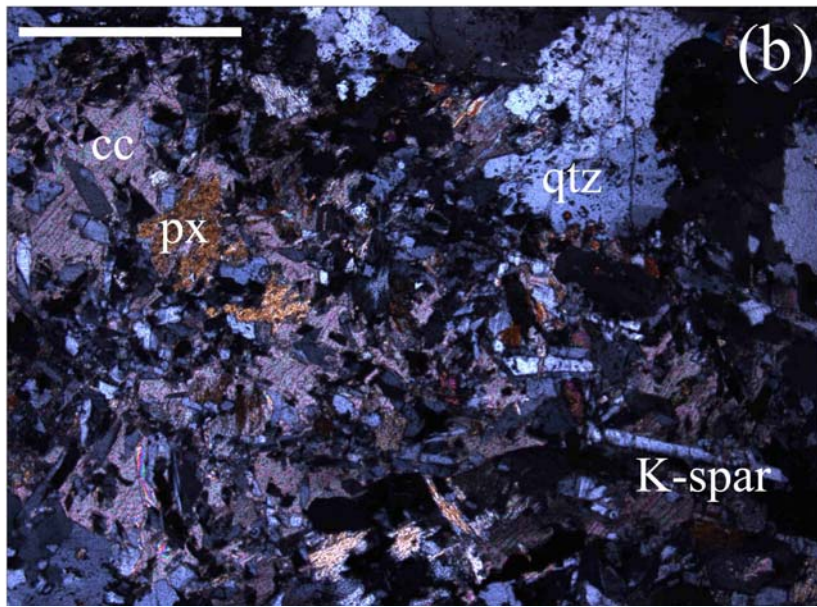
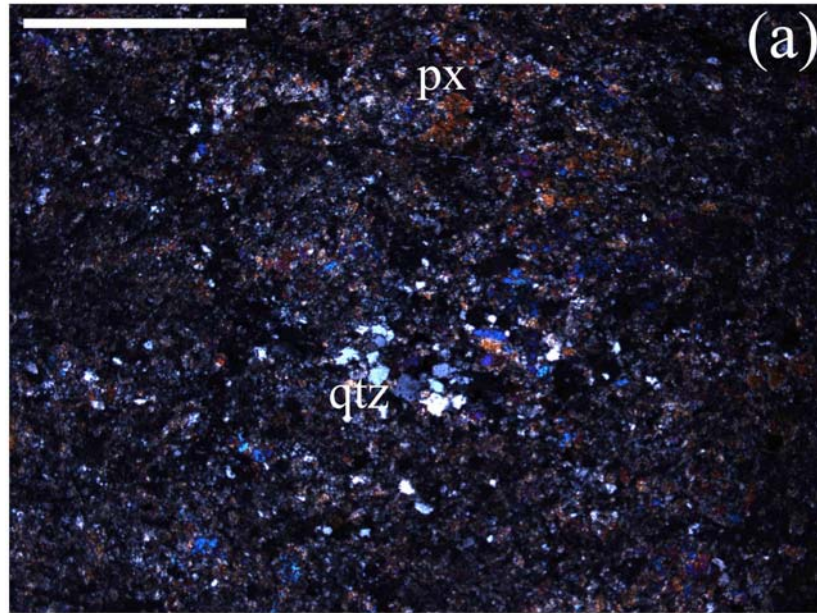


Figure 9. (a) Finer-grained alteration adjacent to quartz-scheelite vein in Open Pit orebody. (b) Coarser-grained skarn alteration 15 cm from the quartz-scheelite veins. Both views under cross polarized light. Scale bars are 0.5 mm in length. Abbreviations: cc = calcite; K-spar = potassium feldspar; px = clinopyroxene; qtz = quartz.

## Trace Metal Analysis

Due to their simple mineralogy, consisting dominantly of quartz, scheelite, and pyrrhotite, it is difficult to link the quartz-scheelite veins definitively to a particular event in the protracted history of skarn formation at Cantung. Trace metal concentrations may be helpful in determining the source(s) of metals and fluid(s) responsible for deposition of quartz-scheelite veins in the Open Pit orebody.

Potential metal sources may include magmas and igneous rocks, or metals remobilized from country rocks. Magmatic sources could have metal suites similar to those of the Mine Stock-related E-Zone skarn ores, namely  $W \pm Mo$ . Alternatively, aplite-related sources could have distinct metal suites (Stern et al., 1986). It is possible that some magmatic/igneous metal sources may have metal suites, including Au, Bi, Cu, and Ag, similar to those in regional quartz veins of the Cantung area thought to represent Intrusion Related Gold Deposits (IRGD) (Lang et al., 2000; Baker et al., 2005).

Alternatively, if the quartz-scheelite veins in the Open Pit orebody at Cantung formed in a shallow, possibly meteoric, hydrothermal system after uplift, metals could have been leached from many different lithologies, including metasedimentary and igneous rocks.

Trace metal concentrations (ppm) and tungsten ore grades (wt. %  $WO_3$ ) were determined for fourteen quartz-scheelite veins from the Open Pit orebody by ICP analysis at ACT Labs, Vancouver. Errors are typically 1.0 to 2.0 % of the measured concentration, never exceeding 5.0 %.

## Interpretation of Trace Metal Analysis

The correlation of various trace metals with tungsten were tested to determine if trace metals in the high-grade quartz-scheelite veins from the Open Pit orebody came from the same source as the main skarn ore metal at Cantung. A linear plot of Mo (ppm) versus  $WO_3$  (wt. %) has a regression coefficient (R) of 0.71 (Fig. 10a). This strong correlation is common in tungsten ore deposits because of the similar geochemistry of tungsten and molybdenum (Ivanova, 1986). This implies that tungsten and molybdenum likely had a similar source. A similar correlation should exist for the E-Zone skarn orebody, as molybdenite ( $MoS_2$ ) and powellite ( $CaMoO_4$ ) are present in minor amounts in the scheelite skarn orebodies at Cantung.

A plot of Bi (ppm) versus  $WO_3$  (wt. %) has an R value of 0.46 (Fig. 10b). The lower correlation coefficient for tungsten and bismuth, compared to that for tungsten and molybdenum, implies that bismuth was likely derived from a different source than tungsten (or molybdenum).

By contrast, a plot of Bi (ppm) versus Au (ppm) has the highest correlation,  $R = 0.92$  (Fig. 10c). This correlation implies that the source for bismuth is likely the same as that for gold. Copper and silver (ppm) have correlation coefficients of 0.59 and 0.69, respectively, when plotted versus bismuth (Fig. 17, Appendix VI). Thus, copper and silver may also reflect a similar source with bismuth and gold that is different from the source of tungsten in the Cantung mine.

Mathieson and Clark (1984) reported that bismuth and copper were byproducts of tungsten ores of the E-Zone skarn orebody. I have documented correlated enrichments of Au, Ag, and Cu with Bi in high-grade quartz-scheelite veins of the Open Pit orebody,

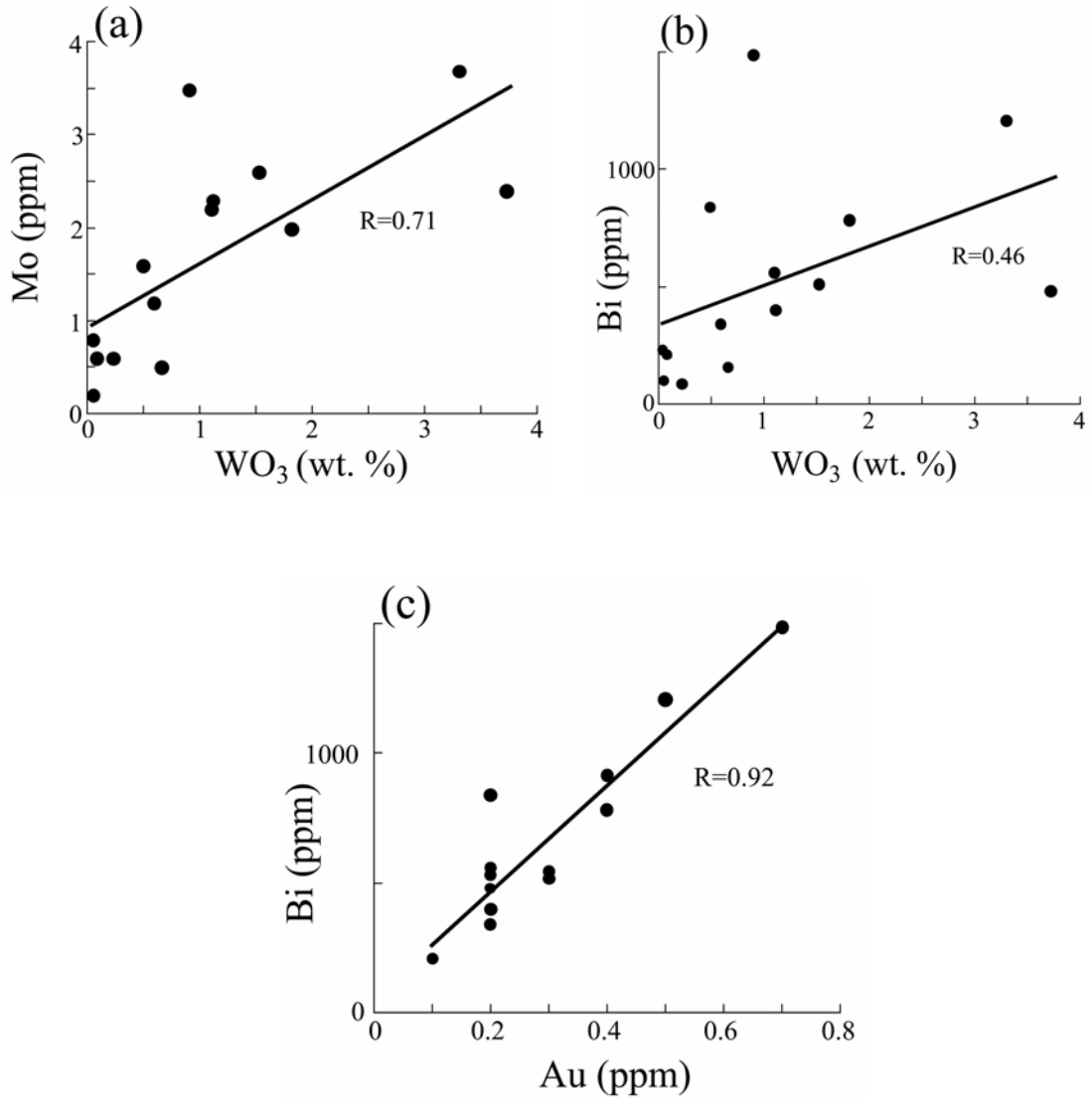


Figure 10. Plots of trace metal contents and tungsten ore grades of high-grade quartz-scheelite veins from the Open Pit orebody. (a) Mo (ppm) versus  $WO_3$  (wt %). (b) Bi (ppm) versus  $WO_3$  (wt. %). (c) Bi (ppm) versus Au (ppm).

300 m vertically above the E-Zone skarn orebody. I hypothesize that byproduct Bi and Cu (as well as Au and Ag) in the underground E-Zone skarn orebody may be the result of an overprint by a late-stage magmatic-hydrothermal system responsible for the quartz-scheelite veins in the overlying Open Pit orebody.

## **Previous Geochemical Studies**

Previous geochemical studies at Cantung have focused on the T-P-X conditions of formation of the E-Zone and Open Pit skarn orebodies. Fluid inclusion studies by Zaw (1976) and Mathieson and Clark (1984) interpreted a low-salinity (< 10 wt. % equiv. NaCl), aqueous brine fluid as the ore fluid. Geobarometry based on the Fe content of sphalerite coexisting with pyrrhotite and pyrite led Zaw (1976) to conclude that the E-Zone orebody formed at pressures of ~1.0 to 2.0 kbar. Based on that pressure estimate, Mathieson and Clark (1984) determined that initial hydrothermal activity began at about 450° to 500°C and continued to lower temperatures near 270°C.

Oxygen isotope thermometry in the E-Zone orebody by Bowman et al. (1985) confirmed the temperature estimates of Mathieson and Clark (1984). Their stable isotope studies of the E-Zone orebody concluded that the ore-forming fluid had an igneous origin, either magmatic water or possibly other waters that equilibrated with the Mine Stock or aplite dikes. The ore fluid was determined to have a limited meteoric water component.

More recently, Marshall et al. (2003) refined the T-P-X conditions of skarn formation by analyzing primary CO<sub>2</sub>-bearing fluid inclusions in apatites from the E-Zone skarn orebody. Combining fluid inclusion analysis with F-OH thermometry from biotite

and apatite, they determined that the E-Zone orebody formed at temperatures of 400° to 520°C and pressures of 2 to 3 kbar.

## **Fluid Inclusion Studies**

Thirty-two quartz vein and five aplite dike samples from the Open Pit and E-Zone orebodies were prepared as 100- $\mu$ m-thick doubly polished thin sections for fluid inclusion analysis. The abundance and quality of fluid inclusions resulted in thirty-three of the doubly polished thin sections yielding usable data.

Microthermometric data were obtained using a FLUID Inc. gas-flow heating/freezing stage calibrated with pure CO<sub>2</sub> and H<sub>2</sub>O inclusions (Shelton and Orville, 1980). Temperatures of total homogenization (T<sub>h</sub>) have standard errors of  $\pm 2^\circ\text{C}$ , and temperatures of melting (T<sub>m</sub> of ice, clathrate, and solid CO<sub>2</sub>) and homogenization of the carbonic phase (T<sub>h CO2</sub>) have standard errors of  $\pm 0.2^\circ\text{C}$ . The composition and density of trapped fluids were determined from thermometric data using the MacFlinCor program (Brown and Hagemann, 1995) and the compiled data of Kerrick and Jacobs (1981), Bodnar and Vityk (1994), and Thiery et al. (1994).

## **Occurrence and Compositional Types of Fluid Inclusions**

Fluid inclusions were found in quartz and scheelite from quartz veins and in tourmaline and quartz grains from aplite dikes. Two compositional types of fluid inclusions have been identified based on their phase relationships at 20°C and behavior upon cooling: H<sub>2</sub>O-CO<sub>2</sub>-NaCl $\pm$ CH<sub>4</sub> fluids and aqueous brines.

*H<sub>2</sub>O-CO<sub>2</sub>-NaCl $\pm$ CH<sub>4</sub> Inclusions:* These inclusions are present as isolated inclusions and three-dimensional clusters of inclusions in quartz, tourmaline, and scheelite, indicating a primary origin. This fluid type is interpreted to be the ore fluid.

At 20°C, these inclusions consist of either two (liquid H<sub>2</sub>O + CO<sub>2</sub> dominant liquid) or three phases (liquid H<sub>2</sub>O + liquid CO<sub>2</sub> + vapor CO<sub>2</sub>). Upon cooling, the two-phase inclusions generated a third phase, vapor CO<sub>2</sub>. The volume percentage of liquid + vapor CO<sub>2</sub> in these inclusions is typically between 25 and 55 %. Typical XCO<sub>2</sub> + CH<sub>4</sub> values range from 0.02 to 0.30.

These inclusions have more regular shapes than the aqueous brine inclusions and range from < 5 to 30 µm in length (Fig. 11a). Negative crystal shapes are common among these inclusions, especially when hosted by scheelite.

*Aqueous Brine Inclusions:* All samples examined contain these two-phase (liquid + vapor) aqueous inclusions (Fig. 11b). They occur in trails or healed fracture planes that crosscut grain boundaries, indicating a secondary origin. Vapor occupies 5 to 30 vol % of these inclusions. Aqueous brine inclusions are < 5 to 20 µm in length, typically near 10 µm. Aqueous brine inclusions have highly irregular shapes. They are frequently elongated and may appear to impart a lineation to the samples (Figs. 7 and 11).

Many fluid inclusion studies of other Western Canadian deposits have noted the presence of ubiquitous aqueous brine inclusions. These inclusions have been variously interpreted to represent (1) fluids integral to the ore-forming event (Nesbitt et al., 1986), (2) synore fluids that are not the ore fluid (Goldfarb et al., 1988), or (3) post-ore fluids (Kerrick and King, 1993; Fayek and Kyser, 1995; Jia et al., 2003; Shelton et al., 2004).

Similar aqueous brine inclusions were observed at Cantung by Zaw (1976) and Mathieson and Clark (1984). These inclusions were interpreted by those authors to be the ore fluid, likely because of their overwhelming abundance and ubiquitous occurrence.

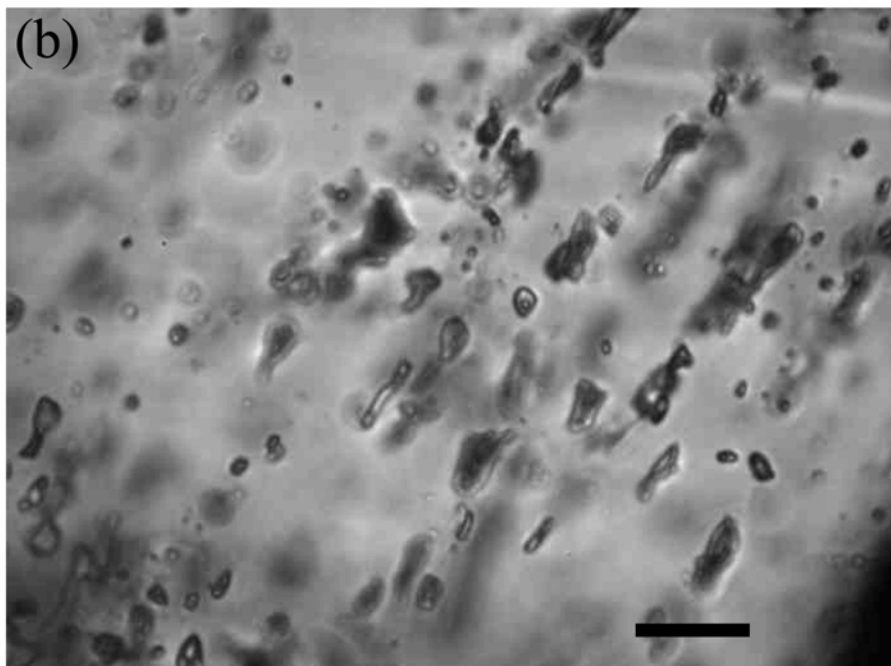
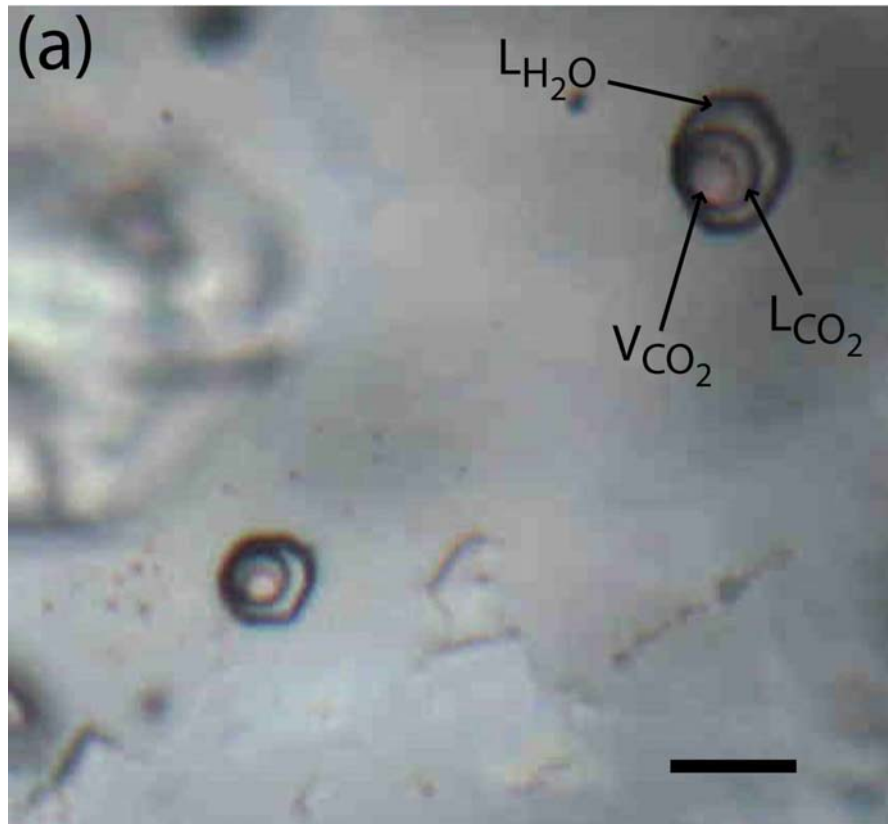




Figure 11. (a) Primary  $\text{H}_2\text{O}-\text{CO}_2-\text{NaCl}\pm\text{CH}_4$  inclusions in scheelite. These three-phase inclusions (vapor  $\text{CO}_2$ , liquid  $\text{CO}_2$ , and liquid  $\text{H}_2\text{O}$ ) typically have negative crystal shapes. Scale bar is  $30\ \mu\text{m}$ . (b) Two-phase aqueous brine inclusions in vein quartz. Scale bar is  $20\ \mu\text{m}$ . These inclusions are typically arranged in linear trails indicating a likely secondary origin. The trails appear to impart a lineation to the samples, similar to those observed in Figure 7.

However, based on textural relationships and reconstructed isochores (Fig. 20, Appendix VI), I believe that the aqueous brine inclusions are secondary fluids unrelated to ore formation.

### **Heating and Freezing Data**

Approximately 200 H<sub>2</sub>O-CO<sub>2</sub>-NaCl±CH<sub>4</sub> inclusions and 300 aqueous brine inclusions were measured. The vast majority of fluid inclusions in samples are aqueous brine inclusions with a subordinate amount of H<sub>2</sub>O-CO<sub>2</sub>-NaCl±CH<sub>4</sub> inclusions.

However, because aqueous brine inclusions are secondary and are not representative of the ore fluid, I chose to measure a percentage of H<sub>2</sub>O-CO<sub>2</sub>-NaCl±CH<sub>4</sub> inclusions that is disproportionate to their occurrence.

*H<sub>2</sub>O-CO<sub>2</sub>-NaCl±CH<sub>4</sub> Inclusions:* These inclusions contain solid and vapor CO<sub>2</sub> and ice when cooled to approximately -150°C. Upon heating, the first melting of the solid CO<sub>2</sub> (T<sub>f</sub> CO<sub>2</sub>) occurs between -125.9° and -76.2°C.

Final melting temperatures of the solid CO<sub>2</sub> (T<sub>m</sub> CO<sub>2</sub>) form two groups, from -64.4° to -56.6°C and -110.6° to -82.1°C (Fig. 12). The higher temperature group is present in all samples analyzed. The carbonic phase of these inclusions has XCH<sub>4</sub> values of 0.00 to 0.21.

The lower temperature group is present in aplite dikes, in quartz-scheelite veins from the Open Pit orebody, and in one quartz vein from the E-Zone orebody. This quartz vein from the E-Zone orebody was collected from an aplite/quartz vein transition zone, and therefore, may have more of an affinity to aplite dike fluids than other quartz veins from the E-Zone orebody. In these inclusions, the carbonic phase has XCH<sub>4</sub> values from 0.93 to 0.96.

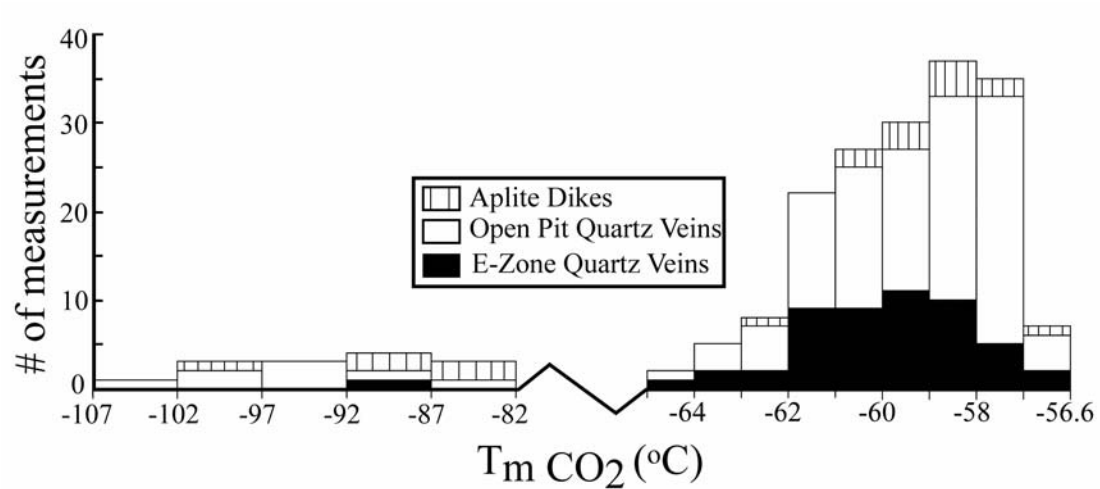


Figure 12. Frequency diagram for the temperature of last CO<sub>2</sub> solid melt (T<sub>m</sub>CO<sub>2</sub>) for primary H<sub>2</sub>O-CO<sub>2</sub>-NaCl±CH<sub>4</sub> fluid inclusions in aplite dikes, quartz-scheelite veins from the Open Pit orebody, and quartz veins from the E-Zone orebody. Note the horizontal scale is different for the left and right sides of the diagram.

The carbonic phases of H<sub>2</sub>O-CO<sub>2</sub>-NaCl±CH<sub>4</sub> inclusions in quartz-scheelite veins from the Open Pit orebody have homogenization temperatures (T<sub>h CO2</sub>) that vary from -86.4° to +28.7°C, dominantly to the liquid phase. The T<sub>h CO2</sub> values yield carbonic phase densities of 0.28 to 0.91 g/cm<sup>3</sup>. Similar inclusions in quartz veins from the E-Zone orebody have T<sub>h CO2</sub> values of -6.8° to +23.9°C, corresponding to carbonic phase densities of 0.39 to 0.81 g/cm<sup>3</sup>. H<sub>2</sub>O-CO<sub>2</sub>-NaCl±CH<sub>4</sub> inclusions in aplite dikes from the E-Zone and Open Pit orebodies have T<sub>h CO2</sub> values of -87.8° to +8.1°C, yielding carbonic phase densities of 0.28 to 0.97 g/cm<sup>3</sup>.

Clathrate melting temperatures (T<sub>m clath</sub>) are 2.1° to 18.3°C. Methane clathrates are known to melt as high as 18°C (Roedder, 1984). T<sub>m clath</sub> values correspond to fluid salinity values (calculated up to only 10°C, because of the limits of the MacFlinCor program) of 0.2 to 9.5 wt. % equiv. NaCl (Diamond, 1992; Brown and Hagemann, 1995). The low T<sub>f CO2</sub> values and T<sub>m CO2</sub> values, below -56.6°C, along with high T<sub>m clath</sub> values (> 10°C), indicate that other species, such as H<sub>2</sub>S and CH<sub>4</sub>, are present in the H<sub>2</sub>O-CO<sub>2</sub>-NaCl±CH<sub>4</sub> fluid (Collins, 1979; Burruss, 1981).

Total homogenization temperatures (T<sub>h</sub>) range from 218° to 401°C (Figure 13a). As they were nearing homogenization, about half of the H<sub>2</sub>O-CO<sub>2</sub>-NaCl±CH<sub>4</sub> inclusions decrepitated.

*Aqueous Brine Inclusions:* First ice melting temperatures (T<sub>e</sub>) in aqueous brine inclusions range from -49.7° to -21.5°C, which attests to the presence of other salts in addition to NaCl, such as CaCl<sub>2</sub> and KCl (Crawford, 1981; Zhang and Frantz, 1989). Final ice melting temperatures (T<sub>m ice</sub>) are between -0.4° and -8.8°C, yielding salinity values between 0.7 and 12.6 wt. % equiv. NaCl. These salinity values are similar to

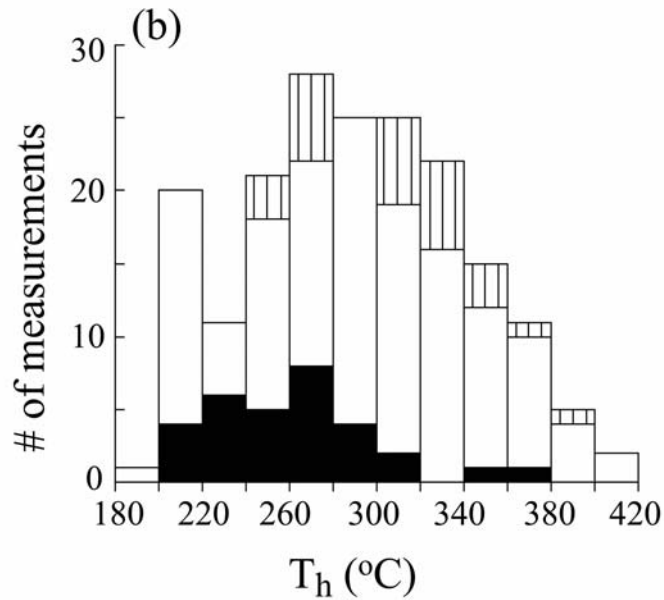
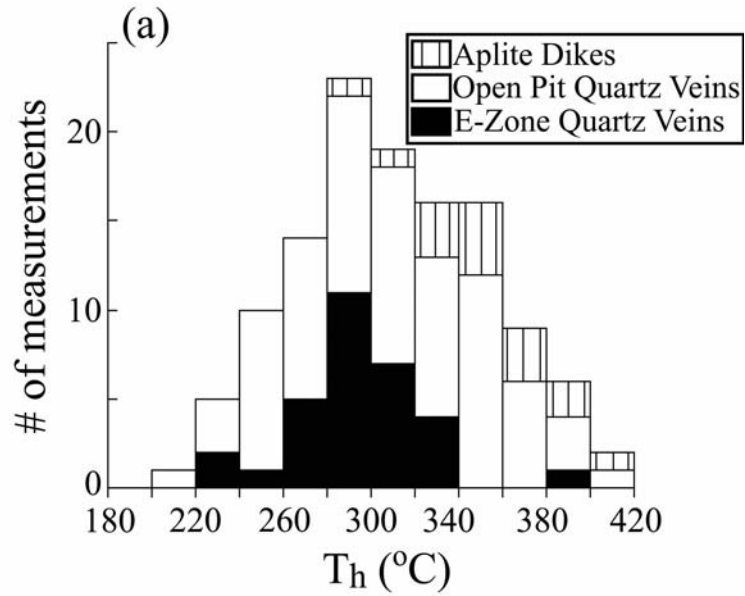


Figure 13. Frequency diagram of total homogenization temperatures ( $T_h$ ) for (a)  $H_2O$ - $CO_2$ - $NaCl \pm CH_4$  inclusions and (b) aqueous brine inclusions. Diagram includes inclusions that decrepitated at temperatures near the homogenization temperatures of adjacent inclusions.

values of 4 to 14 wt. % equiv. NaCl found by Mathieson and Clark (1984).  $T_h$  values, to the liquid phase, range from 188° to 404°C (Figure 13b).

### **Interpretation of Fluid Inclusion Data**

Primary ore fluids in quartz-scheelite veins from the Open Pit orebody, quartz veins from the E-Zone orebody, and aplite dikes from both orebodies are grossly similar  $H_2O-CO_2-NaCl\pm CH_4$  fluids. However, plots of  $T_{mCO_2}$  versus  $T_{hCO_2}$  values (Fig. 14a) and salinity versus  $T_h$  values (Fig. 14b), indicate that two distinct end-member fluids exist, a skarn-related fluid and an aplite-related fluid.

Figure 14a is a plot of  $T_{mCO_2}$  versus  $T_{hCO_2}$  values. The vertical axis,  $T_{mCO_2}$ , is dependant on the  $CH_4$  content of the carbonic phase of  $H_2O-CO_2-NaCl\pm CH_4$  inclusions, with higher  $XCH_4$  values at lower temperatures and lower  $XCH_4$  values at higher temperatures. The horizontal axis,  $T_{hCO_2}$ , is dependant on the density of the carbonic phase of  $H_2O-CO_2-NaCl\pm CH_4$  inclusions, with lower densities at lower temperatures and higher densities at higher temperatures. Fluids in aplite dikes (from both the E-Zone and Open Pit orebodies) define a broad field at low  $T_{mCO_2}$  and  $T_{hCO_2}$  values (higher  $CH_4$ , lower density fluid). Fluids in skarn-related quartz veins from the E-Zone orebody are restricted to a narrower field of higher  $T_{mCO_2}$  and  $T_{hCO_2}$  values (lower  $CH_4$ , higher density fluid). Fluids in high-grade quartz-scheelite veins from the Open Pit orebody overlap both end-member fluid fields.

The low  $T_{hCO_2}$ -low  $T_{mCO_2}$  cluster in Figure 14a represent extremely  $CH_4$ -rich, low density fluids hosted in three different quartz veins from the Open Pit orebody. These three veins occur adjacent to and up to 70 m away from the exposed aplite dike in the Open Pit.

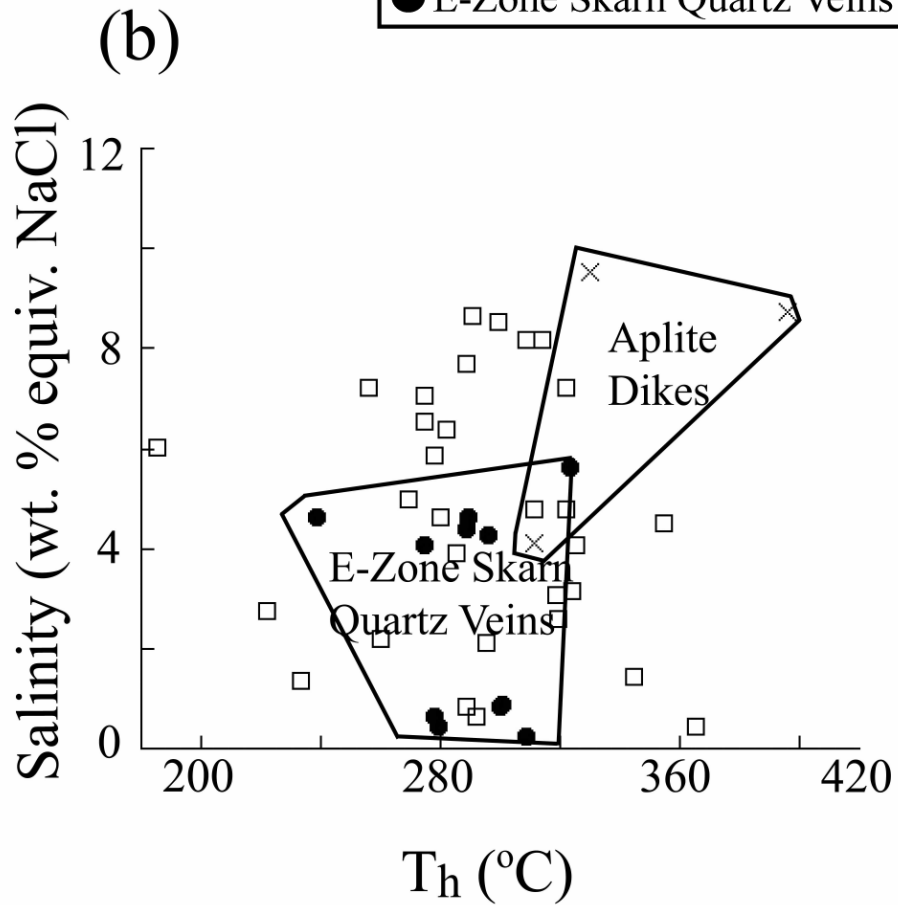
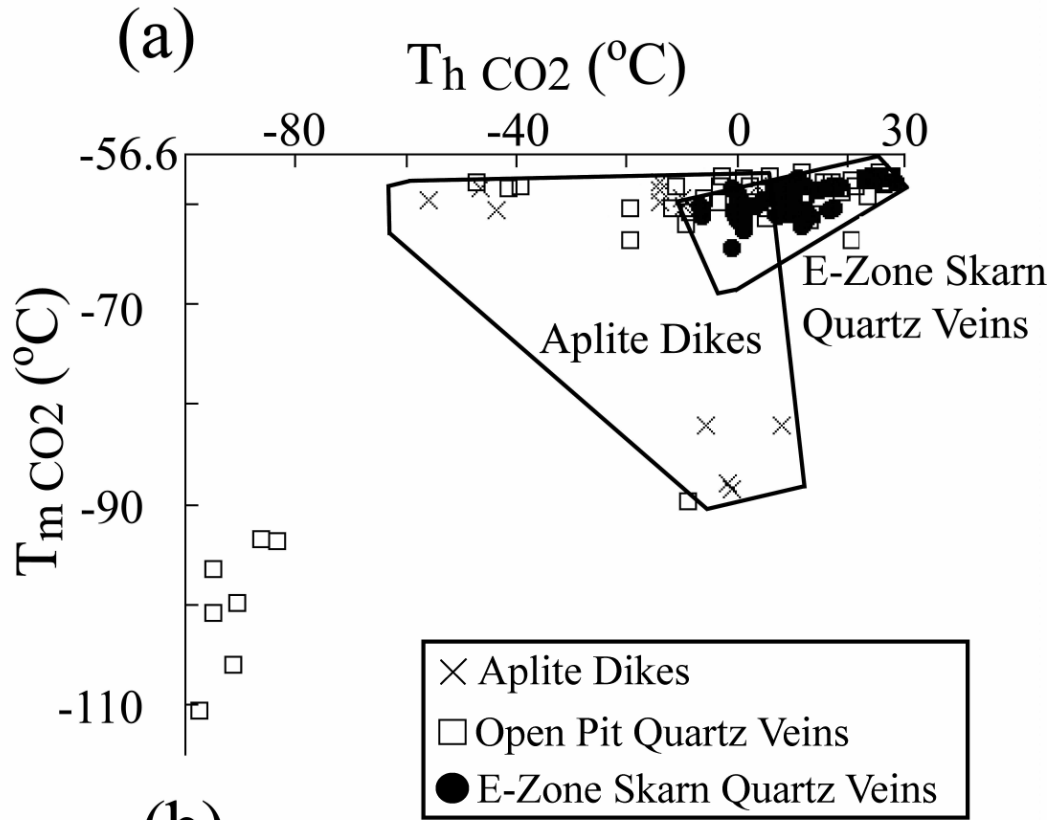


Figure 14. (a)  $T_{h\text{CO}_2}$  versus  $T_{m\text{CO}_2}$  values for  $\text{H}_2\text{O}-\text{CO}_2-\text{NaCl}\pm\text{CH}_4$  inclusions. Fluids in aplite dikes plot at lower  $T_{h\text{CO}_2}$  values (lower densities) and lower  $T_{m\text{CO}_2}$  values (higher  $X\text{CH}_4$ ). Fluids in skarn-related quartz veins from the E-Zone orebody plot at higher  $T_{m\text{CO}_2}$  values (higher densities) and higher  $T_{h\text{CO}_2}$  values (less  $X\text{CH}_4$ ). Fluids in high-grade quartz-scheelite veins from the Open Pit orebody overlap both fields outlined by the end-member fluids. (b) Salinity versus  $T_h$  values for  $\text{H}_2\text{O}-\text{CO}_2-\text{NaCl}\pm\text{CH}_4$  inclusions. Fluids in aplite dikes and those in skarn-related quartz veins from the E-Zone orebody form distinct end-member fields. Fluids in high-grade quartz-scheelite veins from the Open Pit orebody overlap both fields.



Figure 14b is a plot of salinity versus  $T_h$  values. Fluids in aplite dikes (from both the E-Zone and Open Pit orebodies) define a field of higher  $T_h$  and salinity values. Fluids in skarn-related quartz veins from the E-Zone orebody form a distinct field of lower  $T_h$  and salinity values. As in Figure 14a, fluids in high-grade quartz-scheelite veins from the Open Pit orebody overlap both end-member fluid fields.

Regardless of whether they overlap the aplite dike field or the skarn-related E-Zone quartz vein field of Figure 14,  $H_2O-CO_2-NaCl\pm CH_4$  fluid inclusions in high-grade quartz-scheelite veins from the Open Pit orebody are primary inclusions. This observation requires that both end-member fluids entrapped in the veins were present contemporaneously. The fluid end-members may have been trapped individually, or the fluids may have mixed, with the entrapped fluids consisting of various mixtures of the fluid components. In either scenario, there is an apparent influence of aplite dike-related fluids on the quartz-scheelite vein swarm even though veins occur up to 70 meters laterally from the nearest visible aplite dike. We envision a scenario in which quartz-scheelite veins and aplite dikes utilized the same structures to ascend from the subjacent Mine Stock, so it should be no surprise that the quartz veins entrapped an aplite-related fluid.

## **P-T Considerations**

There is no evidence for unmixing of the ore fluids in the Cantung hydrothermal system. There is a lack of fluid inclusions homogenizing to the vapor phase. Most inclusions have similar vapor to liquid ratios. I did not recognize a high salinity inclusion assemblage nor a high  $X_{CO_2} + CH_4$  inclusion assemblage that might be expected from unmixing along the right limb of the solvus in Figure 15. The lack of unmixing implies a

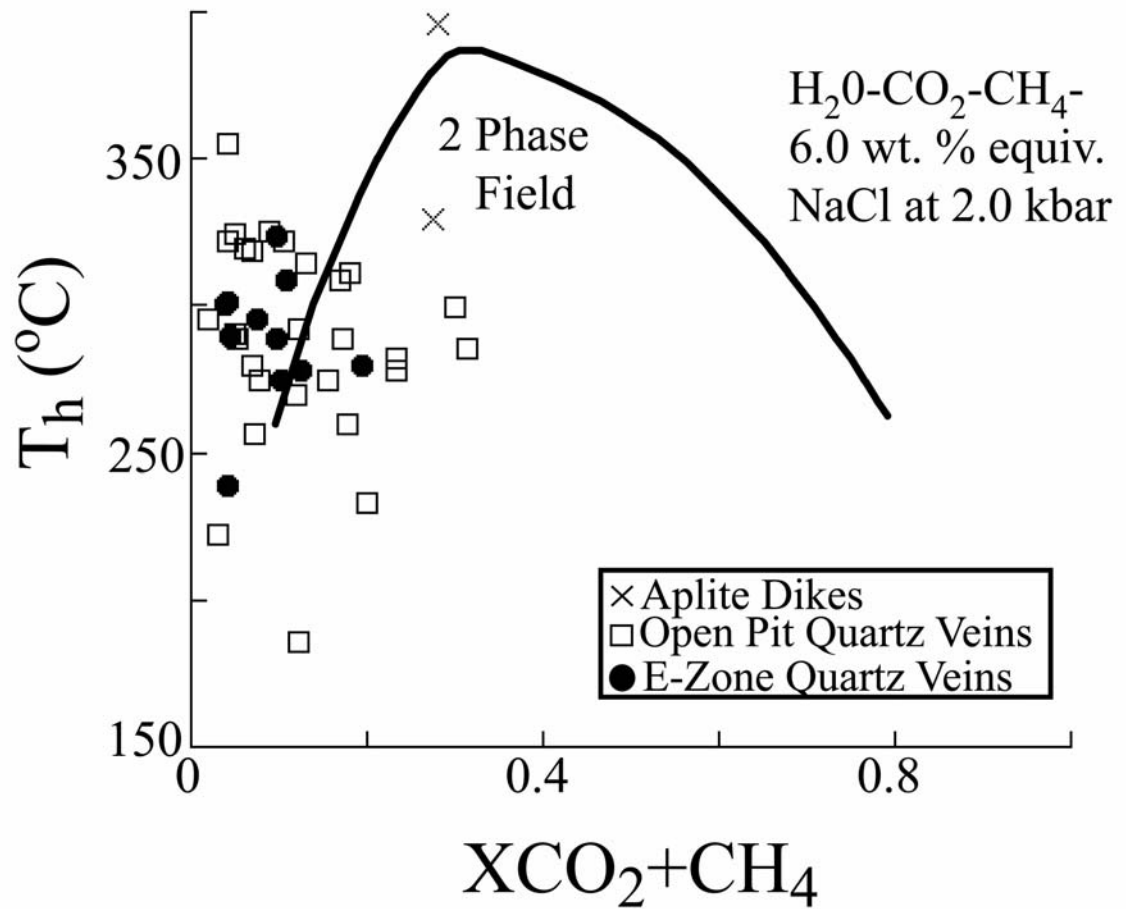


Figure 15.  $T_h$  versus  $X_{\text{CO}_2} + \text{CH}_4$  values for  $\text{H}_2\text{O}-\text{CO}_2-\text{NaCl}\pm\text{CH}_4$  inclusions at Cantung. Solvus of the system  $\text{H}_2\text{O}-\text{CO}_2-\text{CH}_4$ -6.0 wt. % equiv. NaCl at 2.0 kbar is from Gehrig (1980).

minimum pressure of 2 kbar to prevent unmixing of fluids in the high-grade quartz-scheelite veins from the Open Pit orebody (Gehrig, 1980).

Better estimates of pressure can be made using representative isochores for primary  $\text{H}_2\text{O}-\text{CO}_2-\text{NaCl}\pm\text{CH}_4$  fluid inclusions in quartz-scheelite veins from the Open Pit orebody (Fig. 16). Isochores were calculated using the MacFlinCor program (Brown and Hagemann, 1995) and my microthermometric data. Temperatures are constrained by quartz-scheelite oxygen isotope thermometry (Table 1). Using a temperature range of 430° to 595°C, fluid inclusion isochores yield pressure estimates for quartz-scheelite vein formation of 2 to 4 kbar.

Isochores for  $\text{H}_2\text{O}-\text{CO}_2-\text{NaCl}\pm\text{CH}_4$  fluid inclusions in aplite dikes reflect temperatures and pressures similar to those calculated for quartz-scheelite veins from the Open Pit orebody. The pressure range for quartz-scheelite veins from the Open Pit orebody and aplite dikes from both orebodies at Cantung corresponds to depths of approximately 6 to 9 km, assuming purely lithostatic pressure conditions. Rasmussen (2004) stated that the Mine Stock was emplaced at a depth of about 6.6 to 12.7 km, comparable to our depth estimates based on fluid inclusions.

Using F-OH thermometry and fluid inclusions from E-Zone orebody apatites, Marshall et al. (2003) concluded that the skarn ore formed at temperatures of 400° to 520°C and pressures of ~2 to 3 kbar. These temperatures and pressures for the deeper E-Zone skarn orebody are similar to my P-T estimates for the shallower quartz-scheelite veins from the Open Pit orebody. This suggests that no significant uplift and cooling of the magmatic-hydrothermal system had occurred prior to high-grade quartz-scheelite vein

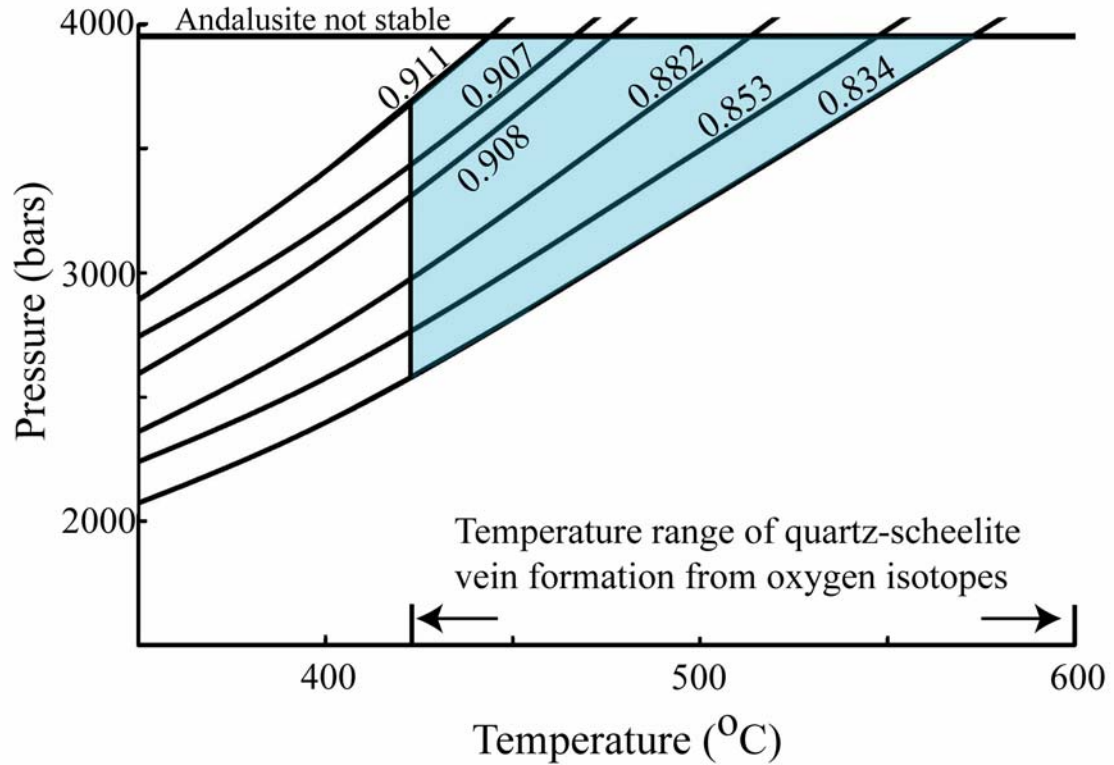


Figure 16. Representative isochores ( $\text{g}/\text{cm}^3$ ) for primary  $\text{H}_2\text{O}-\text{CO}_2-\text{NaCl}\pm\text{CH}_4$  fluid inclusions in scheelite from quartz-scheelite veins from the Open Pit orebody. Combined with temperatures of  $430^\circ$  to  $595^\circ\text{C}$  (from oxygen isotope thermometry, Table 1) and the stability of andalusite in the metasedimentary rocks (Marshall et al., 2003), these isochores indicate pressures of approximately 2 to 4 kbar for quartz-scheelite vein formation. The shaded area represents pressure and temperature conditions for formation of the high-grade quartz-scheelite veins from the Open Pit orebody. The positions of the 0.907 and 0.908 isochores are real and are the result of differences in  $\text{CH}_4$  content of the inclusions.

formation. Therefore, quartz-scheelite veins at Cantung may be thought of as a distal expression of a protracted magmatic-hydrothermal skarn-forming event.

### **Relevance of Aqueous Brine Inclusions**

The aqueous brine inclusions are obviously secondary, but could they represent a non-ore fluid present penecontemporaneously with the  $\text{H}_2\text{O}-\text{CO}_2-\text{NaCl}\pm\text{CH}_4$  ore fluid? Isochores were determined for aqueous brine inclusions. These isochores rarely intersect isochores for  $\text{H}_2\text{O}-\text{CO}_2-\text{NaCl}\pm\text{CH}_4$  inclusions at reasonable temperature and pressure conditions for ore formation (Fig. 20, Appendix VI). They instead likely represent a temperature and pressure range below  $400^\circ\text{C}$  and 2.0 kbar related to uplift of the Cantung mine area. Thus, the aqueous brine fluids are not believed to be an integral part of the scheelite ore-forming magmatic-hydrothermal event.

### **Comparison to Other Scheelite Skarn and Vein Deposits**

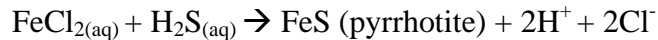
High-grade quartz-scheelite veins from the Open Pit orebody at the Cantung mine formed at temperatures of  $430^\circ$  to  $595^\circ\text{C}$  and pressures of 2 to 4 kbar.  $\text{H}_2\text{O}-\text{CO}_2-\text{NaCl}\pm\text{CH}_4$  fluids in quartz-scheelite veins have magmatic affinities. These T-P-X conditions are similar to those of other scheelite skarn deposits (e.g. Mactung, Northwest Territories, Canada: Gerstner et al., 1989; Dongmyeong mine, Korea: Choi et al., 1992).

In contrast to Cantung, most quartz-scheelite vein deposits are not the result of deep magmatic systems, but are more typically related to shallower granitic hydrothermal systems (Grey River, Newfoundland: Higgins and Kerrich, 1982; Weolag, Republic of Korea: So et al., 1983). In many cases, the early magmatic stages of these vein systems are progressively inundated by meteoric waters coincident with scheelite deposition (e.g.

Dae Hwa, Gyeongchang, and Susan, Republic of Korea: Shelton et al., 1987; So et al., 1991; So and Yun, 1994; Beuchat et al., 2004).

## **Quartz-Scheelite Vein Deposition at Cantung**

Mathieson and Clark (1984) linked the deposition of scheelite in the E-Zone skarn orebody with pyrrhotite deposition through the reaction:



This reaction fixes  $\text{Fe}^{+2}$  in pyrrhotite and increases acidity. The resultant fluid has a greater ability to react with Ca-bearing wall rocks and liberate  $\text{Ca}^{+2}$  from calcite and/or calc-silicate minerals. Because  $\text{Fe}^{+2}$  is sequestered in pyrrhotite, wolframite does not form, and tungsten is able to react with  $\text{Ca}^{+2}$  to form scheelite.

These same conditions would have led to the precipitation of scheelite in high-grade quartz-scheelite veins from the Open Pit orebody. Highly reactive fluids likely moved upward along vertical faults and fractures through the unreactive argillites (Fig. 2). When these fluids encountered the more reactive Ore and Swiss Cheese Limestones of the Open Pit orebody,  $\text{Ca}^{+2}$  was liberated from the wall rock adjacent to quartz-scheelite veins. This scenario for scheelite deposition is evident in thin section (Fig. 9). Finer-grained, dark green alteration selvages adjacent to quartz-scheelite veins in the Open Pit orebody show complete removal of calcite that is present in the earlier coarser-grained skarn assemblage.

## **Oxygen Isotope Studies**

Samples of vein-hosted quartz and scheelite and whole-rock aplite from the Open Pit and E-Zone orebodies were collected for oxygen isotope studies. Samples were

separated by hand, crushed, sieved between 80 and 100 mesh sizes, and analyzed following the procedures of Clayton and Mayeda (1963). Isotopic data are reported in standard  $\delta$  notation relative to Vienna SMOW and the standard error for each analysis is approximately  $\pm 0.1$  ‰ (Table 1). Four quartz veins and one aplite dike were collected from the E-Zone skarn orebody. Five high-grade quartz-scheelite veins and two aplite dikes were sampled from the Open Pit orebody. I carefully selected quartz-scheelite pairs in contact with one another from one quartz vein from the E-Zone orebody and three high-grade quartz-scheelite veins from the Open Pit orebody for isotope thermometry.

### **Isotope Results**

Quartz in veins from the E-Zone skarn orebody has  $\delta^{18}\text{O}$  values of 11.9 to 13.1 ‰ and quartz from high-grade veins in the Open Pit orebody has values of 12.2 to 13.1 ‰. An aplite dike from the E-Zone orebody has a  $\delta^{18}\text{O}$  value of 12.4 ‰ and two aplite dikes from the Open Pit orebody have values of 9.9 and 11.3 ‰. Vein-hosted scheelite from the E-Zone skarn orebody has a  $\delta^{18}\text{O}$  value of 6.8 ‰, whereas scheelite in veins from the Open Pit orebody has  $\delta^{18}\text{O}$  values of 6.6 to 7.2 ‰.

*Oxygen Isotope Thermometry:* The  $\Delta^{18}\text{O}_{\text{quartz-scheelite}}$  values for four quartz-scheelite pairs from quartz veins are 5.1 to 6.5 ‰. Using the oxygen isotope fractionation equations of Clayton et al. (1972) for quartz-water and Wesolowski and Ohmoto (1986) for scheelite-water, calculated equilibrium isotope temperatures for these mineral pairs are 430° to 595°  $\pm$  45°C. These calculated temperatures are in good agreement with temperatures of

Table 1. Oxygen isotope data for quartz, scheelite, and aplite dike samples from Cantung.

Sample	Mineral/ rock	$\delta^{18}\text{O}$ (‰)	$\Delta^{18}\text{O}_{\text{qtz-sch}}$ (‰)	Isotope T (°C)	$\delta^{18}\text{O}_{\text{water}}$ (‰)*
<b>E-Zone Orebody</b>					
HF03-05	quartz	12.1			8.5 - 11.0
HF03-74	quartz	11.9			10.8
	scheelite	6.8	5.1	595 ± 45	10.8
HF03-90	quartz	12.9			9.3 - 11.8
HF03-92	quartz	13.1			9.7 - 12.0
3900Pow	aplite	12.4			9.9 - 11.9
<b>Open Pit Orebody</b>					
HF03-17	quartz (clear)	12.4			11.0
HF03-17	scheelite	7.1	5.3	565 ± 45	11.0
HF03-17	quartz (milky)	12.8			9.2 - 11.7
HF03-25	quartz	12.9			9.5 - 11.8
Pit Vein 2	quartz	12.8			10.9
	scheelite	7.2	5.6	525 ± 45	10.9
Pit Vein 28	quartz	13.1			9.7
	scheelite	6.6	6.5	430 ± 45	9.7
HF03-94	quartz	12.2			8.8 - 11.1
HF03-94-I	aplite	10.0			7.5 - 9.5
	aplite	9.9			7.4 - 9.5
HF03-94-II	aplite	10.9			8.4 - 10.5
	aplite	11.3			8.8 - 10.9

Equilibrium isotope temperatures and  $\delta^{18}\text{O}_{\text{water}}$  values were calculated using the equations of Wesolowski and Ohmoto (1986), Freidman and O'Neil (1977), and Clayton et al. (1972). \*  $\delta^{18}\text{O}_{\text{water}}$  values were calculated at 430° and 595°C for all samples except those with quartz-scheelite pairs, which were calculated at their own equilibrium isotope temperatures.



400° to 520°C suggested for skarn formation by Mathieson and Clark (1984), Bowman et al. (1985), and Marshall et al. (2003).

High-grade quartz-scheelite veins from the Open Pit orebody are related to a deep, hot, magmatic-hydrothermal system. The veins likely represent a distal expression of the magmatic-hydrothermal skarn-forming event. They are not the result of a cooler system associated with uplift of the area.

*Calculated  $\delta^{18}O_{\text{water}}$  Values:* Ranges of  $\delta^{18}O_{\text{water}}$  values responsible for quartz vein precipitation were calculated using the quartz-water curve of Clayton et al. (1972) and a temperature range of 430° to 595°C, based on isotope thermometry. The  $\delta^{18}O_{\text{water}}$  values in equilibrium with quartz in veins from the Open Pit orebody range from 8.8 to 11.8 ‰, and  $\delta^{18}O_{\text{water}}$  values in equilibrium with quartz in veins from the E-Zone orebody are 8.5 to 12.0 ‰. These overlapping ranges indicate that isotopically similar fluids deposited vein quartz from both orebodies.

Since aplite dikes have all have been altered to various degrees, their  $\delta^{18}O_{\text{water}}$  values correspond to the fluids responsible for alteration. Ranges of  $\delta^{18}O_{\text{water}}$  values responsible for aplite dike alteration were calculated using the feldspar-water curve of Freidman and O'Neil (1977). The  $\delta^{18}O$  values of waters responsible for altering the aplite dikes range from 8.4 to 11.9 ‰.

The  $\delta^{18}O_{\text{water}}$  values for high-grade quartz-scheelite veins from the Open Pit orebody and aplite dikes are in good agreement with values of 8.9 to 10.4 ‰ calculated by Bowman et al. (1985) for waters that deposited the E-Zone skarn orebody. The  $\delta^{18}O_{\text{water}}$  values are consistent with waters that equilibrated with igneous and metasedimentary rocks at high temperatures and low water/rock ratios. The fluids that

deposited high-grade quartz-scheelite veins of the Open Pit orebody are likely magmatic-related fluids similar isotopically to those that deposited the underlying E-Zone skarn orebody. There is no isotopic evidence of meteoric water involvement in these vein systems.

## **Summary**

Isochores from primary  $\text{H}_2\text{O}-\text{CO}_2-\text{NaCl}\pm\text{CH}_4$  inclusions in quartz-scheelite veins from the Open Pit orebody, constrained by temperature estimates from oxygen isotope thermometry ( $430^\circ$  to  $595^\circ\text{C}$ ), yield pressures of 2 to 4 kbar. These temperature and pressure estimates are similar to those for the deeper E-Zone skarn orebody ( $400^\circ$  to  $520^\circ\text{C}$  and 2 to 3 kbar). These temperatures and pressures indicate that the high-grade quartz-scheelite veins are related to a deep magmatic-hydrothermal system and are likely a distal expression of a protracted skarn-forming event. Quartz-scheelite veins did not form in a shallower, cooler, hydrothermal system during uplift.

Primary ore fluids in quartz-scheelite veins from the Open Pit orebody, in skarn-related quartz veins from the E-Zone orebody, and in aplite dikes are grossly similar  $\text{H}_2\text{O}-\text{CO}_2-\text{NaCl}\pm\text{CH}_4$  fluids. However, two distinct end-member fluids have been documented: aplite-related fluids and skarn-related fluids. Fluids in high-grade quartz-scheelite veins contain components of both end-member fluids.

High-grade quartz-scheelite veins from the Open Pit orebody share a common structural attitude with aplite dikes. Fluids in quartz-scheelite veins contain an aplite-related fluid end-member even when occurring up to 70 meters from the nearest aplite dike. Thus, quartz-scheelite veins and aplite dikes in the Open Pit orebody may have a genetic relationship in addition to their structural relationship.

High-grade quartz-scheelite veins from the Open Pit orebody represent a distal expression of a protracted magmatic skarn-forming event. The presence of magmatic ore fluids distal to intrusions is intriguing as it has significant implications for mineral resource assessment in the region.

### **Comparison to Other Distal Skarn Systems**

*Distal Skarns:* Distal skarns are not uncommon in reactive carbonate rocks. They are found 100's of meters to several kilometers away from parental intrusions (e.g. Mines Gaspé, Quebec: Shelton and Rye, 1982; Shelton, 1983; Malo et al., 2000; Riba de Alva, Portugal: Gaspar and Inverno, 2000). Although these systems have magmatic components, in comparison to Cantung, they typically involve large volumes of meteoric water and shallower intrusions (1 to 2.5 km depth).

*Veins in Distal Skarns:* Hydrothermal vein systems within distal skarns are less well known. The W-Mo deposits of the Hwanggangri district, Republic of Korea (Weolag mine: So et al., 1983) illustrate the interplay of host rock geometry and fault/fracture control on ore fluid migration. Similar to the Cantung mine, ore fluid flow at the Weolag mine was concentrated through fractures in folded carbonate rocks. However, in contrast to the Cantung mine, wolframite was the dominant ore mineral deposited during the magmatic stage in the Hwanggangri District, whereas scheelite was deposited during progressive meteoric water inundation of the ore-forming system.

The high-grade quartz-scheelite veins from the Open Pit orebody at the Cantung mine are unusual because they are exclusively magmatic and formed at greater depths than most other scheelite vein deposits. The fluids that formed the high-grade quartz-scheelite veins in the Open Pit orebody more closely resemble magmatic fluids associated

with scheelite skarn deposits than fluids associated with quartz-wolframite-scheelite vein systems.

### **Conceptual Model for Cantung**

I envision a conceptual model for the Cantung magmatic-hydrothermal system in which ore-grade tungsten deposits formed where ore fluids emerged from the granite and encountered rocks favorable for skarn development (e.g. cleaner 'Ore Limestone' versus cherty 'Swiss Cheese Limestone'). Due to the folded geometry of the sedimentary sequence, in other areas along the granite contact, the fluids emerging from the granite encountered strata less favorable to skarn development (i.e. argillite). Where these less favorable units were breached by fracture systems, potential skarn-forming fluids (and aplite dikes) gained access to host rocks more conducive to ore development vertically distal to the granite contact.

These deposits need not be only massive skarn deposits, but could also be manifested as vein and replacement-type deposits in metasedimentary rocks. Deposits can take on various forms depending on wall rock composition. For example, in wall rocks that contain K-feldspar, acidic fluids, that would have created skarn in carbonate rocks, might instead form greisen deposits. Such a scenario is seen in tungsten showings in the nearby Rifle Range Creek. If these same fluids moved along quartzite-argillite contacts, vein-type deposits, like those of the nearby HY prospect, might develop.

### **Distal Vein Deposits of the Cantung Region**

High-grade quartz-scheelite veins from the Open Pit orebody are a distal expression of a protracted, magmatic skarn-forming event. These veins have trace metal signatures similar to regional gold-bearing quartz veins.

*Intrusion-Related Gold Deposits:* The association of gold mineralization with Cretaceous intrusions of the Tombstone and Mayo plutonic suites of the Tintina Gold Province (Fig. 1) is so prevalent that it has provided a foundation for intrusion-related gold deposit (IRGD) models (Thompson et al., 1999; Lang et al., 2000; Baker, 2002; Baker et al., 2005; Goldfarb et al., 2005). Fluids in IRGD have low salinities, are CO<sub>2</sub>-bearing, and have T<sub>h</sub> values of 200° to 400°C, similar to primary ore fluids in high-grade quartz-scheelite veins from the Open Pit orebody at Cantung.

Recently, Hart and Lewis (2006) suggested that some of these deposits maybe orogenic gold deposits. Rather than forming as distal products of magmatic fluids, they were thought to be related to metamorphic fluid flow focused along faults.

*Reconnaissance Fluid Inclusion Studies of Outlying Deposits:* To shed light on this controversy on the origin of regional quartz veins, I collected skarn and vein samples in several tungsten and gold deposits and mineral showings in the Cantung area (see Appendix VII). A quartz vein sample and a greisen alteration sample crosscut by quartz veins were collected from glacial debris near the Rifle Range Creek tungsten showing. Two distal skarn samples and one quartz vein sample contained within skarn alteration were collected from the Lened W ± Mo showing. One quartz vein was collected from the Au-Ag-base metal showing at Zantung Creek. Two quartz veins (ribboned and massive varieties) were collected from the HY gold prospect for fluid inclusion analysis.

Primary H<sub>2</sub>O-CO<sub>2</sub>-NaCl±CH<sub>4</sub> fluid inclusions were observed in samples from all localities. H<sub>2</sub>O-CO<sub>2</sub>-NaCl±CH<sub>4</sub> fluids similar to the skarn-related end-member fluid observed in high-grade quartz-scheelite veins from the Open Pit orebody at Cantung (T<sub>m</sub> CO<sub>2</sub> values of -65.0° to -56.6°C and T<sub>h</sub> values of 230° to 315°C) were found in samples

from Rifle Range Creek, Zantung Creek, and both vein types from the HY showing.  $\text{H}_2\text{O}-\text{CO}_2-\text{NaCl}\pm\text{CH}_4$  fluids resembling those of the aplite-related end-member fluid observed in high-grade quartz-scheelite veins from the Open Pit orebody at Cantung ( $T_{\text{mCO}_2}$  values below  $-65^\circ\text{C}$  and  $T_{\text{h}}$  values of  $300^\circ$  to  $340^\circ\text{C}$ ) were found in a massive vesuvianite skarn sample from the Lened prospect. I believe that it is probable that the  $\text{H}_2\text{O}-\text{CO}_2-\text{NaCl}\pm\text{CH}_4$  fluids in samples from Rifle Range Creek, Lened, Zantung Creek, and HY gold prospect have a magmatic affinity, similar to the  $\text{H}_2\text{O}-\text{CO}_2-\text{NaCl}\pm\text{CH}_4$  fluids at Cantung.

Because  $\text{H}_2\text{O}-\text{CO}_2-\text{NaCl}\pm\text{CH}_4$  fluids in all of these outlying deposits are grossly similar, a likely factor that controlled the type of ore deposit formed is the mineralogy of the host lithologic units. Deposits that result from the interaction of magmatic  $\text{H}_2\text{O}-\text{CO}_2-\text{NaCl}\pm\text{CH}_4$  fluids need not be manifested as massive skarns if the fluids encountered mineralogically diverse, but reactive, lithologic units that were not limestones.

*Reinterpretation of the HY Gold Prospect:* The HY gold showing was interpreted to be of orogenic (metamorphic) origin by Hart and Lewis (2006) because evidence supporting an intrusion-related gold model was thought to be absent (i.e. plutons or dikes are not present, skarns are not developed locally, and metal zonations typical of IRGD do not exist).

However, one of the quartz veins I sampled from the HY prospect contained abundant scheelite (Fig. 21, Appendix VII). Additionally, both quartz vein samples from the HY gold prospect that I examined contain primary  $\text{H}_2\text{O}-\text{CO}_2-\text{NaCl}\pm\text{CH}_4$  fluid inclusions, similar to the magmatic skarn-related end-member fluid in high-grade quartz-

scheelite veins at Cantung. These observations suggest that there is a magmatic signature contained within gold-bearing quartz veins of the HY gold prospect.

Although I am unable to speculate on the origin of gold at the HY prospect, the magmatic signature (i.e. scheelite and magmatic H<sub>2</sub>O-CO<sub>2</sub>-NaCl±CH<sub>4</sub> inclusions) could have formed two different ways. First, the entire vein system could be intrusion-related. The gold and tungsten could have a magmatic source and the entire vein system may instead be intrusion-related. Second, the tungsten could have been introduced into the vein system during a later magmatic event. This later event could have introduced tungsten into the HY vein system by reactivating faults and other ore-fluid conduits (Bierlein and McKnight, 2005). No matter which scenario occurred, there is an apparent magmatic signature associated with these gold-bearing veins.

*Implications for Exploration:* I have documented the presence of H<sub>2</sub>O-CO<sub>2</sub>-NaCl±CH<sub>4</sub> fluids in quartz vein and skarn samples from a variety of deposit types in the Cantung region, which resemble the distal, magmatic fluids found in high-grade quartz-scheelite veins from the Open Pit orebody at Cantung. It is possible that these and other deposits in the region may be intrusion-related deposits.

Vein and replacement-type deposits in metasedimentary rocks of the Cantung region frequently have been assumed to represent older ore events. Their origins should be re-evaluated, as some of them could instead represent distal, intrusion-related deposits.

The documentation of ore-mineralizing fluids distal to the intrusion-country rock contact expands the potential exploration area for ore targets. Exploration strategies in the Cantung region should not focus solely on intrusion-country rock contacts. They

should also consider the interplay of host rock geometry and fault/fracture control that could allow fluids to form distal magmatic ore deposits.



## References

- Baker, T., 2002, Emplacement depth and carbon dioxide-rich fluid inclusions in intrusion-related gold deposits: *ECONOMIC GEOLOGY*, v. 97, p. 1111-1117.
- Baker, T., Pollard, P.J., Mustard, R., Mark, G., and Graham, J.L., 2005, A comparison of granite-related tin, tungsten, and gold-bismuth deposits: Implications for exploration: *Society of Economic Geologist Newsletter*, no. 61, p. 5-17.
- Beuchat, S., Moritz, R., and Pettke, T., 2004, The magmatic to hydrothermal transition and its bearing on ore-forming processes: *Chemical Geology*, v. 210, p. 201-224.
- Bierlein, F.P., and McKnight, S., 2005, Possible intrusion-related gold systems in the western Lachlan orogen, southeast Australia: *ECONOMIC GEOLOGY*, v. 100, p. 385-398.
- Blusson, S.L., 1967, Geology and tungsten deposits near the headwaters of the Flat River, Yukon Territory and District of Mackenzie, Canada: *Canadian Geological Survey Paper 67-22*, 77 pp.
- Bodnar, R.J., and Vityk, M.O., 1994, Interpretation of microthermometric data for H<sub>2</sub>O-NaCl fluid inclusions: *in* De Vivo, B., and Frezzotti, M.L., eds., *Fluid inclusions in minerals: Methods and applications*: Blacksburg, Virginia Polytechnic Institute and State University, p. 11-130.
- Bowman, J.R., Covert, J.J., Clark, A.H., and Mathieson, G.A., 1985, The CanTung E Zone scheelite skarn orebody, Tungsten, Northwest Territories: Oxygen, hydrogen, and carbon isotope studies: *ECONOMIC GEOLOGY*, v. 80, p. 1872-1895.
- Brown, C.J., 1961, The geology of the Flat River Tungsten Deposits Canada Tungsten Mining Corporation Limited: *Canadian Mining and Metallurgical Bulletin*, v. 94, p. 510-513.
- Brown, P.E., and Hagemann, S.G., 1995, MacFlinCor and its application to fluids in Archean lode-gold deposits: *Geochimica et Cosmochimica Acta*, v. 19, p. 3943-3952.
- Burruss, R.C., 1981, Analysis of phase equilibria in C-O-H-S fluid inclusions: *in* Hollister, L.S., and Crawford, M.L., eds., *Fluid inclusions: Applications to petrology*: Mineralogical Association of Canada, Short Course Handbook, v. 6, p. 39-74.
- Cathro, R.J., 1969, Tungsten in Yukon: Archer, Cathro, and Associates Ltd., 8 pp.

- Choi, S.H., So, C.S., and Shelton, K.L., 1992, Skarn evolution and tungsten mineralization at the Dongmyeong mine, Republic of Korea: *Neues Jahrbuch für Mineralogie Abhandlungen*, v. 164, p. 57-93.
- Christiansen, E.H., and Keith, J.D., 1996, Trace element systematics in silicic magmas: A metallogenic perspective: *in* Wyman, D.A., ed., Trace element geochemistry of volcanic rocks: Applications for massive sulphide exploration: Geological Association of Canada, Short Course Notes, v. 12, p. 115-151.
- Clayton, R.N., and Mayeda, T.K., 1963, The use of bromine-pentafluoride in the extraction of oxygen from oxides and silicates for isotopic analyses: *Geochimica et Cosmochimica Acta*, v. 27, p. 43-52.
- Clayton, R.N., O'Neil, J.R., and Mayeda, T.K., 1972, Oxygen isotope exchange between quartz and water: *Journal of Geophysical Research*, v. 77, p. 3057-3067.
- Collins, P.L.F., 1979, Gas hydrates in CO<sub>2</sub>-bearing fluid inclusions and the use of freezing data for the estimation of salinity: *ECONOMIC GEOLOGY*, v. 74, p. 1435-1444.
- Crawford, M.L., 1981, Phase equilibria in aqueous fluid inclusions: *in* Hollister, L.S., and Crawford, M.L., eds., Fluid inclusions: Applications to petrology: Mineralogical Association of Canada, Short Course Handbook, v. 6, p. 75-100.
- Crawford, W.J.P., 1963, Geology of the Canada Tungsten Mine, SW District of Mackenzie, Canada: Unpublished M.S. thesis, University of Washington, Seattle, 80 pp.
- Cummings, W.W., and Bruce, D.E., 1977, Canada Tungsten – Change to underground mining and description of mine-mill procedures: *Canada Mining and Metallurgy Bulletin*, v. 70, p. 94-101.
- Diamond, L., 1992, Stability of CO<sub>2</sub> clathrate hydrate + CO<sub>2</sub> liquid + CO<sub>2</sub> vapor + aqueous KCl-NaCl solutions: Experimental determination and application to salinity estimates of fluid inclusions: *Geochimica et Cosmochimica Acta*, v. 56, p. 273-280.
- Dick, L.A., 1980, A comparative study of the geology, mineralogy, and conditions of formation of contact metasomatic mineral deposits in the NE Canadian Cordillera: Unpublished Ph.D. dissertation, Kingston, Queen's University, 473 pp.
- Dick, L.A., and Hodgson, C.J., 1982, The MacTung W-Cu(Zn) contact metasomatic and related deposits of the northeastern Canadian Cordillera: *ECONOMIC GEOLOGY*, v. 77, p. 845-867.

- Fayek, M., and Kyser, T.K., 1995, Characteristics of auriferous and barren fluids associated with the Proterozoic Contact Lake gold deposit, Saskatchewan, Canada: *ECONOMIC GEOLOGY*, v. 90, p. 385-406.
- Friedman, I., and O'Neil, J.R., 1977, Compilation of stable isotope fractionation factors of geochemical interest: *in* Fleischer, M., ed., *Data of Geochemistry*, sixth ed., Chapter KK, U.S. Geological Survey Professional Paper 440-KK, 12 pp.
- Gaspar, L.M., and Inverno, C.M.C., 2000, Mineralogy and metasomatic evolution of distal strata-bound scheelite skarns in the Riba de Alva mine, northeastern Portugal: *ECONOMIC GEOLOGY*, v. 95, p. 1259-1275.
- Gehrig, M., 1980, Phasengleichgewichte und PVT-Daten ternärer Mischungen aus Wasser Kohlendioxid und Natriumchlorid bis 3 kbar und 550°C: Unpublished Ph.D. dissertation, Institut für Physikalische Chemie, Universität Karlsruhe, Karlsruhe.
- Gerstner, M.R., Bowman, J.R., and Pasteris, J.D., 1989, Skarn formation at the Macmillan Pass tungsten deposit (Mactung), Yukon and Northwest Territories. I. P-T-V-X characterization of the methane-bearing, skarn-forming fluids: *Canadian Mineralogist*, v. 27, p. 545-563.
- Goldfarb, R.J., Leach, D.L., and Pickthorn, W.J., 1988, Accretionary tectonics, fluid migration, and gold genesis in the Pacific border ranges and coast mountains, southern Alaska: *in* Kisvarsanyi, G., and Grant, S.K., eds., *North American conference on tectonic control of ore deposits and the vertical and horizontal extent of ore systems: Proceedings volume*, Rolla, University of Missouri-Rolla Press, p. 67-79.
- Goldfarb, R.J., Baker, T., Dubé, B., Hart, C.J.R., and Gosslin, P., 2005, Distribution, character, and genesis of gold deposits in metamorphic terranes: *in* Hedenquist, J.W., Thompson, J.F.H., Goldfarb, R.J., and Richards, J.P., eds., *Economic Geology 100<sup>th</sup> Anniversary Volume*, p. 407-450.
- Hart, C.J.R., and Lewis, L.L., 2006, Gold mineralization in the upper Hyland River area: A non-magmatic origin: *in* Emond, D.S., Bradshaw, G.D., Lewis, L.L., and Weston, L.H., eds., *Yukon Exploration and Geology 2005: Yukon Geological Survey*, Whitehorse, p. 109-125.
- Higgins, N.C., and Kerrich, R., 1982, Progressive <sup>18</sup>O depletion during CO<sub>2</sub> separation from a carbon dioxide-rich hydrothermal fluid: Evidence from the Grey River tungsten deposit, Newfoundland: *Canadian Journal of Earth Science*, v. 19, p. 2247-2257.
- Hodgson, C.J., 2000, Exploration potential at the Cantung Mine, District of Mackenzie, NWT: Andean Engineering, Cantung Internal Files, 26 pp.

- Ishihara, S., 1977, The magnetite-series and ilmenite-series granitic rocks: *Mining Geology*, v. 27, p. 293-305.
- Ivanova, G.F., 1986, Geochemistry of tungsten: *in* Beus, A.A., ed., *Geology of Tungsten*: Belgium, Unesco, p. 11-44.
- Jia, Y., Kerrich, R., and Goldfarb, R., 2003, Metamorphic origin of ore-forming fluids for orogenic gold-bearing quartz vein systems in the North American Cordillera: Constraints from a reconnaissance study of  $\delta^{15}\text{N}$ ,  $\delta\text{D}$ ,  $\delta^{18}\text{O}$ : *ECONOMIC GEOLOGY*, v. 98, p. 109-123.
- Kerrick, D.M., and Jacobs, G.K., 1981, A modified Redlich-Kwong equation for  $\text{H}_2\text{O}$ ,  $\text{CO}_2$ , and  $\text{H}_2\text{O}-\text{CO}_2$  mixtures at elevated pressures and temperatures: *American Journal of Science*, v. 281, p. 735-767.
- Kerrick, R., and King, R., 1993, Hydrothermal zircon and baddeleyite in Val-d'Or Archean mesothermal gold deposits: Characteristics, compositions, and fluid-inclusion properties, with implications for timing of primary gold mineralization: *Canadian Journal of Earth Sciences*, v. 30, p. 2334-2351.
- Lang, J.R., Baker, T., Hart, C.J.R., and Mortensen, J.K., 2000, An exploration model for intrusion-related gold systems: *Society of Economic Geologists Newsletter*, no. 40, p. 1-15.
- Malo, M., Moritz, R., Dubé, B., Chagnon, A., Roy, F., and Pelchat, C., 2000, Base metal skarns and Au occurrences in the Southern Gaspé Appalachians: Distal products of a faulted and displaced magmatic-hydrothermal system along the Grand Pabos-Restigouche fault system: *ECONOMIC GEOLOGY*, v. 95, p. 1297-1318.
- Marshall, D., Falck, H., Mann, B., Kirkham, G., and Mortensen, J., 2003, Geothermometry and fluid inclusion studies of the E-Zone biotite skarn, CanTung Mine, Tungsten, NWT: Abstracts of the 31<sup>st</sup> Yellowknife Geoscience Forum, p. 60.
- Mathieson, G.A., and Clark, A.H., 1984, The CanTung E-zone scheelite skarn orebody, Tungsten, Northwest Territories: A revised genetic model: *ECONOMIC GEOLOGY*, v. 79, p. 883-901.
- Mortensen, J.K., Hart, C.J.R., Murphy, D.C., and Heffernan, S., 2000, Temporal evolution of Early and mid-Cretaceous magmatism in the Tintina Gold Belt: *in* Jambor, J., ed., *The Tintina Gold Belt: Concepts, Exploration, and Discoveries*: British Columbia and Yukon Chamber of Mines, Special Volume 2, p. 49-57.
- Nesbitt, B.E., Murowchick, J.B., and Muehlenbachs, K., 1986, Dual origins of lode gold deposits in the Canadian Cordillera: *Geology*, v. 14, p. 506-509.

- Rasmussen, K.L., 2004, The aplitic dykes of the Cantung Mine: Petrography, geochemistry, and implications for the mineralization process: Unpublished B.Sc. thesis, University of Calgary, Calgary, 157 pp.
- Rasmussen, K.L., Mortensen, J.K., and Falck, H., 2006, Geochronological and lithochemical studies of intrusive rocks in the Nahanni region, southwestern Northwest Territories and southeastern Yukon: *in* Emond, D.S., Bradshaw, G.D., Lewis, L.L., and Weston, L.H., eds., Yukon Exploration and Geology 2005: Yukon Geological Survey, Whitehorse, p. 287-298.
- Roedder, E., 1984, Fluid inclusions: Mineralogical Society of America, Reviews in Mineralogy, v. 12, 646 pp.
- Shelton, K.L., 1983, Composition and origin of ore-forming fluids in a carbonate-hosted porphyry copper and skarn deposit: A fluid inclusion and stable isotope study of Mines Gaspé, Quebec: *ECONOMIC GEOLOGY*, v. 78, p. 387-419.
- Shelton, K.L., McMenamy, T.A., van Hees, E.H.P., and Falck, H., 2004, Deciphering the complex fluid history of a greenstone-hosted gold deposit: Fluid inclusion and stable isotope studies of the Giant Mine, Yellowknife, Northwest Territories, Canada: *ECONOMIC GEOLOGY*, v. 99, p. 1643-1663.
- Shelton, K.L., and Orville, P.M., 1980, Formation of synthetic fluid inclusions in natural quartz: *American Mineralogist*, v. 65, p. 1233-1236.
- Shelton, K.L., and Rye, D.M., 1982, Sulfur isotopic compositions of ores from Mines Gaspé, Quebec: An example of sulfate-sulfide isotopic disequilibria in ore-forming fluids with applications to other porphyry-type deposits: *ECONOMIC GEOLOGY*, v. 77, p. 1688-1709.
- Shelton, K.L., Taylor, R.P., and So, C.S., 1987, Stable isotope studies of the Dae Hwa tungsten-molybdenum mine, Republic of Korea: Evidence of progressive meteoric water interaction in a tungsten-bearing hydrothermal system: *ECONOMIC GEOLOGY*, v. 82, p. 471-481.
- So, C.S., Rye, D.M., and Shelton, K.L., 1983, Carbon, hydrogen, oxygen, and sulfur isotope and fluid inclusion study of the Weolag tungsten-molybdenum deposit, Republic of Korea: Fluid histories of metamorphic and ore-forming events: *ECONOMIC GEOLOGY*, v. 78, p. 1551-1572.
- So, C.S., Shelton, K.L., Chi, S.J., and Yun, S.T., 1991, Geochemical studies of the Gyeongchang W-Mo mine, Republic of Korea: Progressive meteoric water inundation of a magmatic hydrothermal system: *ECONOMIC GEOLOGY*, v. 86, p. 750-767.

- So, C.S., and Yun, S.T., 1994, Origin and evolution of W-Mo producing fluids in a granitic hydrothermal system: Geochemical studies of quartz vein deposits around the Susan granite, Hwanggangri District, Republic of Korea: *ECONOMIC GEOLOGY*, v. 89, p. 246-267.
- Stern, L.A., Brown Jr., G.E., Bird, D.K., Jahns, R.H., Foord, E.E., Shigley, J.E., and Spaulding Jr., L.B., 1986, Mineralogy and geochemical evolution of the Little Three pegmatite-aplite layered intrusive, Romona, California: *American Mineralogist*, v. 71, p. 406-427.
- Thiery, R., van den Kerkhof, A.M., and Dubessy, J., 1994, vX properties modeling of CH<sub>4</sub>-CO<sub>2</sub> and CO<sub>2</sub>-N<sub>2</sub> fluid inclusions (T < 31°C, P < 400 bars): *European Journal of Mineralogy*, v. 6, p. 753-771.
- Thompson, J.F.H., Silltoe, R.H., Baker, T., Lang, J.R., and Mortensen, J.K., 1999, Intrusion-related gold deposits associated with tungsten-tin provinces: *Mineralium Deposita*, v. 34, p. 323-334.
- Wesolowski, D., and Ohmoto, H., 1986, Calculated oxygen isotope fractionation factors between water and the minerals scheelite and powellite: *ECONOMIC GEOLOGY*, v. 81, p. 471-477.
- Yukon Geological Survey, 2005, Canada's Yukon tungsten: Yukon Geological Survey Brochure, 4 pp.
- Yuvan, J.G., Shelton, K.L., Falck, H., and Marshall, D., 2004, High-grade quartz-scheelite veins in the Cantung Mine, Northwest Territories: A late magmatic-hydrothermal event: *Geological Society of America Abstracts with Programs*, v. 36, no. 5, p. 355.
- Yuvan, J.G., Shelton, K.L., and Falck, H., 2005, A distal expression of a protracted skarn-forming event?: Oxygen isotope and fluid inclusion studies of quartz-scheelite veins in the Cantung Mine, NWT: *Abstracts of the 33<sup>rd</sup> Yellowknife Geoscience Forum*, p. 128.
- Zaw, U.K., 1976, The CanTung E-zone orebody, Tungsten, Northwest Territories: A major scheelite skarn deposit: Unpublished Ph.D. dissertation, Queens University, Kingston, Ontario, 409 pp.
- Zhang, Y.G., and Frantz, J.D., 1989, Experimental determination of the compositional limits of immiscibility in the system CaCl<sub>2</sub>-H<sub>2</sub>O-CO<sub>2</sub> at high temperatures and pressures using synthetic fluid inclusions: *Chemical Geology*, v. 74, p. 289-308.

## CHAPTER 3: CONCLUSIONS

Conclusions that can be reached from geochemical studies of quartz-scheelite veins from the Open Pit orebody, quartz veins from the E-Zone orebody, and aplite dikes from both orebodies are:

1. Isochores from primary  $\text{H}_2\text{O}-\text{CO}_2-\text{NaCl}\pm\text{CH}_4$  inclusions in quartz-scheelite veins from the Open Pit orebody, constrained by temperature estimates from oxygen isotope thermometry ( $400^\circ$  to  $595^\circ\text{C}$ ), yield pressures of 2 to 4 kbar. These temperature and pressure estimates are similar to those for the deeper E-Zone skarn orebody ( $400^\circ$  to  $520^\circ\text{C}$  and 2 to 3 kbar) and indicate that the high-grade quartz-scheelite veins are related to a deep magmatic-hydrothermal system. Quartz-scheelite veins did not form in a shallower, cooler, hydrothermal system during uplift.
2. Primary ore fluids in quartz-scheelite veins from the Open Pit orebody, in skarn-related quartz veins from the E-Zone orebody, and in aplite dikes are grossly similar  $\text{H}_2\text{O}-\text{CO}_2-\text{NaCl}\pm\text{CH}_4$  fluids. However, two distinct end-member fluids have been documented: aplite-related fluids and skarn-related fluids. Fluids in high-grade quartz-scheelite veins contain components of both end-member fluids.
3. High-grade quartz-scheelite veins from the Open Pit orebody share a common structural attitude with aplite dikes. Fluids in quartz-scheelite veins contain an aplite-related fluid end-member even when occurring up to 70 meters from the nearest aplite dike. Thus, quartz-scheelite veins and aplite dikes in the Open Pit orebody may have a genetic relationship in addition to their structural relationship.
4. High-grade quartz-scheelite veins from the Open Pit orebody represent a distal expression of a protracted magmatic-hydrothermal skarn-forming event. The presence of

magmatic ore fluids distal to intrusions is intriguing as it has significant implications for mineral resource assessment in the region.

I envision a conceptual model for the Cantung magmatic-hydrothermal system in which ore-grade tungsten deposits formed where fluids emerged from the granite and encountered rocks favorable for skarn development (e.g. cleaner 'Ore Limestone' versus cherty 'Swiss Cheese Limestone'). Due to the folded geometry of the sedimentary sequence, in other areas along the granite contact, the fluids emerging from the granite encountered strata less favorable to skarn development (i.e. argillite). Where these less favorable units were breached by fracture systems, potential skarn-forming fluids (and aplite dikes) gained access to host rocks more conducive to ore development vertically distal to the granite contact.

The conceptual model proposed for the Cantung magmatic-hydrothermal system can be extrapolated to other regions. I have identified a process and geological environment in which magmatic ore fluids may pass through unreactive lithologies and deposit economic grade mineral deposits at significant distances from their igneous source regions. The documentation of ore-mineralizing fluids distal to the intrusion-country rock contact expands the potential exploration area for ore targets. Distal exploration targets need not be manifested as massive skarns, but could take on various forms depending on the geometry and chemistry of the host lithologic units.



## APPENDIX I

### Sample Descriptions

Sample No.

- HF03-05: Underground quartz vein from West Incline. White massive to ribboned quartz vein with chalcopyrite, pyrrhotite, and locally green fluorescing powellite.
- HF03-14: Quartz-scheelite vein from the Open Pit orebody. Massive white quartz with small wallrock fragments, adjacent to calcite-quartz-pyrite fault zone.
- HF03-15: Quartz-scheelite vein from the Open Pit orebody, 30 cm wide.
- HF03-16: Quartz-scheelite vein from the Open Pit orebody, 75 cm wide. Massive white quartz with chalcopyrite in core of vein.
- HF03-17: Quartz-scheelite vein from the Open Pit orebody, 30 cm wide, with coarse scheelite in core of vein.
- HF03-18: Quartz-scheelite vein from the Open Pit orebody, 15 to 20 cm wide. Pyrrhotite and chalcopyrite in fractures and in wall rock margins.
- HF03-19: Duplicate of Open Pit quartz-scheelite vein 14.
- HF03-20: Quartz-scheelite vein from the Open Pit orebody. In the Chert ore near the Open Pit wall. It is accompanied by pyritization of the wall rock.

- HF03-21: Quartz-scheelite vein from the Open Pit orebody.
- HF03-22: Quartz-scheelite vein 12 from the Open Pit orebody.  
Massive white quartz, from the pit floor in the corner of the pit.
- HF03-23: Quartz-scheelite vein 31 from the Open Pit orebody, 20 to 30 cm wide. Minor pyrrhotite and some biotite alteration present.
- HF03-24: Quartz-scheelite vein 340 from the Open Pit orebody, 10 cm wide. Chalcopyrite filled fractures and along the wall rock contact.
- HF03-25: Quartz-scheelite vein 23 from the Open Pit orebody. Series of quartz veins with 7 to 8 vein segments with iridescent biotite wall-rock alteration.
- HF03-26: Quartz-scheelite vein 27 from the Open Pit orebody. In pit wall near vein 10. It is an irregular vein rich in chalcopyrite.
- HF03-27: Quartz-scheelite vein 28 from the Open Pit orebody.  
Contorted folded quartz vein with chalcopyrite, pyrrhotite, and scheelite. On the Open Pit side of the fault zone.
- HF03-74: Underground quartz vein from 3850 Stope. Coarse biotite wall rock alteration.
- HF03-90: Underground quartz vein from 3940-109. Quartz vein sample from an aplite/quartz vein transition zone.

- HF03-91: Quartz-scheelite vein 8 from the Open Pit orebody.
- HF03-92: Underground quartz vein from 108 Stope in Room 2.  
Quartz vein from the hanging wall contact with the skarn and the chert in Lift 3 of the stope.
- HF03-93: High-grade quartz-scheelite vein sample from a subhorizontal vein in the Open Pit along the north face from near the Aplite Bench.
- HF04-94: Quartz-scheelite vein from the Open Pit orebody. Sampled at contact zone with limestone adjacent to aplite dike.
- HF03-95: Quartz-scheelite vein from the Open Pit orebody, on the North Face.
- HF03-98: Quartz-scheelite vein from the Open Pit orebody with coarse scheelite. In Swiss Cheese Limestone.
- HF03-99: Quartz-scheelite vein 28 from the Open Pit orebody. In back wall of the Open Pit, with coarse scheelite.
- HF03-100: Quartz-scheelite vein 2 from Open Pit orebody, with coarse scheelite.
- 15-4: Aplite dike from underground 1102 E Ramp, two samples.
- 3900 POW: Aplite dike from 3900 level underground at Cantung.  
Sample contains quartz, k-spar, biotite, and powellite.
- Aplite I: Aplite dike from the Open Pit orebody. Phenocrysts of quartz, k-spar, and tourmaline. Same sample as Aplite II.

Cantung Pit Vein 7: Quartz-scheelite vein from the Open Pit orebody. Open Pit vein number 7 with abundant scheelite.

Cantung Pit Vein 2: Quartz-scheelite vein from the Open Pit orebody. Open Pit vein number 2 with abundant scheelite.

JY-05-CAN4100: E-Zone skarn sample with garnet, calcite, quartz, and scheelite from the 4100 level underground at Cantung.

PIT SCHEELITE: Quartz-scheelite vein from the Open Pit orebody with abundant scheelite.

KS-05-RR2: Euhedral quartz vein from the Rifle Range Creek tungsten showing. Vein is composed of quartz and scheelite.

KS-05-RR1: Quartz-scheelite vein from the Rifle Range Creek in greisen, containing quartz and scheelite.

KS-05-HY1B: Quartz vein from the HY gold showing. Vein is composed of massive, white quartz.

KS-05-HY1A: Quartz vein from the HY gold showing. Vein is ribbon-banded and contains scheelite.

KS-05-LEN2: Quartz-idocrase skarn from Lened showing.

KS-05-LEN5: Core sample from Lened. Sample contains quartz, pyroxene, and garnet.

KS-03-LENV1: Quartz vein from Lened.

Zantung Creek: Massive, white quartz vein from Zantung (Zenchuk) Creek.

APPENDIX II

Cantung Fluid Inclusion Data

Sample (Chip)	Inclusion # (mineral if not quartz) Type	Fluid Inclusion	T <sub>CO2</sub> (°C)	T <sub>m,CO2</sub> (°C)	T <sub>s,CO2</sub> (°C)	T <sub>m</sub> (°C)	T <sub>m,asph</sub> (°C)	T <sub>h</sub> (°C)	Vapor % Homogenization (h) or Decapitated (d)	Density (g/cm <sup>3</sup> )	XCO <sub>2</sub>	XCH <sub>4</sub>	Bulk Inclusion XH <sub>2</sub> O (wt% equiv. NaCl)	Salinity (wt% equiv. NaCl)	XCO <sub>2</sub> +XCH <sub>4</sub>	Location	Carbonic Phase XCO <sub>2</sub>	XCH <sub>4</sub>	Density (g/cm <sup>3</sup> )
15-4-1 (1) Apilite	2 (tourmaline)	Aqueous Brine	-125.9	-87.9	-43.6	-6.0	10.8	311.3	23.0 h	0.8020				9.19		Pit Cantung			
15-4-1 (1) Apilite	1 (tourmaline)	H <sub>2</sub> O-CO <sub>2</sub> -NaCl±CH <sub>4</sub>	-125.9	-87.9	-43.6	-6.0	10.8	298.6	24.0 h							Pit Cantung			
15-4-1 (2) Apilite	3 (tourmaline)	Aqueous Brine	-47.2	-7.3	-4.7	-7.3	271.7	17.7 h		0.8770				10.85		Pit Cantung			
15-4-1 (2) Apilite	1 (tourmaline)	Aqueous Brine	-44.9	-6.1	-4.9	-6.1	268.8	16.4 h		0.8650				9.32		Pit Cantung			
15-4-1 (2) Apilite	2 (tourmaline)	Aqueous Brine	-41.6	-5.4	-4.1	-5.4	264.1	35.8 h		0.8610				7.96		Pit Cantung			
15-4-1 (4) Apilite	1 (tourmaline)	Aqueous Brine	-45.2	-5.1	-4.5	-5.1	252.9	25.0 h		0.8720				8.38		Pit Cantung			
15-4-1 (5) Apilite	2 (tourmaline)	Aqueous Brine	-44.2	-5.4	-4.2	-5.4	325.1	23.2 h		0.8760				8.38		Pit Cantung			
15-4-1 (5) Apilite	1 (tourmaline)	Aqueous Brine	-39.6	-3.5	-3.6	-3.5	268.8	35.8 h		0.8250				5.62		Pit Cantung			
15-4-2 (1) Apilite	2 (tourmaline)	Aqueous Brine	-39.9	-6.5	-3.9	-6.5	7.1	317.2	20.8 h	0.8020				9.84		Pit Cantung			
15-4-2 (1) Apilite	1 (tourmaline)	Aqueous Brine	-43.0	-6.6	-4.3	-6.6	324.9	16.4 h		0.7910				9.97		Pit Cantung			
15-4-2 (1) Apilite	4 (tourmaline)	Aqueous Brine	-43.5	-6.6	-4.3	-6.6	315.6	12.7 h		0.7880				8.65		Pit Cantung			
15-4-2 (1) Apilite	7 (tourmaline)	H <sub>2</sub> O-CO <sub>2</sub> -NaCl±CH <sub>4</sub>	-97.1	-87.8	-42.9	-4.5	5.2		d							Pit Cantung			0.038
15-4-2 (1) Apilite	6 (tourmaline)	H <sub>2</sub> O-CO <sub>2</sub> -NaCl±CH <sub>4</sub>	-95.7	-58.4	-46.4	-4.5	12.2	375.1	50.0 h							Pit Cantung			0.279
15-4-2 (2) Apilite	2 (tourmaline)	Aqueous Brine	-41.9	-5.0	-4.9	-5.0	243.5	29.3 h		0.8820				7.82		Pit Cantung			
15-4-2 (2) Apilite	1 (tourmaline)	Aqueous Brine	-47.3	-4.9	-4.7	-4.9	279.1	23.2 h		0.8330				7.68		Pit Cantung			
15-4-2 (2) Apilite	3 (tourmaline)	Aqueous Brine	-46.8	-3.5	-4.6	-3.5	324.9	42.7 h		0.7250				5.62		Pit Cantung			
15-4-2 (2) Apilite	2 (tourmaline)	Aqueous Brine	-112.2	-88.4	-0.9	-8.1	4.6	384.3	48.0 h							Pit Cantung			
15-4-2 (4)	1 (tourmaline)	H <sub>2</sub> O-CO <sub>2</sub> -NaCl±CH <sub>4</sub>	-103.5	-82.1	-5.9	-8.1	7.1	336.2	35.8 h							Pit Cantung			
15-4-2 (4)	2 (tourmaline)	H <sub>2</sub> O-CO <sub>2</sub> -NaCl±CH <sub>4</sub>	-90.8	-82.1	8.1	-8.1	12.1	343.9	25.0 h							Pit Cantung			
15-4-2 (5)	1 (tourmaline)	Aqueous Brine	-33.9	-6.3	-3.9	-6.3			d							Pit Cantung			
3900 POW(1)	5	Aqueous Brine	-41.4	-5.1	-4.1	-5.1			d							Pit Cantung			
3900 POW(1)	1	Aqueous Brine	-35.7	-4.9	-3.5	-4.9			d							Pit Cantung			
3900 POW(1)	4	Aqueous Brine	-36.9	-3.9	-3.6	-3.9			d							Pit Cantung			
3900 POW(1)	6	H <sub>2</sub> O-CO <sub>2</sub> -NaCl±CH <sub>4</sub>	-95.6	-60.6	-43.6	-5.7	9.1	376.6	50.0 d							Pit Cantung			
3900 POW(2)	1	Aqueous Brine	-39.6	-5.7	-3.9	-5.7		381.9	50.0 d	0.6600				8.78		Pit Cantung			
Apilite (1)	1	Aqueous Brine	-43.8	-2.5	-4.3	-2.5			d							Pit Cantung			
Apilite (1)	3	H <sub>2</sub> O-CO <sub>2</sub> -NaCl±CH <sub>4</sub>	-86.5	-59.8	-13.9	-8.1	12.3	349.7	41.0 d							Pit Cantung			
Apilite (1)	2	H <sub>2</sub> O-CO <sub>2</sub> -NaCl±CH <sub>4</sub>	-87.5	-59.4	-10.2	-8.1	6.1	329.8	50.0 d	0.9990	0.249	0.027	0.701	9.53	0.276	Pit Cantung			0.902
Apilite (2)	3	Aqueous Brine	-40.4	-5.5	-4.0	-5.5			d							Pit Cantung			0.088
Apilite (2)	1	H <sub>2</sub> O-CO <sub>2</sub> -NaCl±CH <sub>4</sub>	-84.5	-60.2	-9.7	-8.1	10.5	357.1	50.0 d							Pit Cantung			
Apilite (2)	2	H <sub>2</sub> O-CO <sub>2</sub> -NaCl±CH <sub>4</sub>	-89.5	-58.6	-13.9	-8.1	4.8		d							Pit Cantung			
Apilite (2)	5	H <sub>2</sub> O-CO <sub>2</sub> -NaCl±CH <sub>4</sub>	-90.8	-57.8	-14.1	-8.1	7.1	386.3	50.0 d	1.0240	0.279	0.001	0.691	8.73	0.280	Pit Cantung			0.966
Apilite (2)	4	H <sub>2</sub> O-CO <sub>2</sub> -NaCl±CH <sub>4</sub>	-86.1	-56.8	-14.1	-8.1	13.2	411.5	29.0 d							Pit Cantung			
Apilite (3)	2	Aqueous Brine	-39.8	-5.9	-3.9	-5.9		262.9	18.0 h	0.8700				9.05		Pit Cantung			
Apilite (3)	3	Aqueous Brine	-43.6	-5.5	-4.3	-5.5		349.2	41.0 h	0.7240				8.51		Pit Cantung			
Apilite (3)	1	Aqueous Brine	-44.5	-4.7	-4.5	-4.7		254.7	15.0 h	0.6640				7.39		Pit Cantung			
Apilite (4)	1	H <sub>2</sub> O-CO <sub>2</sub> -NaCl±CH <sub>4</sub>	-86.1	-59.6	-55.8	-4.7	9.4	348.1	40.0 d							Pit Cantung			
Apilite (4)	3	H <sub>2</sub> O-CO <sub>2</sub> -NaCl±CH <sub>4</sub>	-87.7	-57.9	-55.8	-4.7	11.1	362.2	30.0 d							Pit Cantung			
Apilite (5)	2	Aqueous Brine	-39.1	-4.9	-3.9	-4.9		302.4	37.0 h	0.7970				7.68		Pit Cantung			
Apilite (5)	1	Aqueous Brine	-36.7	-3.8	-3.6	-3.8		334.1	22.0 h	0.7140				6.08		Pit Cantung			
Apilite (11)	3	Aqueous Brine	-42.4	-7.6	-4.2	-7.6			d							Pit Cantung			
Apilite (11)	1	Aqueous Brine	-49.4	-7.2	-4.9	-7.2		360.9	30.0 h	0.7400				10.73		Pit Cantung			
Apilite (11)	4	Aqueous Brine	-48.5	-7.1	-4.8	-7.1			d							Pit Cantung			
Apilite (11)	5	Aqueous Brine	-38.2	-5.4	-3.8	-5.4		310.5	18.0 h	0.7930				8.38		Pit Cantung			
Apilite (11)	2	Aqueous Brine	-37.5	-4.2	-3.7	-4.2		333.5	32.0 h	0.7250				6.67		Pit Cantung			
Apilite (11)	6	Aqueous Brine	-39.9	-3.7	-3.9	-3.7			d							Pit Cantung			
Apilite (12)	2	Aqueous Brine	-45.6	-7.5	-4.5	-7.5		309.4	36.2 h	0.6300				11.10		Pit Cantung			
Apilite (12)	8	Aqueous Brine	-32.3	-6.1	-3.2	-6.1		328.1	39.0 h	0.7760				9.32		Pit Cantung			
Apilite (12)	10	Aqueous Brine	-37.8	-4.6	-3.7	-4.6			d							Pit Cantung			
Apilite (12)	6	Aqueous Brine	-41.1	-4.4	-4.1	-4.4		341.7	29.0 h	0.7130				6.96		Pit Cantung			

Sample	Inclusion # (mineral if not quartz)	Fluid Inclusion Type	T <sub>1</sub> (°C)	T <sub>m,coz</sub> (°C)	T <sub>e</sub> (°C)	T <sub>m</sub> (°C)	T <sub>m,deh</sub> (°C)	T <sub>h</sub> (°C)	Vapor % Homogenization (h) or Decrepitated (d)	Density (g/cm <sup>3</sup> )	XCO <sub>2</sub> XCH <sub>4</sub> XH <sub>2</sub> O (wt% equiv. NaCl)	Salinity	XCO <sub>2</sub> +XCH <sub>4</sub> Location	XCO <sub>2</sub> XCH <sub>4</sub> Density (g/cm <sup>3</sup> )
Apile II (2)	5	Aqueous Brine	-95.9	-62.1	-49.7	-4.2	5.6	356.5	40.0 h	0.6760		6.87	Pit Cantung	
Apile II (2)	4	H <sub>2</sub> O-CO <sub>2</sub> -NaCl±CH <sub>4</sub>	-89.5	-58.4			10.3	339.4	40.0 h				Pit Cantung	
Apile II (2)	9	H <sub>2</sub> O-CO <sub>2</sub> -NaCl±CH <sub>4</sub>	-99.8	-56.1	3.6		8.4	311.1	42.7 h	0.9640	0.202 0.011 0.776	4.12	Pit Cantung	0.947 0.053 0.855
Apile II (2)	3	H <sub>2</sub> O-CO <sub>2</sub> -NaCl±CH <sub>4</sub>											Pit Cantung	
Cantung Pit Vein 2(1)	1	Aqueous Brine			-33.8	-4.2			d				Pit Cantung	
Cantung Pit Vein 2(1)	5	Aqueous Brine			-38.4	-4.1			d	0.5970			Pit Cantung	
Cantung Pit Vein 2(1)	2	Aqueous Brine			-36.2	-3.2		376.6	41.0 h	0.5850			Pit Cantung	
Cantung Pit Vein 2(1)	8	Aqueous Brine			-45.3	-3.1		379.8	21.0 h	0.5840			Pit Cantung	
Cantung Pit Vein 2(1)	4	Aqueous Brine			-43.3	-2.6		381.2	42.7 h				Pit Cantung	
Cantung Pit Vein 2(1)	6	Aqueous Brine			-38.7	-2.4			d				Pit Cantung	
Cantung Pit Vein 2(1)	9	H <sub>2</sub> O-CO <sub>2</sub> -NaCl±CH <sub>4</sub>	-93.7	-58.1	-11.1		9.6	299.3	52.0 d	0.9390	0.279 0.021 0.717	8.52	0.300 Pit Cantung	0.929 0.071 0.908
Cantung Pit Vein 2(2)	2	Aqueous Brine			-29.9	-5.5			d	0.6080			Pit Cantung	
Cantung Pit Vein 2(2)	5	Aqueous Brine	-91.5	-59.9	-47.3	-2.4	12.3	360.2	43.0 d			3.92	Pit Cantung	
Cantung Pit Vein 2(2)	4	H <sub>2</sub> O-CO <sub>2</sub> -NaCl±CH <sub>4</sub>	-90.9	-56.3			7.3		d				Pit Cantung	
Cantung Pit Vein 2(2)	1	H <sub>2</sub> O-CO <sub>2</sub> -NaCl±CH <sub>4</sub>					8.3		d				Pit Cantung	
Cantung Pit Vein 7 (1)	7	Aqueous Brine			-24.1				d				Pit Cantung	
Cantung Pit Vein 7 (1)	4	Aqueous Brine			-27.1			9.3					Pit Cantung	
Cantung Pit Vein 7 (1)	8	Aqueous Brine			-23.2			9.8	294.6	7.0 h			Pit Cantung	
Cantung Pit Vein 7 (1)	2	Aqueous Brine			-27.2			9.9	202.7	4.5 h			Pit Cantung	
Cantung Pit Vein 7 (1)	5	Aqueous Brine			-25.1			10.9	220.5	9.0 h			Pit Cantung	
Cantung Pit Vein 7 (1)	3	Aqueous Brine			-32.1			12.6		d			Pit Cantung	
Cantung Pit Vein 7 (1)	10	H <sub>2</sub> O-CO <sub>2</sub> -NaCl±CH <sub>4</sub>	-108.7	-60.7	-8.8		13.1		d				Pit Cantung	
Cantung Pit Vein 7 (1)	1	H <sub>2</sub> O-CO <sub>2</sub> -NaCl±CH <sub>4</sub>	-114.9	-59.7	-3.4		11.9	269.2	50.0 d				Pit Cantung	
Cantung Pit Vein 7 (1)	9	H <sub>2</sub> O-CO <sub>2</sub> -NaCl±CH <sub>4</sub>	-104.6	-57.1	-2.9		7.6		d	0.7690			Pit Cantung	
Cantung Pit Vein 7 (2)	2	Aqueous Brine			-29.2	-4.5		8.2	313.9	10.0 d			Pit Cantung	
Cantung Pit Vein 7 (2)	7	Aqueous Brine					9.2	208.7	9.5 h			7.11	Pit Cantung	
Cantung Pit Vein 7 (2)	2	H <sub>2</sub> O-CO <sub>2</sub> -NaCl±CH <sub>4</sub>	-94.6	-60.4			14.4	272.4	14.0 d				Pit Cantung	
Cantung Pit Vein 7 (2)	4	H <sub>2</sub> O-CO <sub>2</sub> -NaCl±CH <sub>4</sub>	-103.3	-59.9			18.3	262.7	25.0 d				Pit Cantung	
Cantung Pit Vein 7 (2)	6	H <sub>2</sub> O-CO <sub>2</sub> -NaCl±CH <sub>4</sub>	-97.6	-59.8			16.3	257.2	12.7 d				Pit Cantung	
Cantung Pit Vein 7 (3)	7	Aqueous Brine			-23.9		5.1		d				Pit Cantung	
Cantung Pit Vein 7 (3)	8	H <sub>2</sub> O-CO <sub>2</sub> -NaCl±CH <sub>4</sub>	-110.3	-83.5	-86.4		16.5		d			0.048 0.952 0.282	Pit Cantung	
Cantung Pit Vein 7 (3)	3	H <sub>2</sub> O-CO <sub>2</sub> -NaCl±CH <sub>4</sub>	-107.1	-63.5	-19.4		15.1	326.8	11.5 d				Pit Cantung	
Cantung Pit Vein 7 (3)	4	H <sub>2</sub> O-CO <sub>2</sub> -NaCl±CH <sub>4</sub>	-106.4	-62.2			250.3	16.0 d	d				Pit Cantung	
Cantung Pit Vein 7 (3)	3	H <sub>2</sub> O-CO <sub>2</sub> -NaCl±CH <sub>4</sub>	-101.8	-61.9	-9.2		12.8		d				Pit Cantung	
Cantung Pit Vein 7 (3)	1	H <sub>2</sub> O-CO <sub>2</sub> -NaCl±CH <sub>4</sub>	-106.4	-59.7	8.3		15.1	304.7	21.5 d				Pit Cantung	
Cantung Pit Vein 7 (3)	6	H <sub>2</sub> O-CO <sub>2</sub> -NaCl±CH <sub>4</sub>	-102.8	-58.3	-41.6		14.5		d				Pit Cantung	
HF03-05(1)	3	H <sub>2</sub> O-CO <sub>2</sub> -NaCl±CH <sub>4</sub>	-89.7	-63.4			13.6		d				Pit Cantung	
HF03-05(1)	2	H <sub>2</sub> O-CO <sub>2</sub> -NaCl±CH <sub>4</sub>	-100.1	-62.5	1.2		13.1	248.1	d				Underground Cantung	
HF03-05(1)	1	H <sub>2</sub> O-CO <sub>2</sub> -NaCl±CH <sub>4</sub>	-101.6	-61.9	1.1		13.2	289.1	d				Underground Cantung	
HF03-05(1)	4	H <sub>2</sub> O-CO <sub>2</sub> -NaCl±CH <sub>4</sub>	-90.1	-61.1			12.2		d				Underground Cantung	
HF03-05(1)	5	H <sub>2</sub> O-CO <sub>2</sub> -NaCl±CH <sub>4</sub>	-100.1	-60.8	-0.6		14.1		d				Underground Cantung	
HF03-05(2)	3	H <sub>2</sub> O-CO <sub>2</sub> -NaCl±CH <sub>4</sub>	-96.7	-61.8			14.9		d				Underground Cantung	
HF03-05(2)	2	H <sub>2</sub> O-CO <sub>2</sub> -NaCl±CH <sub>4</sub>	-96.7	-59.2			10.9	236.5	h				Underground Cantung	
HF03-05(2)	1	H <sub>2</sub> O-CO <sub>2</sub> -NaCl±CH <sub>4</sub>	-110.2	-58.9	0.1		12.4	275.1	d				Underground Cantung	
HF03-05(3)	1	Aqueous Brine			-35.3	-3.6		204.5	h	0.9080			Underground Cantung	5.78
HF03-05(3)	4	Aqueous Brine			-30.2	-2.8		242.8	h	0.8600			Underground Cantung	5.47
HF03-05(3)	8	Aqueous Brine			-30.2	-2.8		200.2	h	0.9030			Underground Cantung	4.55
HF03-05(3)	6	Aqueous Brine			-24.4	-2.8		222.1	h	0.8780			Underground Cantung	4.55
HF03-05(3)	10	Aqueous Brine			-24.2	-2.8		269.2	h	0.8000			Underground Cantung	3.60
HF03-05(3)	3	Aqueous Brine			-26.4	-2.2		212.5	h	0.8770			Underground Cantung	3.12
HF03-05(3)	2	Aqueous Brine			-28.2	-1.9		12.9	277.3	h			Underground Cantung	
HF03-05(3)	9	H <sub>2</sub> O-CO <sub>2</sub> -NaCl±CH <sub>4</sub>	-105.5	-56.7			12.2	327.6	d				Underground Cantung	
HF03-05(4)	2	H <sub>2</sub> O-CO <sub>2</sub> -NaCl±CH <sub>4</sub>	-98.2	-60.4										

Sample (Chip)	Inclusion # (mineral if not quartz)	Fluid Inclusion Type	T <sub>co2</sub> (°C)	T <sub>m,co2</sub> (°C)	T <sub>co2</sub> (°C)	T <sub>e</sub> (°C)	T <sub>m</sub> (°C)	T <sub>m,adm</sub> (°C)	T <sub>h</sub> (°C)	Vapor % Disreptiated (d)	Density (g/cm <sup>3</sup> )	XCO <sub>2</sub>	XCH <sub>4</sub>	XH <sub>2</sub> O (wt% equiv. NaCl)	Salinity	XCO <sub>2</sub> +XCH <sub>4</sub>	Location	XCO <sub>2</sub>	XCH <sub>4</sub>	Density (g/cm <sup>3</sup> )			
HF03-05(4)	1	H <sub>2</sub> O-CO <sub>2</sub> -NaCl±CH <sub>4</sub>	-98.2	-59.7	0.1		11.8	281.2	d								Underground Cantung						
HF03-05(4)	5	H <sub>2</sub> O-CO <sub>2</sub> -NaCl±CH <sub>4</sub>	-91.9	-59.6			11.4		d								Underground Cantung						
HF03-05(4)	3	H <sub>2</sub> O-CO <sub>2</sub> -NaCl±CH <sub>4</sub>	-111.7	-59.5			10.7	318.7	h								Underground Cantung						
HF03-05(4)	4	H <sub>2</sub> O-CO <sub>2</sub> -NaCl±CH <sub>4</sub>	-106.3	-59.3	-1.1		10.9		d								Underground Cantung						
HF03-05(5)	1	Aqueous Brine				-39.3	-3.5			d							Underground Cantung						
HF03-05(5)	7	Aqueous Brine				-39.9	-4.9			d							Underground Cantung						
HF03-05(5)	2	Aqueous Brine				-38.1	-4.2			d							Underground Cantung						
HF03-05(5)	5	H <sub>2</sub> O-CO <sub>2</sub> -NaCl±CH <sub>4</sub>	-89.3	-61.3			7.9	334.8	13.0								Underground Cantung						
HF03-05(5)	9	H <sub>2</sub> O-CO <sub>2</sub> -NaCl±CH <sub>4</sub>	-91.1	-60.4	17.2		13.4	201.6	18.0								Underground Cantung						
HF03-05(5)	10	H <sub>2</sub> O-CO <sub>2</sub> -NaCl±CH <sub>4</sub>	-96.1	-60.2	3.4		11.6		d								Underground Cantung						
HF03-05(5)	3	H <sub>2</sub> O-CO <sub>2</sub> -NaCl±CH <sub>4</sub>	-87.7	-59.6			9.5	288.8	28.0								Underground Cantung						
HF03-05(5)	4	H <sub>2</sub> O-CO <sub>2</sub> -NaCl±CH <sub>4</sub>	-87.4	-59.4			11.7	297.8	49.0								Underground Cantung						
HF03-05(5)	8	H <sub>2</sub> O-CO <sub>2</sub> -NaCl±CH <sub>4</sub>	-95.2	-58.2			9.8	282.8	17.7	d							Underground Cantung						
HF03-05(5)	6	H <sub>2</sub> O-CO <sub>2</sub> -NaCl±CH <sub>4</sub>					10.2		d								Underground Cantung						
HF03-10(1)	2	Aqueous Brine				-23.1	-4.8			d							Pit Cantung						
HF03-10(1)	8	Aqueous Brine				-22.4	-4.8			d							Pit Cantung						
HF03-10(1)	9	Aqueous Brine				-24.9	-3.8		264.4	4.5	h				6.08		Pit Cantung						
HF03-10(1)	7	Aqueous Brine				-21.7	-3.8			d							Pit Cantung						
HF03-10(1)	3	Aqueous Brine					-3.1			d							Pit Cantung						
HF03-10(1)	6	Aqueous Brine				-25.2	-1.9			d							Pit Cantung						
HF03-10(1)	5	Aqueous Brine					-1.9			d							Pit Cantung						
HF03-10(1)	4	Aqueous Brine				-21.8	-1.4		263.9	29.0	h				2.31		Pit Cantung						
HF03-10(2)	6	(scheelite)					-6.9			d							Pit Cantung						
HF03-10(2)	3	(scheelite)				-22.9	-6.2		204.1	6.5	h				9.45		Pit Cantung						
HF03-10(2)	5	(scheelite)				-22.9	-5.4		285.1	4.0	h				8.38		Pit Cantung						
HF03-10(2)	7	(scheelite)					-3.2			d							Pit Cantung						
HF03-10(2)	4	(scheelite)	-87.2	-57.9	26.4		7.5	311.2	50.0	h					4.80	0.180	Pit Cantung			0.950	0.050	0.517	
HF03-10(2)	2	(scheelite)	-81.1	-57.3	26.7		5.5	314.3	38.2	h					8.19	0.132	Pit Cantung			0.971	0.029	0.638	
HF03-10(2)	1	(scheelite)	-85.2	-57.1	26.6		5.5	308.5	43.0	h					8.19	0.169	Pit Cantung			0.975	0.025	0.643	
HF03-10(3)	3	(scheelite)	-91.8	-57.8	26.6		6.8	185.4	41.0	d					6.03	0.122	Pit Cantung			0.948	0.052	0.470	
HF03-10(3)	1	(scheelite)	-99.9	-57.6	24.5		6.7			d							Pit Cantung						
HF03-10(3)	2	(scheelite)	-85.5	-57.4	24.1		5.8	288.9	16.4						7.70	0.052	Pit Cantung			0.965	0.035	0.663	
HF03-10(3)	5	(scheelite)	-83.5	-57.3	25.6		6.1	286.2	22.0	d					7.21	0.073	Pit Cantung			0.971	0.029	0.666	
HF03-10(3)	4	(scheelite)	-97.8	-57.3	27.6		6.1	322.1	36.0						7.21	0.106	Pit Cantung			0.967	0.033	0.501	
HF03-10(3)	6	(scheelite)	-91.9	-57.3	27.2		6.4			d							Pit Cantung						
HF03-10(3)	7	(scheelite)	-89.8	-57.1	27.7		6.0			d							Pit Cantung						
HF03-14(1)	11	Aqueous Brine				-33.9	-2.4		230.1	4.0	h				3.92		Pit Cantung						
HF03-14(1)	1	Aqueous Brine					-1.3		285.3	15.0	h				2.14		Pit Cantung						
HF03-14(1)	2	Aqueous Brine					-1.0		311.1	12.0	h				1.65		Pit Cantung						
HF03-14(1)	7	H <sub>2</sub> O-CO <sub>2</sub> -NaCl±CH <sub>4</sub>	-106.3	-63.6	20.5					d							Pit Cantung						
HF03-14(1)	4	H <sub>2</sub> O-CO <sub>2</sub> -NaCl±CH <sub>4</sub>	-99.4	-60.3	-19.5		10.1	353.3	55.0	h							Pit Cantung						
HF03-14(1)	5	H <sub>2</sub> O-CO <sub>2</sub> -NaCl±CH <sub>4</sub>	-104.3	-58.8			10.4	338.7	22.0	d							Pit Cantung						
HF03-14(1)	6	H <sub>2</sub> O-CO <sub>2</sub> -NaCl±CH <sub>4</sub>	-102.2	-58.1	21.3					d							Pit Cantung						
HF03-14(1)	10	H <sub>2</sub> O-CO <sub>2</sub> -NaCl±CH <sub>4</sub>	-100.8	-57.8			10.9			d							Pit Cantung						
HF03-14(1)	3	H <sub>2</sub> O-CO <sub>2</sub> -NaCl±CH <sub>4</sub>	-100.7	-66.7			13.2			d							Pit Cantung						
HF03-15(1)	4	Aqueous Brine				-23.2	-5.2			d							Pit Cantung						
HF03-15(1)	2	H <sub>2</sub> O-CO <sub>2</sub> -NaCl±CH <sub>4</sub>	-81.7	-61.6	12.9		8.9			d							Pit Cantung						
HF03-15(1)	3	H <sub>2</sub> O-CO <sub>2</sub> -NaCl±CH <sub>4</sub>	-81.6	-61.4	5.2		9.3	295.4	6.5	h					2.11	0.019	Pit Cantung			0.768	0.212	0.604	
HF03-15(1)	5	H <sub>2</sub> O-CO <sub>2</sub> -NaCl±CH <sub>4</sub>	-85.8	-60.9	13.3		8.6	222.1	10.5	h					2.77	0.031	Pit Cantung			0.848	0.152	0.583	
HF03-15(1)	1	H <sub>2</sub> O-CO <sub>2</sub> -NaCl±CH <sub>4</sub>	-88.7	-60.5	6.8		9.3			d							Pit Cantung						
HF03-15(1)	8	H <sub>2</sub> O-CO <sub>2</sub> -NaCl±CH <sub>4</sub>	-82.2	-59.9	8.6		8.1			d							Pit Cantung						
HF03-15(1)	7	H <sub>2</sub> O-CO <sub>2</sub> -NaCl±CH <sub>4</sub>	-84.1	-59.9	10.2		8.9	259.9	41.0	h					2.20	0.179	Pit Cantung			0.873	0.127	0.699	

Sample (Chip)	Inclusion # (mineral if not quartz)	Fluid inclusion Type	T <sub>1</sub> (°C)	T <sub>2</sub> (°C)	T <sub>3</sub> (°C)	T <sub>hom</sub> (°C)	T <sub>m</sub> (°C)	T <sub>m</sub> (°C)	T <sub>h</sub> (°C)	Vapor % Homogenization (h) or Decapitated (d)	Density (g/cm <sup>3</sup> )	XCO <sub>2</sub>	XCH <sub>4</sub>	XH <sub>2</sub> O	Salinity (wt% equiv NaCl)	XCO <sub>2</sub> +XCH <sub>4</sub>	Location	XCO <sub>2</sub>	XCH <sub>4</sub>	Density (g/cm <sup>3</sup> )
HF03-15(1)	6	H <sub>2</sub> O-CO <sub>2</sub> -NaCl±CH <sub>4</sub>	-819	-57.3	1.2	8.2	322.2	10.5	d	10.5	1.0160	0.041	0.001	0.943	4.80	0.042	Pit/Cantung	0.981	0.019	0.887
HF03-16(1)	8	Aqueous Brine	-22.1	-6.5			322.6	17.7	h		0.7930				9.84		Pit/Cantung			
HF03-16(1)	4	Aqueous Brine	-29.5	-5.3					d								Pit/Cantung			
HF03-16(1)	6	Aqueous Brine	-25.7	-4.6					d								Pit/Cantung			
HF03-16(1)	5	Aqueous Brine	-24.2	-2.6					d								Pit/Cantung			
HF03-16(1)	3	Aqueous Brine	-24.4	-2.4			308.2	10.5	h		0.7320				3.92		Pit/Cantung			
HF03-16(1)	7	Aqueous Brine	-24.3	-2.4			204.7	9.0	d		0.8930				3.92		Pit/Cantung			
HF03-16(1)	2	H <sub>2</sub> O-CO <sub>2</sub> -NaCl±CH <sub>4</sub>	-91.1	-56.9			9.8	308.4	36.2	d							Pit/Cantung			
HF03-16(1)	1	H <sub>2</sub> O-CO <sub>2</sub> -NaCl±CH <sub>4</sub>	-83.2	-67.9			13.4	257.3	36.2	d							Pit/Cantung			
HF03-16(2)	2	Aqueous Brine	-26.2	-5.6					d								Pit/Cantung			
HF03-16(2)	3	Aqueous Brine	-26.2	-4.6			288.8	2.5	h		0.8130				7.25		Pit/Cantung			
HF03-16(2)	8	Aqueous Brine	-28.1	-3.4					d								Pit/Cantung			
HF03-16(2)	6	Aqueous Brine	-24.1	-3.2					d								Pit/Cantung			
HF03-16(2)	5	H <sub>2</sub> O-CO <sub>2</sub> -NaCl±CH <sub>4</sub>	-89.6	-59.6	11.7	8.2			d								Pit/Cantung			
HF03-16(2)	1	H <sub>2</sub> O-CO <sub>2</sub> -NaCl±CH <sub>4</sub>	-80.6	-59.3	-6.2	9.7	324.2	12.5	d		1.0020	0.046	0.005	0.940	3.15	0.051	Pit/Cantung	0.906	0.094	0.856
HF03-16(2)	4	H <sub>2</sub> O-CO <sub>2</sub> -NaCl±CH <sub>4</sub>	-82.9	-58.1	2.2	8.2			d								Pit/Cantung			
HF03-17(1)	7	H <sub>2</sub> O-CO <sub>2</sub> -NaCl±CH <sub>4</sub>	-82.2	-57.6			8.8		d								Pit/Cantung			
HF03-17(1)	10	Aqueous Brine	-88.1	-61.1	11.6	11.6	353.1	40.0	h								Pit/Cantung			
HF03-17(1)	11	H <sub>2</sub> O-CO <sub>2</sub> -NaCl±CH <sub>4</sub>	-86.8	-60.8	-0.4				d								Pit/Cantung			
HF03-17(1)	9	H <sub>2</sub> O-CO <sub>2</sub> -NaCl±CH <sub>4</sub>	-91.2	-60.3	5.1	5.1	354.9	11.5	h		1.0000	0.035	0.006	0.945	4.51	0.041	Pit/Cantung	0.863	0.137	0.730
HF03-17(1)	6 (scheelite)	H <sub>2</sub> O-CO <sub>2</sub> -NaCl±CH <sub>4</sub>	-80.7	-57.5	20.6	6.4			d								Pit/Cantung			
HF03-17(1)	2 (scheelite)	H <sub>2</sub> O-CO <sub>2</sub> -NaCl±CH <sub>4</sub>	-89.9	-57.5	24.6	6.9	277.9	53.0	h		0.8340	0.224	0.009	0.753	5.86	0.233	Pit/Cantung	0.863	0.037	0.639
HF03-17(1)	1 (scheelite)	H <sub>2</sub> O-CO <sub>2</sub> -NaCl±CH <sub>4</sub>	-92.2	-57.5	23.9	7.4	289.4	33.0	h		0.9110	0.116	0.004	0.866	4.98	0.120	Pit/Cantung	0.965	0.035	0.656
HF03-17(1)	7 (scheelite)	H <sub>2</sub> O-CO <sub>2</sub> -NaCl±CH <sub>4</sub>	-79.5	-57.4	23.2	6.6	282.1	52.0	h		0.8530	0.225	0.008	0.752	6.37	0.233	Pit/Cantung	0.867	0.033	0.666
HF03-17(1)	4 (scheelite)	H <sub>2</sub> O-CO <sub>2</sub> -NaCl±CH <sub>4</sub>	-76.2	-57.1	25.4	6.2	274.8	23.2	h		0.9600	0.076	0.002	0.901	7.04	0.078	Pit/Cantung	0.975	0.025	0.669
HF03-17(1)	3 (scheelite)	H <sub>2</sub> O-CO <sub>2</sub> -NaCl±CH <sub>4</sub>	-86.2	-56.7	25.7	6.5	274.8	39.0	h		0.9070	0.154	0.001	0.827	6.54	0.155	Pit/Cantung	0.992	0.008	0.683
HF03-17(2)	1	Aqueous Brine	-25.9	-5.6			357.4		d		0.7100				8.65		Pit/Cantung			
HF03-17(2)	3	Aqueous Brine	-22.6	-2.6					d								Pit/Cantung			
HF03-17(2)	2	Aqueous Brine	-23.1	-2.2					d								Pit/Cantung			
HF03-17(2)	5 (scheelite)	Aqueous Brine	-28.8	-1.9					d								Pit/Cantung			
HF03-17(2)	4	Aqueous Brine	-23.3	-1.8					d								Pit/Cantung			
HF03-17(2)	7 (scheelite)	H <sub>2</sub> O-CO <sub>2</sub> -NaCl±CH <sub>4</sub>	-79.6	-61.9	1.1	11.7			d		0.7080				2.96		Pit/Cantung			
HF03-17(3)	3	Aqueous Brine	-45.1	-6.1			202.4	10.0	h		0.9370				9.32		Pit/Cantung			
HF03-17(3)	5 (scheelite)	Aqueous Brine	-38.9	-5.5			305.1	67.0	h		0.8030				8.51		Pit/Cantung			
HF03-17(3)	2 (scheelite)	Aqueous Brine	-45.1	-4.6					d								Pit/Cantung			
HF03-17(3)	4	H <sub>2</sub> O-CO <sub>2</sub> -NaCl±CH <sub>4</sub>	-80.7	-59.8			7.8		d								Pit/Cantung			
HF03-17(3)	1	H <sub>2</sub> O-CO <sub>2</sub> -NaCl±CH <sub>4</sub>	-82.6	-59.8	9.9	7.9	325.3	23.2	d		0.9660	0.078	0.010	0.900	4.07	0.088	Pit/Cantung	0.882	0.118	0.719
HF03-17(5)	4 (scheelite)	Aqueous Brine	-88.8	-59.2	11.9	7.6	284.6	8.2	h		0.8100				6.52		Pit/Cantung			
HF03-17(5)	6 (scheelite)	H <sub>2</sub> O-CO <sub>2</sub> -NaCl±CH <sub>4</sub>	-84.7	-58.8	9.7	12.1	301.8	39.0	h		0.9790	0.062	0.007	0.917	4.62	0.069	Pit/Cantung	0.895	0.105	0.718
HF03-17(5)	3 (scheelite)	H <sub>2</sub> O-CO <sub>2</sub> -NaCl±CH <sub>4</sub>	-89.4	-58.2			10.2		d								Pit/Cantung			
HF03-17(5)	5 (scheelite)	H <sub>2</sub> O-CO <sub>2</sub> -NaCl±CH <sub>4</sub>	-86.7	-57.7	15.6	9.7	291.8	30.0	h		0.8320	0.117	0.004	0.877	0.63	0.121	Pit/Cantung	0.865	0.035	0.764
HF03-17(5)	2 (scheelite)	H <sub>2</sub> O-CO <sub>2</sub> -NaCl±CH <sub>4</sub>	-89.6	-57.2			7.2		d								Pit/Cantung			
HF03-17(6)	1 (scheelite)	H <sub>2</sub> O-CO <sub>2</sub> -NaCl±CH <sub>4</sub>	-86.3	-58.9	9.2	9.4	233.1	45.0	d		0.9190	0.184	0.017	0.795	1.36	0.201	Pit/Cantung	0.915	0.085	0.767
HF03-17(6)	2 (scheelite)	H <sub>2</sub> O-CO <sub>2</sub> -NaCl±CH <sub>4</sub>	-89.8	-58.1	9.6	9.3			d								Pit/Cantung			
HF03-18(1)	7	Aqueous Brine	-27.1	-4.9			248.4	37.0	d		0.8740				7.68		Pit/Cantung			
HF03-18(1)	5	Aqueous Brine	-23.9	-3.2			202.9	6.0	h		0.8950				4.23		Pit/Cantung			
HF03-18(1)	3	Aqueous Brine	-23.2	-3.2					d								Pit/Cantung			
HF03-18(1)	4	Aqueous Brine	-21.7	-2.6			228.4	17.7	h		0.8670				4.23		Pit/Cantung			
HF03-18(1)	6	H <sub>2</sub> O-CO <sub>2</sub> -NaCl±CH <sub>4</sub>	-87.4	-58.1	-39.2	9.1	256.6	26.5	d								Pit/Cantung			
HF03-18(2)	1 (scheelite)	Aqueous Brine	-25.9	-2.8					d		0.9290				3.92		Pit/Cantung			
HF03-18(2)	2 (scheelite)	Aqueous Brine	-23.1	-2.4			169.8	31.0	d								Pit/Cantung			



Sample (Chip)	Inclusion # (mineral if not quartz)	Fluid Inclusion Type	T <sub>m,co2</sub> (°C)	T <sub>m,co2</sub> (°C)	T <sub>e,co2</sub> (°C)	T <sub>m</sub> (°C)	T <sub>m,depl</sub> (°C)	T <sub>h</sub> (°C)	Vapor % Homogenization (h) or Depleted (d)	Density (g/cm <sup>3</sup> )	XCO <sub>2</sub>	XCH <sub>4</sub>	XH <sub>2</sub> O (wt% equiv. NaCl)	Salinity	XCO <sub>2</sub> +XCH <sub>4</sub>	Location	XCO <sub>2</sub>	XCH <sub>4</sub>	Density (g/cm <sup>3</sup> )
HF03-19-1(1)	3	Aqueous Brine	-39.2	-7.6	-39.2	366.3			h	0.7370			11.22			Pit Cantung			
HF03-19-1(1)	2	Aqueous Brine	-30.9	-3.9	-48.2	272.7			d	0.8130			5.17			Pit Cantung			
HF03-19-1(1)	4	Aqueous Brine	-48.2	-3.2	-29.9	312.9			d	0.8800			5.01			Pit Cantung			
HF03-19-1(1)	6	Aqueous Brine	-29.9	-3.1	-26.6	312.9			h	0.6930			2.14			Pit Cantung			
HF03-19-1(1)	5	Aqueous Brine	-26.6	-1.3		13.3			h							Pit Cantung			
HF03-19-1(1)	1	H <sub>2</sub> O-CO <sub>2</sub> -NaCl±CH <sub>4</sub>	-97.4	-61.1					d							Pit Cantung			
HF03-19-2(1)	3	Aqueous Brine	-48.7	-4.5					d	0.8560			5.78			Pit Cantung			
HF03-19-2(1)	4	Aqueous Brine	-28.8	-3.6	-37.3	247.9			23.0 h	0.8440			3.60			Pit Cantung			
HF03-19-2(1)	7	Aqueous Brine	-37.3	-2.2		240.3			28.0 h							Pit Cantung			
HF03-19-2(1)	1	H <sub>2</sub> O-CO <sub>2</sub> -NaCl±CH <sub>4</sub>	-90.5	-58.7	18.9	7.1			d	1.0230	0.050	0.000	0.922	8.86	0.050	Pit Cantung	0.992	0.008	0.792
HF03-19-2(1)	2	H <sub>2</sub> O-CO <sub>2</sub> -NaCl±CH <sub>4</sub>	-90.7	-57.8	17.1	5.2	290.8	14.0 h	d	0.5180			4.70			Pit Cantung			
HF03-20(1)	5	Aqueous Brine			-21.6	-2.9			h							Pit Cantung			
HF03-20(1)	6	H <sub>2</sub> O-CO <sub>2</sub> -NaCl±CH <sub>4</sub>	-97.5	-61.1		15.5	400.1		d							Pit Cantung			
HF03-20(1)	4	H <sub>2</sub> O-CO <sub>2</sub> -NaCl±CH <sub>4</sub>	-99.5	-60.4		10.3	375.1		d							Pit Cantung			
HF03-20(1)	1	H <sub>2</sub> O-CO <sub>2</sub> -NaCl±CH <sub>4</sub>	-100.2		-83.2	16.6	329.8		h							Pit Cantung			
HF03-20(2)	4	H <sub>2</sub> O-CO <sub>2</sub> -NaCl±CH <sub>4</sub>	-101.1	-63.8		2.1			d							Pit Cantung			
HF03-20(2)	5	H <sub>2</sub> O-CO <sub>2</sub> -NaCl±CH <sub>4</sub>	-99.8	-61.9		12.7			d							Pit Cantung			
HF03-20(2)	2	H <sub>2</sub> O-CO <sub>2</sub> -NaCl±CH <sub>4</sub>	-95.5	-61.4		13.4	388.5		d							Pit Cantung			
HF03-20(2)	1	H <sub>2</sub> O-CO <sub>2</sub> -NaCl±CH <sub>4</sub>	-96.9	-60.9		10.4	329.5		d							Pit Cantung			
HF03-20(2)	3	H <sub>2</sub> O-CO <sub>2</sub> -NaCl±CH <sub>4</sub>	-95.1	-60.1		10.4	383.8		h							Pit Cantung			
HF03-20(2)	6	H <sub>2</sub> O-CO <sub>2</sub> -NaCl±CH <sub>4</sub>	-96.9	-58.5		10.5	382.9		h							Pit Cantung			
HF03-20(3)	7	H <sub>2</sub> O-CO <sub>2</sub> -NaCl±CH <sub>4</sub>	-98.5	-57.7		13.8			d							Pit Cantung			
HF03-20(3)	4	Aqueous Brine			-21.5	-1.8			d							Pit Cantung			
HF03-20(3)	6	Aqueous Brine				12.9	354.1		d							Pit Cantung			
HF03-20(3)	7	H <sub>2</sub> O-CO <sub>2</sub> -NaCl±CH <sub>4</sub>	-106.1	-62.5		14.6			h							Pit Cantung			
HF03-20(3)	9	H <sub>2</sub> O-CO <sub>2</sub> -NaCl±CH <sub>4</sub>	-113.4	-61.1		12.6	376.8		d							Pit Cantung			
HF03-20(3)	2	H <sub>2</sub> O-CO <sub>2</sub> -NaCl±CH <sub>4</sub>	-101.9	-59.1		15.3	352.6		d							Pit Cantung			
HF03-20(3)	3	H <sub>2</sub> O-CO <sub>2</sub> -NaCl±CH <sub>4</sub>	-114.4	-58.4		4.9	305.6		d							Pit Cantung			
HF03-20(3)	1	H <sub>2</sub> O-CO <sub>2</sub> -NaCl±CH <sub>4</sub>	-91.4	-57.6		16.2			d							Pit Cantung			
HF03-20(3)	8	H <sub>2</sub> O-CO <sub>2</sub> -NaCl±CH <sub>4</sub>	-118.5		-81.4				d							Pit Cantung			
HF03-23(1)	3	Aqueous Brine	-38.2	-6.8		297.6			d	0.8360			10.23			Pit Cantung			
HF03-23(1)	5	Aqueous Brine	-38.6	-4.8		270.1			23.2 h	0.8440			7.54			Pit Cantung			
HF03-23(1)	2	Aqueous Brine	-39.2	-3.9		325.8			5.0 h	0.7340			6.23			Pit Cantung			
HF03-23(1)	4	Aqueous Brine	-36.8	-3.7					23.2 h							Pit Cantung			
HF03-23(1)	6	Aqueous Brine	-28.9	-2.6					d							Pit Cantung			
HF03-23(1)	7	Aqueous Brine	-38.5	-2.5					d							Pit Cantung			
HF03-23(1)	1	H <sub>2</sub> O-CO <sub>2</sub> -NaCl±CH <sub>4</sub>	-100.5	-64.1		12.3	318.2		d	0.7640			7.35			Pit Cantung			
HF03-23(2)	3	Aqueous Brine	-24.6	-4.6		311.2			17.7 h	0.7520			5.62			Pit Cantung			
HF03-23(2)	2	Aqueous Brine	-36.7	-3.5		7.3	351.2		21.0 h							Pit Cantung			
HF03-23(2)	1	H <sub>2</sub> O-CO <sub>2</sub> -NaCl±CH <sub>4</sub>	-96.8	-59.1					60.0 h							Pit Cantung			
HF03-25(1)	8	Aqueous Brine	-28.4	-4.8					d							Pit Cantung			
HF03-25(1)	1	Aqueous Brine	-27.7	-4.8		289.5			d	0.8100			7.11			Pit Cantung			
HF03-25(1)	9	Aqueous Brine	-24.8	-4.5		325.9			28.3 h	0.7450			6.96			Pit Cantung			
HF03-25(1)	5	Aqueous Brine	-27.6	-4.4		345.4			39.0 h	0.8480			6.96			Pit Cantung			
HF03-25(1)	3	Aqueous Brine	-24.1	-4.4					12.7 h	0.6900			6.08			Pit Cantung			
HF03-25(1)	2	Aqueous Brine	-26.5	-3.8					40.0 h							Pit Cantung			
HF03-25(1)	6	Aqueous Brine	-28.1	-3.1					d	0.5240			4.07			Pit Cantung			
HF03-25(1)	7	Aqueous Brine	-22.9	-2.5		393.9			2.5 h	0.9310	0.183	0.012	0.805	0.44	0.195	Pit Cantung	0.940	0.060	0.809
HF03-25(1)	4	H <sub>2</sub> O-CO <sub>2</sub> -NaCl±CH <sub>4</sub>	-95.5	-58.4	7.7	9.9	279.4	41.0 h	d							Pit Cantung			
HF03-25(2)	6	Aqueous Brine	-22.1	-6.6					d							Pit Cantung			
HF03-25(2)	8	Aqueous Brine	-28.8	-5.4					d	0.6640			7.54			Pit Cantung			
HF03-25(2)	4	Aqueous Brine	-22.5	-4.9		369.1			d	0.7620			5.47			Pit Cantung			
HF03-25(2)	3	Aqueous Brine	-26.9	-4.8		304.9			12.0 h							Pit Cantung			
HF03-25(2)	7	Aqueous Brine	-23.1	-3.4					6.5 h							Pit Cantung			

Sample (Chip)	Inclusion # (mineral if not quartz)	Fluid Inclusion Type	T <sub>coz</sub> (°C)	T <sub>m,coz</sub> (°C)	T <sub>h,coz</sub> (°C)	T <sub>e</sub> (°C)	T <sub>m</sub> (°C)	T <sub>m,em</sub> (°C)	T <sub>h</sub> (°C)	Vapor % Homogenization (h) or Decriptated (d)	Density (g/cm <sup>3</sup> )	XCO <sub>2</sub>	XCH <sub>4</sub>	XH <sub>2</sub> O (wt% equiv. NaCl)	Salinity	XCO <sub>2</sub> +XCH <sub>4</sub>	Location	XCO <sub>2</sub>	XCH <sub>4</sub>	Density (g/cm <sup>3</sup> )
HF03-25(2)	1	H <sub>2</sub> O-CO <sub>2</sub> -NaCl±CH <sub>4</sub>	-88.1	-58.3	16.6	-24.7	-3.9	9.6	288.6	4.0	0.9300	0.163	0.010	0.824	0.83	0.173	Pit Cantung	0.940	0.080	0.733
HF03-25(2)	5	H <sub>2</sub> O-CO <sub>2</sub> -NaCl±CH <sub>4</sub>	-85.8	-58.1	17.8	-24.7	-3.9	8.7	319.3	18.0	0.9600	0.058	0.004	0.931	2.58	0.062	Pit Cantung	0.937	0.063	0.699
HF03-25(2)	2	H <sub>2</sub> O-CO <sub>2</sub> -NaCl±CH <sub>4</sub>	-95.2	-58.1	18.2	-24.7	-3.9	9.9	308.8	30.0	0.9020	0.100	0.009	0.891	0.22	0.108	Pit Cantung	0.919	0.081	0.655
HF03-26(1)	4	Aqueous Brine				-38.7	-3.7	203.9	317.7	20.0	0.7490			6.23		Pit Cantung				
HF03-26(1)	1	Aqueous Brine				-38.7	-3.7	317.7	20.0	10.0	0.9100			5.93		Pit Cantung				
HF03-26(2)	8	H <sub>2</sub> O-CO <sub>2</sub> -NaCl±CH <sub>4</sub>	-110.2	-96.4	-94.9	-23.5	-6.1	10.4	359.1	58.5	0.8100				9.32		Pit Cantung	0.058	0.942	0.312
HF03-26(2)	1	Aqueous Brine				-22.4	-5.3	307.8	39.0	d	0.7150			8.24		Pit Cantung				
HF03-26(2)	2	Aqueous Brine				-28.9	-4.8	351.8	12.5	d	0.5290			5.47		Pit Cantung				
HF03-26(2)	4	Aqueous Brine				-27.4	-3.4	403.9	10.0	d	0.6420			5.32		Pit Cantung				
HF03-26(2)	5	Aqueous Brine				-22.9	-3.3	359.8	58.0	d	0.3002					Pit Cantung				
HF03-26(2)	6	Aqueous Brine				-22.3	-2.1			h	0.2376					Pit Cantung				
HF03-26(2)	3	Aqueous Brine				-99.8				h	0.1215					Pit Cantung				
HF03-26(2)	9	Aqueous Brine				-85.5				h	0.8380					Pit Cantung				
HF03-26(2)	11	Aqueous Brine				-83.2				h						Pit Cantung				
HF03-27-1(1)	7	Aqueous Brine				-32.1	-3.4			d						Pit Cantung				
HF03-27-1(1)	5	Aqueous Brine				-26.2	-3.4		258.3	13.0					5.47		Pit Cantung			
HF03-27-1(1)	1	H <sub>2</sub> O-CO <sub>2</sub> -NaCl±CH <sub>4</sub>	-87.8	-61.6				13.9		d						Pit Cantung				
HF03-27-1(1)	4	H <sub>2</sub> O-CO <sub>2</sub> -NaCl±CH <sub>4</sub>	-91.6	-61.3				12.9		d						Pit Cantung				
HF03-27-1(1)	2	H <sub>2</sub> O-CO <sub>2</sub> -NaCl±CH <sub>4</sub>	-83.6	-60.9				13.7	184.7	55.0						Pit Cantung				
HF03-27-1(1)	6	H <sub>2</sub> O-CO <sub>2</sub> -NaCl±CH <sub>4</sub>	-99.4	-59.2	23.6	-44.2	-5.3	14.6	266.5	33.0						Pit Cantung				
HF03-27-2(3)	4 (scheelite)	Aqueous Brine				-45.7	-3.7		298.2	23.2	0.7800				5.93		Pit Cantung			
HF03-27-2(3)	2 (scheelite)	Aqueous Brine				-45.7	-3.7		359.3	43.0					8.24		Pit Cantung			
HF03-27-2(3)	1 (scheelite)	H <sub>2</sub> O-CO <sub>2</sub> -NaCl±CH <sub>4</sub>	-97.4	-59.3		-36.4	-5.3	8.1	329.1	15.0						Pit Cantung				
HF03-27-2(1)	3	Aqueous Brine				-28.6	-4.4		355.6	25.3					6.67		Pit Cantung			
HF03-27-2(1)	9	Aqueous Brine				-36.5	-3.8		289.3	29.0					6.08		Pit Cantung			
HF03-27-2(1)	6	Aqueous Brine				-25.6	-3.4		359.5	22.0					5.32		Pit Cantung			
HF03-27-2(1)	4	Aqueous Brine				-37.4	-3.3		-23.2	-2.6						Pit Cantung				
HF03-27-2(1)	5	Aqueous Brine				-38.8	-3.3		-38.7	-1.8						Pit Cantung				
HF03-27-2(1)	8	Aqueous Brine				-23.2	-2.6		-88.7	-1.8						Pit Cantung				
HF03-27-2(1)	7	Aqueous Brine				-33.2	-2.6		282.2	6.0					2.96		Pit Cantung			
HF03-27-2(1)	2	H <sub>2</sub> O-CO <sub>2</sub> -NaCl±CH <sub>4</sub>	-87.5	-59.4		-24.5	-5.3	7.5	353.4	h						Pit Cantung				
HF03-27-2(1)	1	Aqueous Brine				-35.7	-4.1			d						Pit Cantung				
HF03-27-2(2)	3	Aqueous Brine				-24.5	-3.4		351.7	50.0					5.47		Pit Cantung			
HF03-27-2(2)	2	Aqueous Brine				-31.5	-2.5			d						Pit Cantung				
HF03-27-2(2)	5	Aqueous Brine				-42.5	-1.2			d						Pit Cantung				
HF03-27-2(2)	4	Aqueous Brine				-42.5	-1.2			d						Pit Cantung				
HF03-27-2(2)	1	Aqueous Brine				-25.7	-2.6			d						Underground Cantung				
HF03-27-2(2)	3	Aqueous Brine				-25.7	-2.6			d						Underground Cantung				
HF03-74(1)	7	Aqueous Brine				-105.5	-63.9		13.4	390.3	50.0					Underground Cantung				
HF03-74(1)	2	H <sub>2</sub> O-CO <sub>2</sub> -NaCl±CH <sub>4</sub>	-105.5	-63.9		-27.2	-4.6			d						Underground Cantung				
HF03-74(1)	1	H <sub>2</sub> O-CO <sub>2</sub> -NaCl±CH <sub>4</sub>	-97.8	-57.1	-59.2	-27.2	-4.6			d						Underground Cantung				
HF03-74(1)	6	H <sub>2</sub> O-CO <sub>2</sub> -NaCl±CH <sub>4</sub>	-104.6			-32.3	-3.8		245.9	9.0					6.08		Underground Cantung			
HF03-74(2)	4	Aqueous Brine				-25.4	-2.4		222.4	5.0					3.92		Underground Cantung			
HF03-74(2)	2	Aqueous Brine				-41.6	-1.3		282.7	16.0					2.14		Underground Cantung			
HF03-74(2)	8	Aqueous Brine				-104.6	-58.3			d						Underground Cantung				
HF03-74(2)	12	Aqueous Brine				-105.3	-58.1			d						Underground Cantung				
HF03-74(2)	3	H <sub>2</sub> O-CO <sub>2</sub> -NaCl±CH <sub>4</sub>	-104.6	-58.3		-98.1	-57.4	11.4		d						Underground Cantung				
HF03-74(2)	13	H <sub>2</sub> O-CO <sub>2</sub> -NaCl±CH <sub>4</sub>	-105.3	-58.1		-57.2	-23.9	13.6		d						Underground Cantung				
HF03-74(2)	9	H <sub>2</sub> O-CO <sub>2</sub> -NaCl±CH <sub>4</sub>	-98.1	-57.4	23.7	-57.2	-23.9	9.8		d						Underground Cantung				
HF03-74(2)	7	H <sub>2</sub> O-CO <sub>2</sub> -NaCl±CH <sub>4</sub>	-96.9	-57.2	23.9	-102.6	-56.6			d						Underground Cantung				
HF03-74(2)	5	H <sub>2</sub> O-CO <sub>2</sub> -NaCl±CH <sub>4</sub>	-102.6	-56.6		-106.5	-107.9	12.9	327.8	27.0						Underground Cantung				
HF03-74(2)	1	H <sub>2</sub> O-CO <sub>2</sub> -NaCl±CH <sub>4</sub>	-106.5	-107.9		-32.2	-4.8	10.9		d						Underground Cantung				
HF03-74(2)	10	H <sub>2</sub> O-CO <sub>2</sub> -NaCl±CH <sub>4</sub>	-107.9							d						Underground Cantung				

Sample (Chip)	Inclusion # (mineral if not quartz)	Fluid Inclusion Type	T <sub>1000</sub> (°C)	T <sub>m,coz</sub> (°C)	T <sub>m,coz</sub> (°C)	T <sub>e</sub> (°C)	T <sub>m</sub> (°C)	T <sub>m,deh</sub> (°C)	T <sub>h</sub> (°C)	Vapor % Decriptated (d)	Density (g/cm <sup>3</sup> )	XCO <sub>2</sub> XCH <sub>4</sub> XH <sub>2</sub> O (wt% equiv. NaCl)	XCO <sub>2</sub> +XCH <sub>4</sub> Location	XCO <sub>2</sub> XCH <sub>4</sub> Density (g/cm <sup>3</sup> )
HF03-74(2)	11	H <sub>2</sub> O-CO <sub>2</sub> -NaCl±CH <sub>4</sub>	-96.6	-67.2	12.4	12.4	12.4	12.4	12.4	d			Underground Cantung	
HF03-74(2)	6	H <sub>2</sub> O-CO <sub>2</sub> -NaCl±CH <sub>4</sub>	-100.9	-57.2	14.5	14.5	14.5	14.5	14.5	d			Underground Cantung	
HF03-74(3)	3	Aqueous Brine				-35.2	-8.8		363.6	18.0	0.7850	12.63	Underground Cantung	
HF03-74(3)	1	Aqueous Brine				-31.6	-4.6		346.2	41.0	0.7090	7.25	Underground Cantung	
HF03-74(3)	2	Aqueous Brine				-33.8	-4.4		318.8	55.0	0.7580	6.96	Underground Cantung	
HF03-74(3)	5	Aqueous Brine				-38.3	-3.4						Underground Cantung	
HF03-90(1)	7	Aqueous Brine				-26.1	-6.9		279.5	23.3	0.8620	10.36	Underground Cantung	
HF03-90(1)	10	Aqueous Brine				-23.5	-6.9		302.8	33.0	0.8270	10.10	Underground Cantung	
HF03-90(1)	6	Aqueous Brine				-29.2	-6.7		278.4	22.5	0.8600	9.97	Underground Cantung	
HF03-90(1)	8	Aqueous Brine				-25.7	-6.6		265.9	17.5	0.8710	9.58	Underground Cantung	
HF03-90(1)	13	Aqueous Brine				-24.2	-6.3						Underground Cantung	
HF03-90(1)	9	Aqueous Brine				-25.8	-6.1						Underground Cantung	
HF03-90(1)	11	Aqueous Brine				-28.2	-5.2		284.6	13.5	0.8230	7.54	Underground Cantung	
HF03-90(1)	14	Aqueous Brine				-26.4	-4.8		210.6	27.5	0.9110	6.96	Underground Cantung	
HF03-90(1)	5	Aqueous Brine				-28.6	-4.4						Underground Cantung	
HF03-90(1)	16	Aqueous Brine				-4.4	-4.4						Underground Cantung	
HF03-90(1)	1	Aqueous Brine				-27.8	-2.9		221.1	9.0	0.8800	4.70	Underground Cantung	
HF03-90(1)	12	Aqueous Brine				-28.8	-2.8		259.6	21.0	0.8260	4.55	Underground Cantung	
HF03-90(1)	3	H <sub>2</sub> O-CO <sub>2</sub> -NaCl±CH <sub>4</sub>	-96.4	-61.2	7.4			9.4	300.8	15.0	0.9410	0.88	Underground Cantung	0.788 0.212 0.635
HF03-90(1)	4	H <sub>2</sub> O-CO <sub>2</sub> -NaCl±CH <sub>4</sub>	-100.5	-58.4	6.4			9.8					Underground Cantung	
HF03-90(1)	2	H <sub>2</sub> O-CO <sub>2</sub> -NaCl±CH <sub>4</sub>	-104.9	-57.8	28.7			7.9	295.7	19.0	0.9900	0.071 0.005 0.912	Underground Cantung	0.937 0.063 0.812
HF03-90(2)	2	Aqueous Brine				-27.5	-3.7		10.1	290.4	25.0		Underground Cantung	
HF03-90(2)	3	Aqueous Brine				-26.2	-3.3		287.9	h	0.7880	5.83	Underground Cantung	
HF03-90(2)	7	Aqueous Brine				-33.4	-4.2		270.4	38.0	0.8180	5.32	Underground Cantung	
HF03-90(2)	8	Aqueous Brine				-35.5	-2.6						Underground Cantung	
HF03-90(2)	7	H <sub>2</sub> O-CO <sub>2</sub> -NaCl±CH <sub>4</sub>	-102.3	-91.6	10.2			10.2	312.9	41.0			Underground Cantung	
HF03-90(2)	5	H <sub>2</sub> O-CO <sub>2</sub> -NaCl±CH <sub>4</sub>	-91.8	-62.2	11.5			11.5	298.6	22.0			Underground Cantung	
HF03-90(2)	1	H <sub>2</sub> O-CO <sub>2</sub> -NaCl±CH <sub>4</sub>	-99.9	-60.2	10.6			10.6	314.5	41.0			Underground Cantung	
HF03-90(2)	6	H <sub>2</sub> O-CO <sub>2</sub> -NaCl±CH <sub>4</sub>	-97.1	-57.4	10.2			10.2	312.9	28.0			Underground Cantung	
HF03-90(3)	1	Aqueous Brine				-41.4	-6.7				0.8330		Underground Cantung	
HF03-90(3)	6	Aqueous Brine				-39.4	-4.9		271.2	12.5			Underground Cantung	
HF03-90(3)	5	Aqueous Brine				-33.4	-4.2						Underground Cantung	
HF03-90(3)	2	Aqueous Brine				-34.2	-3.1						Underground Cantung	
HF03-90(3)	4	Aqueous Brine				-35.4	-2.4		262.4	19.0		6.67	Underground Cantung	
HF03-90(3)	3	H <sub>2</sub> O-CO <sub>2</sub> -NaCl±CH <sub>4</sub>	-84.3	-61.1	13.2			9.6	300.3	18.0	0.8150	3.92	Underground Cantung	0.765 0.215 0.385
HF03-90(3)	1	H <sub>2</sub> O-CO <sub>2</sub> -NaCl±CH <sub>4</sub>	-96.6	-60.8	8.8			7.9	274.5	27.0	0.8890	0.030 0.008 0.959	Underground Cantung	0.785 0.215 0.385
HF03-91-1B(1)	12	Aqueous Brine				-21.9	-4.3				0.9460	0.085 0.017 0.887	Pit Cantung	0.834 0.166 0.664
HF03-91-1B(1)	2	Aqueous Brine				-28.5	-4.2						Pit Cantung	
HF03-91-1B(1)	7	Aqueous Brine				-23.8	-3.8		300.5	10.0	0.7860	6.67	Pit Cantung	
HF03-91-1B(1)	3	Aqueous Brine				-25.2	-3.9		261.7	18.5	0.8420	6.23	Pit Cantung	
HF03-91-1B(1)	4	Aqueous Brine				-23.4	-3.6		259.4	14.0	0.8440	6.08	Pit Cantung	
HF03-91-1B(1)	10	Aqueous Brine				-21.8	-3.4		271.5	12.5	0.8220	5.78	Pit Cantung	
HF03-91-1B(1)	5	Aqueous Brine				-21.8	-3.4						Pit Cantung	
HF03-91-1B(1)	8	Aqueous Brine				-21.5	-1.9		253.9	8.2	0.8280	3.92	Pit Cantung	
HF03-91-1B(1)	6	Aqueous Brine				-22.3	-1.6		205.2	4.0	0.8820	2.63	Pit Cantung	
HF03-91-1B(1)	9	H <sub>2</sub> O-CO <sub>2</sub> -NaCl±CH <sub>4</sub>	-101.1	-60.8	12.4			12.4	377.6	62.0			Pit Cantung	
HF03-91-1B(1)	11	H <sub>2</sub> O-CO <sub>2</sub> -NaCl±CH <sub>4</sub>	-110.6	-58.9	12.2			9.3	344.5	70.0	0.8420	0.390 0.036 0.571	0.426 Pit Cantung	0.915 0.085 0.732
HF03-91-1B(1)	1	H <sub>2</sub> O-CO <sub>2</sub> -NaCl±CH <sub>4</sub>	-107.2	-58.4	18.4			9.8	385.2	85.0	0.7540	0.589 0.045 0.365	0.634 Pit Cantung	0.929 0.071 0.680
HF03-91-1B(2)	7	Aqueous Brine				-22.9	-6.4						Pit Cantung	
HF03-91-1B(2)	5	Aqueous Brine				-25.3	-5.1		272.5	6.0	0.8460	7.96	Pit Cantung	
HF03-91-1B(2)	6	Aqueous Brine				-29.7	-4.9		284.9	25.3	0.8240	7.68	Pit Cantung	
HF03-91-1B(2)	4	Aqueous Brine				-23.2	-4.1		222.4	6.5	0.8850	6.52	Pit Cantung	
HF03-91-1B(2)	1	Aqueous Brine				-21.9	-3.5		169.8	12.7	0.9400	5.62	Pit Cantung	
HF03-91-1B(2)	3	Aqueous Brine				-27.2	-3.3		283.9	14.5	0.7870	5.32	Pit Cantung	
HF03-91-1B(2)	2	H <sub>2</sub> O-CO <sub>2</sub> -NaCl±CH <sub>4</sub>	-95.1	-56.7	11.6			12.2	263.9	69.0			Pit Cantung	
HF03-91-2(1)	2	Aqueous Brine				-24.9	-5.8		316.9	25.0	0.7900	8.92	Pit Cantung	

Sample (Chip)	Inclusion # (mineral if not quartz)	Fluid Inclusion Type	T <sub>m,co2</sub> (°C)	T <sub>m,co2</sub> (°C)	T <sub>e</sub> (°C)	T <sub>m</sub> (°C)	T <sub>m,calc</sub> (°C)	T <sub>h</sub> (°C)	Vapor-% Homogenization (h) or Deceptated (d)	Density (g/cm <sup>3</sup> )	XCO <sub>2</sub>	XCH <sub>4</sub>	XH <sub>2</sub> O (wt% equiv. NaCl)	Salinity	XCO <sub>2</sub> +XCH <sub>4</sub>	Location	XCO <sub>2</sub>	XCH <sub>4</sub>	Density (g/cm <sup>3</sup> )
HF03-91-2(1)	4	Aqueous Brine	-28.7	-4.3	-28.7	-4.3			d							Pit Cantung			
HF03-91-2(1)	1	Aqueous Brine	-23.5	-4.2	-23.5	-4.2		385.4	65.0 h	0.8580				6.67		Pit Cantung			
HF03-91-2(1)	3	Aqueous Brine	-25.8	-2.3	-25.8	-2.3			d							Pit Cantung			
HF03-91-2(1)	6	Aqueous Brine	-25.4	-1.4	-25.4	-1.4			d							Pit Cantung			
HF03-91-2(1)	5	H <sub>2</sub> O-CO <sub>2</sub> -NaCl±CH <sub>4</sub>	-81.1	-62.2			11.9		d							Pit Cantung			
HF03-91A(1)	7	Aqueous Brine	-29.6	-5.7	-29.6	-5.7		391.7	46.0 h	0.6280				8.38		Pit Cantung			
HF03-91A(1)	1	Aqueous Brine	-41.9	-5.4	-41.9	-5.4			d							Pit Cantung			
HF03-91A(1)	9	Aqueous Brine	-31.7	-4.4	-31.7	-4.4			d							Pit Cantung			
HF03-91A(1)	3	Aqueous Brine	-29.3	-3.8	-29.3	-3.8			d							Pit Cantung			
HF03-91A(1)	5	Aqueous Brine	-30.3	-3.6	-30.3	-3.6			d							Pit Cantung			
HF03-91A(1)	6	Aqueous Brine	-37.8	-2.8	-37.8	-2.8		362.8	50.0 h	0.6190				4.55		Pit Cantung			
HF03-91A(1)	2	Aqueous Brine	-39.9	-2.4	-39.9	-2.4		389.4	36.2 h	0.5080				3.92		Pit Cantung			
HF03-91A(1)	10	Aqueous Brine	-27.3	-1.8	-27.3	-1.8		321.4	29.0 h	0.8680				2.96		Pit Cantung			
HF03-91A(1)	8	H <sub>2</sub> O-CO <sub>2</sub> -NaCl±CH <sub>4</sub>	-95.8	-60.4	-11.9		9.9	285.1	55.0 d	0.9610	0.273	0.042	0.877	3.90	0.315	Pit Cantung	0.866	0.134	0.835
HF03-91A(1)	4	H <sub>2</sub> O-CO <sub>2</sub> -NaCl±CH <sub>4</sub>	-99.8	-57.7			9.9	350.9	52.0 h							Pit Cantung			
HF03-92(1)	5	Aqueous Brine	-29.6	-4.8	-29.6	-4.8			d							Underground Cantung			
HF03-92(1)	7	Aqueous Brine	-26.2	-4.4	-26.2	-4.4			d							Underground Cantung			
HF03-92(1)	9	Aqueous Brine	-22.5	-4.3	-22.5	-4.3		290.1	6.0 d							Underground Cantung			
HF03-92(1)	2	Aqueous Brine	-25.7	-3.9	-25.7	-3.9		225.1	16.0 h	0.8890				6.23		Underground Cantung			
HF03-92(1)	8	Aqueous Brine	-24.4	-3.7	-24.4	-3.7		225.8	22.0 h	0.8860				5.93		Underground Cantung			
HF03-92(1)	1	Aqueous Brine	-24.8	-3.2	-24.8	-3.2		279.1	9.0 d	0.8030				5.17		Underground Cantung			
HF03-92(1)	10	Aqueous Brine	-22.5	-3.1	-22.5	-3.1			d							Underground Cantung			
HF03-92(1)	4	Aqueous Brine	-28.6	-2.5	-28.6	-2.5		258.9	17.7 h	0.8220				4.07		Underground Cantung			
HF03-92(1)	6	Aqueous Brine	-22.8	-1.7	-22.8	-1.7		233.2	21.5 h	0.8460				2.79		Underground Cantung			
HF03-92(1)	3	Aqueous Brine	-24.1	-1.3	-24.1	-1.3		240.4	4.0 h	0.8280				2.14		Underground Cantung			
HF03-92(2)	5	H <sub>2</sub> O-CO <sub>2</sub> -NaCl±CH <sub>4</sub>	-81.2	-60.5	16.5		9.8		d							Underground Cantung			
HF03-92(2)	8	H <sub>2</sub> O-CO <sub>2</sub> -NaCl±CH <sub>4</sub>	-86.3	-59.9			9.9		d							Underground Cantung			
HF03-92(2)	3	H <sub>2</sub> O-CO <sub>2</sub> -NaCl±CH <sub>4</sub>	-77.1	-59.6	7.1		9.8		d							Underground Cantung			
HF03-92(2)	1	H <sub>2</sub> O-CO <sub>2</sub> -NaCl±CH <sub>4</sub>	-92.3	-59.2	9.5		9.7	278.3	30.0 h	0.8370	0.112	0.012	0.874	0.65	0.124	Underground Cantung	0.903	0.097	0.750
HF03-92(2)	7	H <sub>2</sub> O-CO <sub>2</sub> -NaCl±CH <sub>4</sub>	-86.6	-58.6	14.9		9.6		d							Underground Cantung			
HF03-92(2)	4	H <sub>2</sub> O-CO <sub>2</sub> -NaCl±CH <sub>4</sub>	-87.1	-58.4	17.1		7.6	289.2	12.0 h	0.8900	0.041	0.003	0.942	4.62	0.044	Underground Cantung	0.934	0.066	0.708
HF03-92(2)	2	H <sub>2</sub> O-CO <sub>2</sub> -NaCl±CH <sub>4</sub>	-87.9	-58.2	12.4		10.5	238.9	23.0 h	0.8910	0.041	0.002	0.942	4.62	0.043	Underground Cantung			
HF03-92(2)	6	H <sub>2</sub> O-CO <sub>2</sub> -NaCl±CH <sub>4</sub>	-82.9	-58.1	8.9		12.2		d							Underground Cantung			
HF03-92(3)	1	H <sub>2</sub> O-CO <sub>2</sub> -NaCl±CH <sub>4</sub>	-89.7	-64.4	-1.2		7.9		d							Underground Cantung			
HF03-92(3)	2	H <sub>2</sub> O-CO <sub>2</sub> -NaCl±CH <sub>4</sub>	-90.6	-61.5	0.2		7.8	323.6	25.3 d	0.8710	0.078	0.020	0.886	5.63	0.098	Underground Cantung	0.798	0.202	0.679
HF03-92(3)	6	H <sub>2</sub> O-CO <sub>2</sub> -NaCl±CH <sub>4</sub>	-102.5	-61.2	-6.5		11.2		d							Underground Cantung			
HF03-92(3)	4	H <sub>2</sub> O-CO <sub>2</sub> -NaCl±CH <sub>4</sub>	-87.8	-60.7	1.2		8.5		d							Underground Cantung			
HF03-92(3)	5	H <sub>2</sub> O-CO <sub>2</sub> -NaCl±CH <sub>4</sub>	-77.3	-60.1	-6.8		8.4		d							Underground Cantung			
HF03-92(3)	7	H <sub>2</sub> O-CO <sub>2</sub> -NaCl±CH <sub>4</sub>	-78.6	-59.8	0.6		8.7		d							Underground Cantung			
HF03-92(3)	3	H <sub>2</sub> O-CO <sub>2</sub> -NaCl±CH <sub>4</sub>	-87.2	-59.6	4.7		8.2	288.9	24.0	0.9790	0.087	0.011	0.890	4.37	0.088	Underground Cantung	0.890	0.110	0.774
HF03-93(1)	4	Aqueous Brine	-27.6	-6.4	-27.6	-6.4			5.0 d							Pit Cantung			
HF03-93(1)	6	Aqueous Brine	-30.9	-6.1	-30.9	-6.1		283.6	22.0 h	0.8310				9.32		Pit Cantung			
HF03-93(1)	11	Aqueous Brine	-26.2	-4.1	-26.2	-4.1		339.5	15.0 h	0.7100				6.52		Pit Cantung			
HF03-93(1)	7	Aqueous Brine	-28.3	-3.9	-28.3	-3.9		249.8	3.2 h	0.8580				6.23		Pit Cantung			
HF03-93(1)	13	Aqueous Brine	-28.4	-3.8	-28.4	-3.8		326.5	21.5 h	0.7300				6.08		Pit Cantung			
HF03-93(1)	2	Aqueous Brine	-28.4	-3.5	-28.4	-3.5		334.4	14.0 h	0.7080				5.62		Pit Cantung			
HF03-93(1)	15	Aqueous Brine	-22.8	-3.5	-22.8	-3.5		331.6	23.2 h	0.7110				5.62		Pit Cantung			
HF03-93(1)	16	H <sub>2</sub> O-CO <sub>2</sub> -NaCl±CH <sub>4</sub>	-104.3	-83.5	-23.9	-3.7	11.2		17.0 d							Pit Cantung	0.052	0.948	0.276
HF03-93(1)	1	H <sub>2</sub> O-CO <sub>2</sub> -NaCl±CH <sub>4</sub>	-101.3	-64.2			8.1	367.4	30.0 h							Pit Cantung			
HF03-93(1)	3	H <sub>2</sub> O-CO <sub>2</sub> -NaCl±CH <sub>4</sub>	-94.7	-62.2			13.7	340.6	22.0 h							Pit Cantung			
HF03-93(1)	5	H <sub>2</sub> O-CO <sub>2</sub> -NaCl±CH <sub>4</sub>	-102.1	-62.1				293.2	15.5 h	0.8100				7.54		Pit Cantung			
HF03-93-2(1)	6	Aqueous Brine	-37.9	-4.8	-37.9	-4.8		241.6	5.8 d					7.39		Pit Cantung			
HF03-93-2(1)	2	Aqueous Brine	-36.4	-4.2	-36.4	-4.2		256.1	16.0 h	0.8540				6.67		Pit Cantung			

Sample (Chip)	Inclusion # (mineral if not quartz)	Fluid Inclusion Type	T <sub>1,co2</sub> (°C)	T <sub>m,co2</sub> (°C)	T <sub>e</sub> (°C)	T <sub>m</sub> (°C)	T <sub>m,am</sub> (°C)	T <sub>h</sub> (°C)	Vapor % Homogenization (h) or Decriptated (d)	Density (g/cm <sup>3</sup> )	XCO <sub>2</sub>	XCH <sub>4</sub>	XH <sub>2</sub> O (wt% equiv. NaCl)	XCO <sub>2</sub> +XCH <sub>4</sub> Location	XCO <sub>2</sub>	XCH <sub>4</sub>	Density (g/cm <sup>3</sup> )
HF03-93-2(1)	5	Aqueous Ethne	-109.4	-88.6	-91	-24.4	-2.9	251.5	8.2 h	0.8400				Pit Centung			4.70
HF03-93-2(1)	4	Aqueous Ethne				-27.9	-2.4	300.7	16.0 h	0.7470				Pit Centung			3.92
HF03-93-2(1)	7	Aqueous Ethne				-31.9	-2.2		17.7 d					Pit Centung			
HF03-93-2(1)	1	H <sub>2</sub> O-CO <sub>2</sub> -NaCl±CH <sub>4</sub>	-109.4	-88.6	-91			8.7	24.1 h					Pit Centung			
HF03-93-2(1)	8	H <sub>2</sub> O-CO <sub>2</sub> -NaCl±CH <sub>4</sub>	-99.9	-61.4	11.9			11.2	280.9					Pit Centung			
HF03-93-2(1)	4	Aqueous Ethne				-26.6	-4.4		5.7 d					Pit Centung			
HF03-93-2(2)	8	Aqueous Ethne				-31.9	-4.1	217.4	24.0 h	0.9000				Pit Centung			6.52
HF03-93-2(2)	9	Aqueous Ethne				-29.9	-2.6	352.2	35.8 h	0.6400				Pit Centung			4.23
HF03-93-2(2)	7	Aqueous Ethne				-23.3	-1.8	276.1	36.2 h	0.7790				Pit Centung			2.96
HF03-93-2(2)	3	H <sub>2</sub> O-CO <sub>2</sub> -NaCl±CH <sub>4</sub>	-95.1	-60.9	9.6				75.0 d					Pit Centung			
HF03-93-2(2)	2	H <sub>2</sub> O-CO <sub>2</sub> -NaCl±CH <sub>4</sub>	-100.4	-60.4				9.6	313.8					Pit Centung			
HF03-93-2(2)	6	H <sub>2</sub> O-CO <sub>2</sub> -NaCl±CH <sub>4</sub>	-99.4	-60.1				9.4	314.7					Pit Centung			
HF03-93-2(2)	1	H <sub>2</sub> O-CO <sub>2</sub> -NaCl±CH <sub>4</sub>	-97.6	-56.8				8.4	272.3					Pit Centung			
HF03-94 (1)	8	Aqueous Ethne				-31.3	-5.9		13.0 h					Pit Centung			
HF03-94 (1)	5	Aqueous Ethne				-32.8	-5.2	332.7	16.4 h	0.7640				Pit Centung			9.05
HF03-94 (1)	6	Aqueous Ethne				-41.6	-4.8	328.4	23.2 h	0.7580				Pit Centung			8.10
HF03-94 (1)	9	Aqueous Ethne				-39.8	-4.8	340.9	39.0 h	0.7240				Pit Centung			7.54
HF03-94 (1)	2	Aqueous Ethne				-38.3	-4.4	276.8	7.0 h	0.8340				Pit Centung			7.54
HF03-94 (1)	4	Aqueous Ethne				-43.2	-4.3		d					Pit Centung			
HF03-94 (1)	10	Aqueous Ethne				-38.4	-4.2	304.5	12.5 h	0.7790				Pit Centung			6.67
HF03-94 (1)	1	Aqueous Ethne				-30.2	-4.2	300.8	25.0 h	0.7680				Pit Centung			6.67
HF03-94 (1)	7	Aqueous Ethne				-34.5	-4.1	362.4	10.0 h	0.6600				Pit Centung			6.52
HF03-94 (1)	3	Aqueous Ethne				-38.4	-3.8	283.1	10.0 h	0.8080				Pit Centung			6.08
HF03-94 (2)	6	Aqueous Ethne				-38.5	-3.8	330.1	88.0 d	0.7220				Pit Centung			6.08
HF03-94 (2)	2	Aqueous Ethne				-40.9	-3.5		d					Pit Centung			
HF03-94 (2)	2	H <sub>2</sub> O-CO <sub>2</sub> -NaCl±CH <sub>4</sub>	-83.7	-58.1				9.8	326.9					Pit Centung			
HF03-94 (2)	1	H <sub>2</sub> O-CO <sub>2</sub> -NaCl±CH <sub>4</sub>	-91.6	-58.1	-3.1			10.2	280.2					Pit Centung			
HF03-94 (2)	4	H <sub>2</sub> O-CO <sub>2</sub> -NaCl±CH <sub>4</sub>	-94.1	-57.4				9.2	293.2					Pit Centung			
HF03-94 (2)	7	H <sub>2</sub> O-CO <sub>2</sub> -NaCl±CH <sub>4</sub>	-97.6	-57.1	5.8			8.8	318.4					Pit Centung			
HF03-94 (3)	5	Aqueous Ethne				-36.2	-6.3		d					Pit Centung			
HF03-94 (3)	3	Aqueous Ethne				-39.8	-5.9		d					Pit Centung			
HF03-94 (3)	4	Aqueous Ethne				-35.4	-5.3	375.6	34.0 d	0.6640				Pit Centung			0.24
HF03-94 (3)	1	Aqueous Ethne				-34.7	-3.5	352.3	33.0 d	0.6670				Pit Centung			5.62
HF03-94 (3)	2	Aqueous Ethne				-39.5	-3.0		d					Pit Centung			
HF03-98-1(1)	1	Aqueous Ethne				-26.1	-4.4	207.5	12.5 h	0.9140				Pit Centung			6.96
HF03-98-1(1)	2	Aqueous Ethne				-30.6	-2.3		d					Pit Centung			
HF03-98-1(1)	5	Aqueous Ethne				-31.2	-2.1	188.2	35.8 h	0.9070				Pit Centung			3.44
HF03-98-1(1)	4	Aqueous Ethne				-27.6	-1.7	208.8	4.5 d	0.8790				Pit Centung			2.79
HF03-98-1(1)	3	Aqueous Ethne				-28.1	-1.1	273.2	6.0 h	0.7700				Pit Centung			1.82
HF03-98-1(2)	3	Aqueous Ethne				-23.6	-5.7	212.8	14.0 d	0.9230				Pit Centung			8.78
HF03-98-1(2)	4	Aqueous Ethne				-30.3	-4.3	281.9	25.3 d	0.8180				Pit Centung			6.81
HF03-98-1(2)	2	Aqueous Ethne				-28.6	-3.6		d					Pit Centung			
HF03-98-1(2)	5	Aqueous Ethne				-29.8	-3.1		d					Pit Centung			
HF03-98-1(2)	6	Aqueous Ethne				-22.9	-1.7	236.6	12.7 h	0.8410				Pit Centung			2.79
HF03-98-1(2)	7	Aqueous Ethne				-27.8	-0.4	258.6	1.6 h	0.7810				Pit Centung			0.66
HF03-98-1(2)	1	H <sub>2</sub> O-CO <sub>2</sub> -NaCl±CH <sub>4</sub>	-109.4	-57.1				10.4	246.8					Pit Centung			
HF03-98-2(1)	8	Aqueous Ethne				-26.8	-4.3	309.6	9.0 h	0.7720				Pit Centung			6.81
HF03-98-2(1)	3	Aqueous Ethne				-28.1	-3.3	279.5	3.8 h	0.8040				Pit Centung			5.32
HF03-98-2(1)	7	Aqueous Ethne				-22.9	-1.5		d					Pit Centung			
HF03-98-2(1)	2	H <sub>2</sub> O-CO <sub>2</sub> -NaCl±CH <sub>4</sub>	-119.1	-110.6	-97.6			13.4	229.6					Pit Centung			
HF03-98-2(1)	4	H <sub>2</sub> O-CO <sub>2</sub> -NaCl±CH <sub>4</sub>	-114.2	-106.1	-91.3			10.8						Pit Centung			
HF03-98-2(1)	1	H <sub>2</sub> O-CO <sub>2</sub> -NaCl±CH <sub>4</sub>	-118.7	-100.9	-94.9			11.5	218.1					Pit Centung			
HF03-98-2(1)	5	H <sub>2</sub> O-CO <sub>2</sub> -NaCl±CH <sub>4</sub>	-122.1	-98.8	-90.6			11.8	256.3					Pit Centung			
HF03-98-2(1)	3	Aqueous Ethne				-41.4	-5.9	286.9	2.0 h	0.8380				Pit Centung			9.05
HF03-98-2(1)	5	Aqueous Ethne				-37.7	-5.9	285.4	12.7 h	0.8400				Pit Centung			9.05
HF03-98-2(1)	9	Aqueous Ethne				-26.9	-5.9	241.3	22.0 h	0.8950				Pit Centung			9.05

Sample (Chip)	Inclusion # (mineral if not quartz)	Fluid Inclusion Type	T <sub>m,coz</sub> (°C)	T <sub>m,coz</sub> (°C)	T <sub>h,coz</sub> (°C)	T <sub>o</sub> (°C)	T <sub>m</sub> (°C)	T <sub>a,ash</sub> (°C)	T <sub>h</sub> (°C)	Vapor % Homogenization (h) or Decrepitated (d)	Density (g/cm <sup>3</sup> )	XCO <sub>2</sub> (g/cm <sup>3</sup> )	XCH <sub>4</sub> (g/cm <sup>3</sup> )	XCO <sub>2</sub> +XCH <sub>4</sub> Location	Salinity (wt% equiv. NaCl)	XCO <sub>2</sub> (g/cm <sup>3</sup> )	XCH <sub>4</sub> (g/cm <sup>3</sup> )	Density (g/cm <sup>3</sup> )
HF03-39(1)	8	Aqueous Brine				-39.2	-5.1	207.7	5.0 h		0.9220			Pit Cantung	7.96			
HF03-39(1)	7	Aqueous Brine				-29.8	-5.1	203.9	4.0 h		0.9260			Pit Cantung	7.96			
HF03-39(1)	6	Aqueous Brine				-27.1	-4.7	202.5	17.7 h		0.9230			Pit Cantung	7.39			
HF03-39(1)	1	Aqueous Brine				-29.9	-3.8		d					Pit Cantung				
HF03-39(1)	2	Aqueous Brine				-33.5	-3.4	294.1	2.0 d		0.7810			Pit Cantung	5.47			
HF03-39(1)	4	Aqueous Brine				-27.5	-2.3		d					Pit Cantung				
HF03-39(2)	5	Aqueous Brine				-27.9	-5.0	324.9	17.7 h		0.7800			Pit Cantung	7.82			
HF03-39(2)	2	Aqueous Brine				-28.7	-4.4	261.3	7.0 h		0.8500			Pit Cantung	6.96			
HF03-39(2)	4	Aqueous Brine				-25.7	-3.6		d					Pit Cantung				
HF03-39(2)	3	Aqueous Brine				-34.6	-3.5	286.2	10.0 h		0.7970			Pit Cantung	5.62			
HF03-39(2)	1	Aqueous Brine				-29.5	-2.8	290.8	12.7 h		0.7740			Pit Cantung	4.50			
HF03-39(2)	6	Aqueous Brine				-28.8	-2.7	242.3	12.0 h		0.8500			Pit Cantung	4.39			
HF03-39(2)	7	Aqueous Brine				-24.8	-2.6	279.2	12.7 h		0.7910			Pit Cantung	4.23			
HF03-39(2)	2	Aqueous Brine				-39.2	-1.8		12.0 d					Underground Cantung				
HF03-39(2)	4	Aqueous Brine				-37.9	-2.5		16.0 d					Underground Cantung				
JY-05-CAN4100 (1)	1	H <sub>2</sub> O-CO <sub>2</sub> -NaCl±CH <sub>4</sub>						6.4	251.9	37.0 d				Underground Cantung				
JY-05-CAN4100 (1)	1	H <sub>2</sub> O-CO <sub>2</sub> -NaCl±CH <sub>4</sub>						7.9	279.8	18.0 d				Underground Cantung				
JY-05-CAN4100 (2)	1	Aqueous Brine				-43.9	-3.2	208.8	24.0 h		0.8990			Underground Cantung	5.17			
JY-05-CAN4100 (2)	1	Aqueous Brine				-44.5	-3.4	210.7	20.0 h		0.8990			Underground Cantung	5.47			
JY-05-CAN4100 (2)	2	Aqueous Brine				-44.2	-1.7	278.6	19.0 h		0.7730			Underground Cantung	2.79			
PIT SCHEELITE (1)	1	Aqueous Brine				-44.9	-6.1	324.8	18.0 h		0.7920			Pit Cantung	9.32			
PIT SCHEELITE (1)	3	Aqueous Brine				-37.5	-5.7	337.5	17.7 h		0.7520			Pit Cantung	9.78			
PIT SCHEELITE (1)	2	Aqueous Brine				-37.4	-5.4	353.4	28.0 h		0.7130			Pit Cantung	9.38			
PIT SCHEELITE (1)	6	Aqueous Brine				-41.2	-5.1		d					Pit Cantung				
PIT SCHEELITE (1)	8	Aqueous Brine				-39.2	-4.8		d					Pit Cantung				
PIT SCHEELITE (1)	4	Aqueous Brine				-44.7	-4.5		d					Pit Cantung				
PIT SCHEELITE (1)	5	Aqueous Brine				-44.7	-4.5	329.7	33.0 h		0.7400			Pit Cantung	7.11			
PIT SCHEELITE (1)	7	Aqueous Brine				-23.8	-3.2		d					Pit Cantung				



Sample (Chip)	Inclusion # (mineral if not quartz)	Fluid Inclusion Type	T <sub>1,coz</sub> (°C)	T <sub>m,coz</sub> (°C)	T <sub>h,coz</sub> (°C)	T <sub>e</sub> (°C)	T <sub>m</sub> (°C)	T <sub>m,sub</sub> (°C)	T <sub>h</sub> (°C)	Vapor % Decrepitated (d)	Homogenization (h) or Decrepitated (d)	Density (g/cm <sup>3</sup> )	Bulk Inclusion			Carbonic Phase				
													XCO <sub>2</sub>	XCH <sub>4</sub>	XH <sub>2</sub> O	Salinity (wt% equiv. NaCl)	XCO <sub>2</sub> →XCH <sub>4</sub>	Location	XCO <sub>2</sub>	XCH <sub>4</sub>
Zanbung Creek(2)	3	H <sub>2</sub> O-CO <sub>2</sub> -NaCl±CH <sub>4</sub>	-85.1	-56.6	16.1		6.9	261.7		60.0	d	0.902	0.334	0	0.654	5.855	0.334	Zanbung Creek		
Zanbung Creek(2)	6	H <sub>2</sub> O-CO <sub>2</sub> -NaCl±CH <sub>4</sub>	-83.4	-56.6	25.5		8.8	227.6		12.5	h	0.971	0.04	0	0.953	2.388	0.04	Zanbung Creek		
Zanbung Creek(1)	2	H <sub>2</sub> O-CO <sub>2</sub> -NaCl±CH <sub>4</sub>	-82.6	-58.6	15.7		8.4				d							Zanbung Creek		
Zanbung Creek(1)	3	H <sub>2</sub> O-CO <sub>2</sub> -NaCl±CH <sub>4</sub>	-89.5	-58.2	3.8		8.1				d							Zanbung Creek		
Zanbung Creek(1)	4	H <sub>2</sub> O-CO <sub>2</sub> -NaCl±CH <sub>4</sub>	-73.7	-57.9	13.7		6.2				d							Zanbung Creek		
Zanbung Creek(1)	5	H <sub>2</sub> O-CO <sub>2</sub> -NaCl±CH <sub>4</sub>	-87.2	-57.8	9.6		7.6				d							Zanbung Creek		
Zanbung Creek(1)	1	H <sub>2</sub> O-CO <sub>2</sub> -NaCl±CH <sub>4</sub>	-84.9	-57.8	17.9		8.2	233.7		10.0	h	0.992	0.032	0.002	0.956	3.52	0.034	Zanbung Creek		
Zanbung Creek(1)	11	H <sub>2</sub> O-CO <sub>2</sub> -NaCl±CH <sub>4</sub>	-80.1	-57.6	-9.1		8.4				d							Zanbung Creek		
Zanbung Creek(1)	8	H <sub>2</sub> O-CO <sub>2</sub> -NaCl±CH <sub>4</sub>	-87.1	-57.5	9		5.7	262.7		29.0	h	0.996	0.122	0.004	0.852	7.865	0.126	Zanbung Creek		
Zanbung Creek(1)	6	H <sub>2</sub> O-CO <sub>2</sub> -NaCl±CH <sub>4</sub>	-81.7	-57.4	16.7		6.4				d							Zanbung Creek		
Zanbung Creek(1)	8	H <sub>2</sub> O-CO <sub>2</sub> -NaCl±CH <sub>4</sub>	-78.2	-57.4	7.6		8.8				d							Zanbung Creek		
Zanbung Creek(1)	7	H <sub>2</sub> O-CO <sub>2</sub> -NaCl±CH <sub>4</sub>	-86.8	-57.1	19.8		9.9				d							Zanbung Creek		
Zanbung Creek(1)	10	H <sub>2</sub> O-CO <sub>2</sub> -NaCl±CH <sub>4</sub>	-83.8	-56.6	17.3		8.9	315.1		12.7	h	0.982	0.046	0	0.948	2.196	0.046	Zanbung Creek		



## APPENDIX IV

### Raw Trace Metal Data

SAMPLES	WO <sub>3</sub> (wt. %)	Mo	Cu	Pb	Zn	Ag	Ni	Co	Mn	As	U	Au	Th	Sr	Cd	Sb
		(ppm)	(ppm)	(ppm)	(ppm)	(ppm)	(ppm)	(ppm)	(ppm)	(ppm)	(ppm)	(ppm)	(ppm)	(ppm)	(ppm)	(ppm)
HF03-14	0.23	0.6	32.0	1.1	7	0.1	2.3	3	57				0.1	3	0.1	0.1
HF03-15	0.67	0.5	24.5	1.2	15	0.2	1.4	1	129	1	0.4		1.0	31		0.1
HF03-16	1.82	2.0	520.3	2.4	65	0.9	9.2	14	545		1.2	0.4	4.0	48	0.1	0.2
HF03-17	3.31	3.7	1096.3	3.4	83	2.1	4.1	6	1012	7	1.0	0.5	2.1	38	0.2	0.4
HF03-18	1.12	2.3	916.6	2.4	57	1.0	11	14	643	2	1.5	0.2	4.6	68	0.1	0.1
HF03-19	0.50	1.6	8181.6	4.2	296	5.6	9.7	15	322	221	0.7	0.2	1.9	43	0.7	0.8
HF03-20	1.53	2.6	1535	3.1	106	0.9	25.1	30	1236	3	2.1		6.6	86	0.3	0.2
HF03-21	0.09	0.6	46.2	6.1	16	0.2	4.7	3	82	2	0.9	0.1	5.0	60		0.1
HF03-22	0.60	1.2	212.2	1.6	34	0.5	5.4	5	277	2	0.4	0.2	0.8	34		0.1
HF03-23	0.05	0.2	89.3	1.5	31	0.3	5.7	2	265		0.9		2.8	34		0.1
HF03-24	0.06	0.8	84.4	3.2	46	0.1	11.3	6	333	2	1.8		6.0	54	0.1	0.1
HF03-25	1.11	2.2	338.9	3.7	57	0.6	8.6	11	591	2	1.6	0.2	5.0	62		0.1
		2.2	340	1.8	55	0.6	8.7	11	613	1	1.7	0.3	5.3	65		0.1
HF03-26	0.91	3.5	4097.2	1.4	153	2.6	5.3	14	662		0.4	0.7	1.0	14	0.2	0.3
HF03-27	3.73	2.4	1359.3	1.5	27	0.9	1.0	2	297	2	0.6	0.2	0.8	32	0.1	0.2
HF03-05		1.7	319.9	4.8	9	0.4	28.5	10	86	1	0.5		2.4	40		0.4
HF03-74		0.2	1586	1.4	67	1.2	4.3	50	351	2	0.7		1.2	5	0.2	0.2
HF03-91		1.3	503.9	2.6	27	0.4	15.6	27	311	2	0.9		2.1	72		0.3
HF03-92		0.3	54.8	0.5	21	0.1	1.2	2	188		0.2		0.6	2		
HF03-93		2.9	3137.9	2.0	65	1.4	2.7	26	589	1	0.3	0.2	0.1	3	0.2	0.2
		2.5	3276.5	1.9	66	1.4	2.9	26	610	2	0.4	0.3	0.1	3	0.1	0.3
HF03-95		2.3	216.3	8.9	10	0.2	1.5	1	77	12	6.0		14.3	109		0.1
HF03-98		4.5	1487.8	4.2	123	1.7	10.6	13	1046	2	2.0	0.4	5.2	85	0.3	0.4
HF03-99		0.2	5.0	0.8	2	0.1	0.2		41				0.1	16		
HF03-100		0.9	15.3	1.1	2		1.7		31		0.1			4		0.1

SAMPLES	Bi (ppm)	V (ppm)	La (ppm)	Cr (ppm)	Ba (ppm)	Zr (ppm)	Ce (ppm)	Sn (ppm)	Y (ppm)	Nb (ppm)	Ta (ppm)	Be (ppm)	Sc (ppm)	Li (ppm)	Rb (ppm)	Hf (ppm)
HF03-14	86.1	11	1.0	1.9	4	1.7	3	3.9	3.9			1	7	7.0	4.5	
HF03-15	154.9	24	5.2	4.8	14	3.7	12	5.4	10.0			7	2	18.9	14.8	0.1
HF03-16	783.5	28	22.4	18.6	83	15.0	44	11.1	18.2	0.1		3	4	48.3	78.5	0.4
HF03-17	1207.4	13	13.6	10.0	10	7.4	33	21.7	23.7	0.1		16	2	17.2	13.7	0.3
HF03-18	399.4	27	15.6	19.3	27	18.7	31	20.4	17.6	0.4		9	4	33.6	33.2	0.6
HF03-19	835.2	23	13.4	6.8	40	6.9	29	34.6	20.4	0.6		6	4	37.1	63.5	0.2
HF03-20	507.3	70	23.6	37.9	77	27.1	48	20.4	18.7	8.3	0.2	9	8	91.5	162.3	1
HF03-21	207.2	24	12.6	10.5	96	18.5	25	1.0	7.4	3.3	0.2	3	3	20.9	38.5	0.6
HF03-22	340.3	15	3.7	7.3	19	5.9	10	8.1	13.7			8	3	32.3	18.2	0.2
HF03-23	229.3	23	9.2	13.1	40	15.9	18	4.7	7.0	3.5	0.2	2	3	23.2	36.2	0.6
HF03-24	98.9	45	20.3	28.1	124	31.6	39	8.4	9.7	6.8	0.4	5	6	54.8	80.7	1.2
HF03-25	560.0	36	16.9	25.7	44	24.8	34	13.1	19.5	0.8		9	5	39.2	59.8	0.9
HF03-26	544.7	35	17.1	25.6	42	24.8	34	12.9	20.2	2.0		8	5	39.3	60.7	0.8
HF03-27	1485.8	22	8.9	3.4	58	4.0	24	12.5	62.5	0.2		2	3	64.8	127.4	0.1
HF03-05	477.8	15	11.8	3.5	10	0.5	26	5.7	17.4			6	1	14.1	7.3	
HF03-74	165.4	14	8.4	17.6	64	6.3	16	12.1	5.4	1.7	0.1	1	2	23.3	32.6	0.2
HF03-91	510.7	18	12.5	12.2	22	2.3	25	7.1	10.8	10.5	0.8	1	2	31.7	31.6	0.1
HF03-92	420.7	23	13.6	19.8	153	7.7	31	102.2	33.7	4.5	0.2	19	3	65.5	198.3	0.3
HF03-93	127.4	17	2.0	8.2	20	3.6	4	2.5	1.1	3.4	0.1		1	26.2	58.6	0.1
HF03-95	532.0	11	3.4	9.8	14	1.6	9	5.1	16.7			2	2	26.1	51.8	
HF03-98	516.3	12	3.5	14.5	15	1.5	10	4.9	16.4			4	4	29.2	53.0	
HF03-99	4.0	11	29.5	6.0	92	21.9	59	7.9	5.5	5.1	0.6	4	3	4.5	93.2	1.2
HF03-100	917.1	29	31.1	22.5	55	14.3	67	23.9	46.7	2.9		27	4	53.7	110.6	0.6
HF03-99	123.8	12	0.6	6.8	2	0.9	2	0.7	2.3					9.4	0.9	0.1
HF03-100	12.5	17	4.1	7.8	2	0.3	11	0.2	12.4					12.5	0.5	

APPENDIX V

Raw Structural Data

Quartz Vein (number)	other info	Strike (degrees from N)	Dip (right hand rule, degrees)
1		220	50
1		80	20
1	fractures	150	90
2		45	90
2		70	20
3		70	90
4		50	90
4		50	90
5		30	90
5		10	90
6		62	90
7		40	80
7		340	80
7		30	90
7		50	45
7		10	90
7		40	90
7		70	80
7		45	75
7		50	90
7		10	90
8		60	90
8		30	90
8		33	90
8		45	90
8	fault	50	90
8		30	90
9		50	90
10		320	35
10		340	40
10	fault	30	55
11		250	90
11	fault	340	35
12		20	90
12		10	90
12		20	60
13		195	70
14		10	90
15		70	90
15		330	0
16		15	90
16		150	65
17		15	90

Quartz Vein (number)	other info	Strike (degrees from N)	Dip (right hand rule, degrees)
17		265	0
18		305	35
18		195	70
19		15	90
19		130	0
20		30	90
20		30	0
21		10	90
22		30	90
22	fault	25	90
23		10	0
23		45	0
23		5	70
23		0	90
23		20	90
23		10	90
23		30	90
23		3	90
23		5	90
23		20	90
23		0	90
23		20	90
24		340	60
24		320	90
24		30	90
25		30	90
26		5	90
26		70	90
26		10	90
26		30	90
27		335	90
27		10	90
28		340	60
28		70	90
29		270	20
29		25	90
29	fault	20	90
30		0	90
31		15	90
31		350	90
32		30	90
33		30	90
33		30	90
Lamprophyre Dike	in pit	240	40
Lamprophyre Dike	at Dutchman's Peak	70	90
Lamprophyre Dike	at Dutchman's Peak	120	90
Circular Stock	fault	30	90
Circular Stock	Breccia in Dolomite	340	90

Quartz				
Vein (number)	other info	Strike (degrees from N)	Dip (right hand rule, degrees)	
West Decline (UG ??)	fault	0	90	
West Decline (UG ??)	fault	30	90	
UG 3850 level-101	magnetic fractures	10	90	
UG 3850 level-101	magnetic fractures	30	90	
Argillite (same as above)	fractures	30	80	
Argillite (same as above)	fractures	15	90	
Same Place	fault slip direction	155	60	

## APPENDIX VI

### Other Graphs and Charts

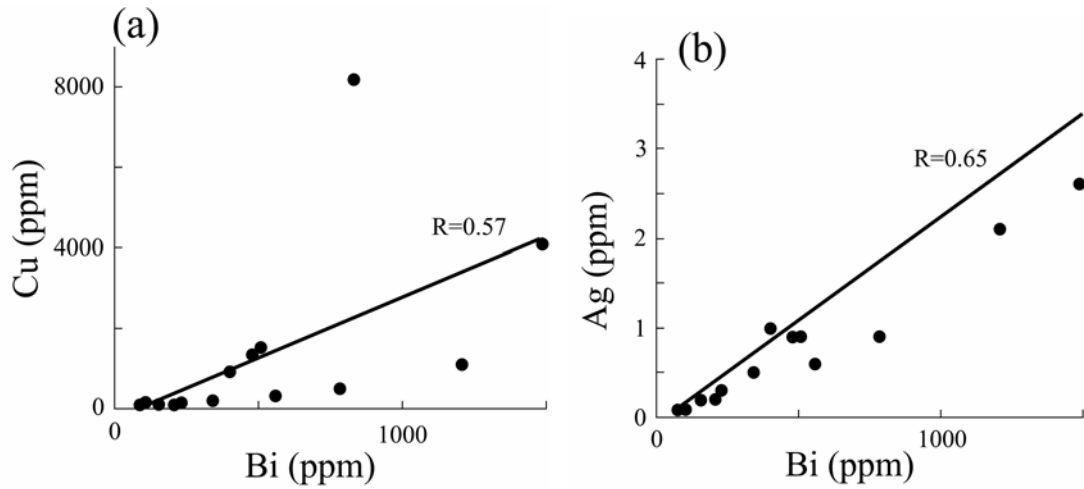


Figure 17. Additional plots of trace metal contents of high-grade quartz-scheelite veins from the Open Pit orebody at Cantung. (a) Cu (ppm) versus Bi (ppm). (b) Ag (ppm) versus Bi (ppm).

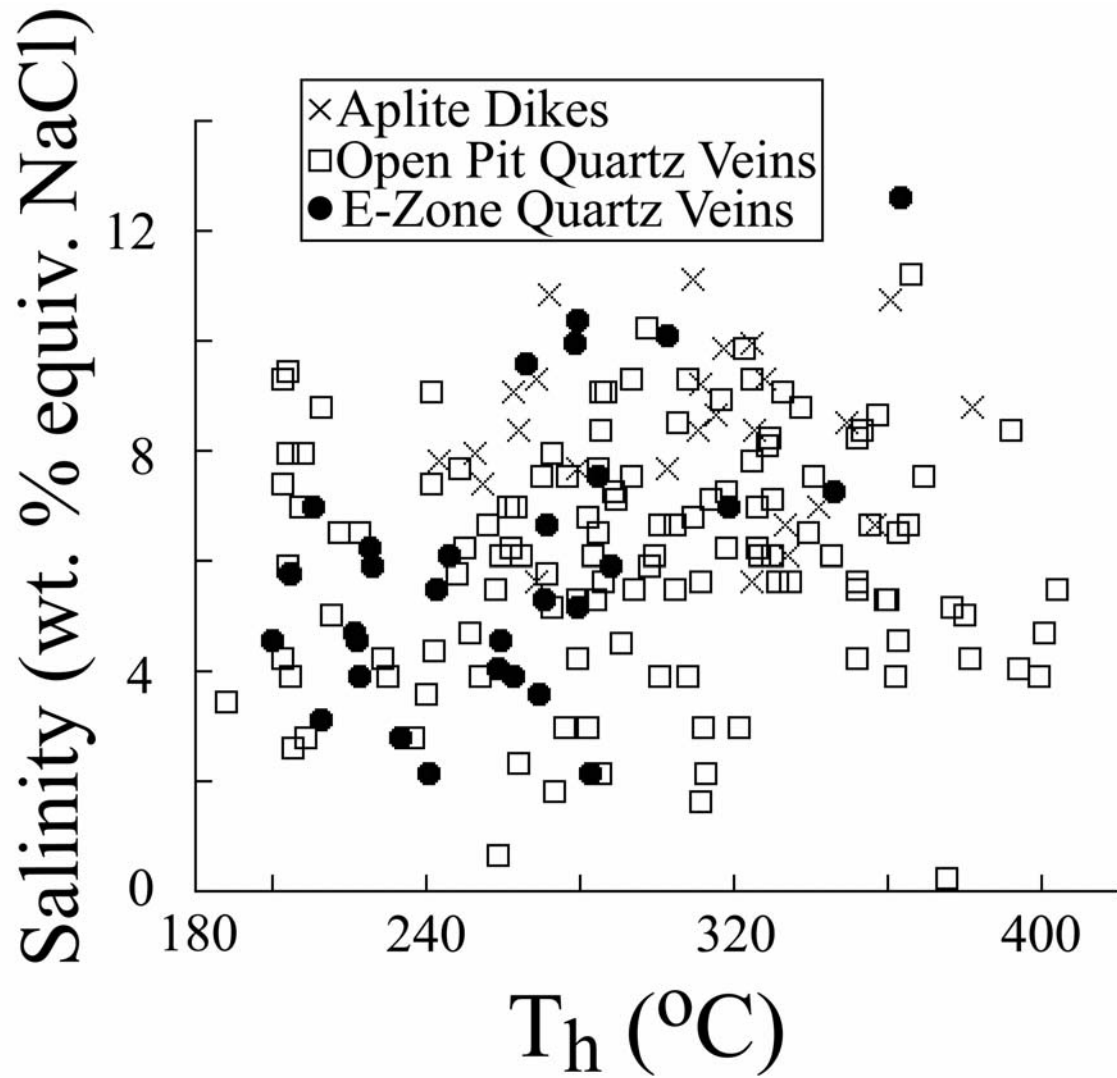


Figure 18. Salinity versus  $T_h$  values for aqueous brine inclusions. No systematic relationship exists between salinity and  $T_h$  values for the aqueous brine inclusions at Cantung.

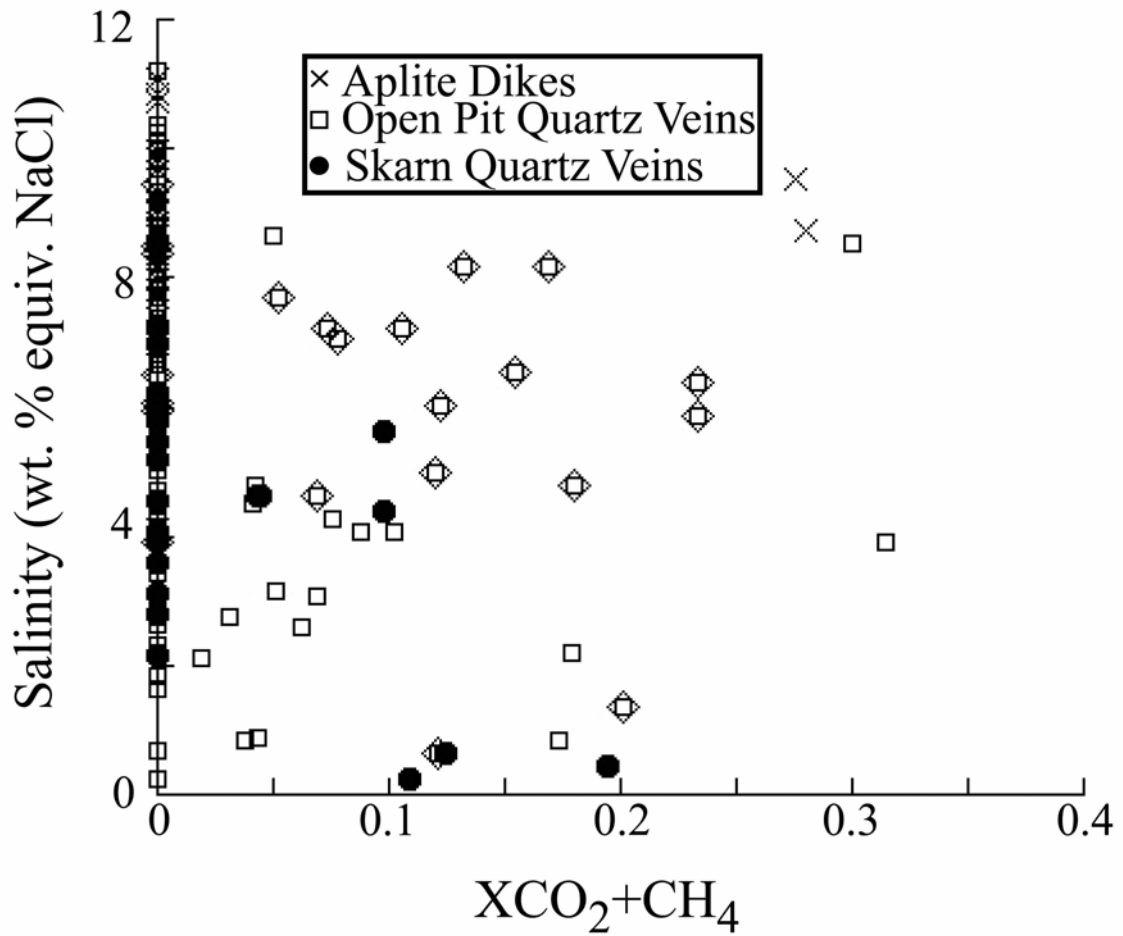


Figure 19. Salinity versus X<sub>CO<sub>2</sub>+CH<sub>4</sub></sub> values for H<sub>2</sub>O-CO<sub>2</sub>-NaCl±CH<sub>4</sub> and aqueous brine inclusions at Cantung. No systematic relationship exists between salinity and carbonic phase contents of the inclusions.



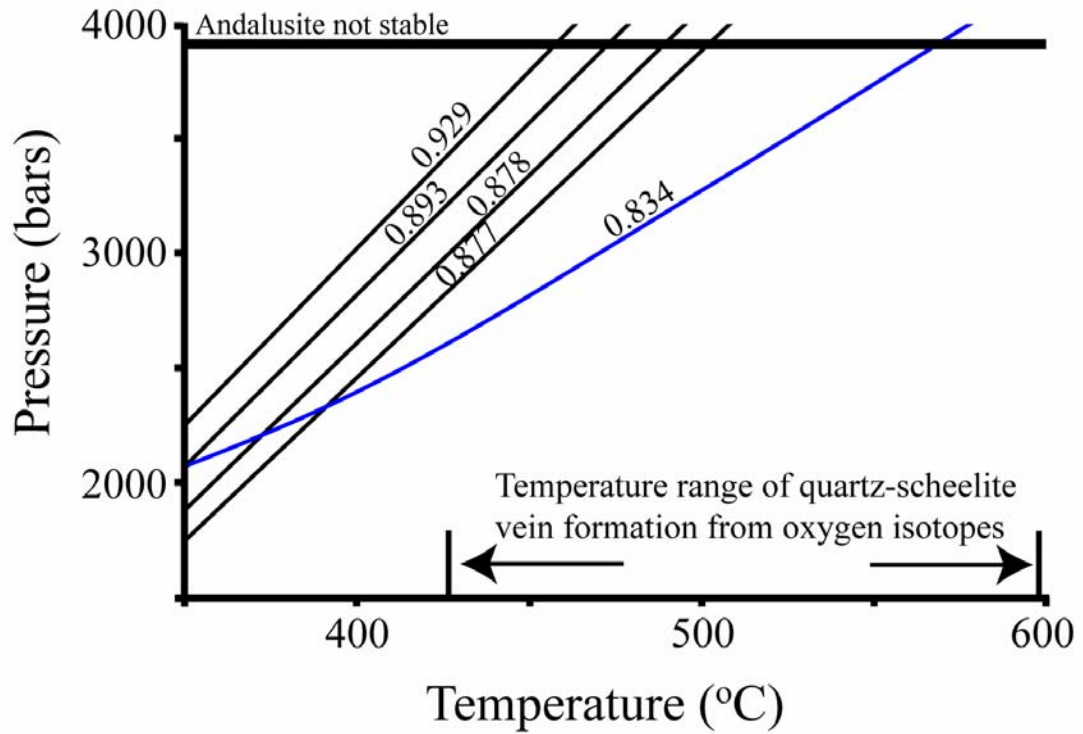


Figure 20. Calculated isochores from secondary aqueous brine fluid inclusions (black lines). One isochore from the primary  $\text{H}_2\text{O}-\text{CO}_2-\text{NaCl}\pm\text{CH}_4$  fluid inclusions also plotted (blue line). The densities of both inclusion assemblages are similar and their isochores do not cross within the pressure and temperature range for high-grade quartz-scheelite vein formation.

## APPENDIX VII

### Reconnaissance Fluid Inclusion Studies of Other Deposits and Showings in the Cantung Area

To evaluate the possibility that other mineral showings may have a magmatic origin, reconnaissance fluid inclusion studies were initiated. Samples were collected for fluid inclusion analysis from various mineral showings proximal to Cantung within the Tombstone-Tungsten plutonic suite (Rifle Range Creek, Lened, Zantung Creek, and HY). *Rifle Range Creek:* The Rifle Range Creek tungsten showing is approximately 15 km east-southeast of the Cantung mine in the Northwest Territories. Tungsten anomalies were measured in float samples at the toe of a glacier.

Two glacial debris samples with mineralization were collected from the toe of the glacier for fluid inclusion analysis. One mineralized sample consists of greisen alteration containing quartz, muscovite, tourmaline, and scheelite crosscut by quartz-scheelite veins. The second sample, a quartz-scheelite vein, contains massive and clear quartz.

In quartz, primary (three-phase)  $\text{H}_2\text{O}-\text{CO}_2-\text{NaCl}\pm\text{CH}_4$  and secondary (two-phase) aqueous brine inclusions were observed.  $\text{H}_2\text{O}-\text{CO}_2-\text{NaCl}\pm\text{CH}_4$  inclusions have  $T_{\text{m CO}_2}$  values of  $-59.4^\circ$  to  $-57.1^\circ\text{C}$ , salinity values of 0.4 to 5.5 wt. % equiv. NaCl, and  $T_{\text{h}}$  values of  $235^\circ$  to  $316^\circ\text{C}$ .

The primary,  $\text{H}_2\text{O}-\text{CO}_2-\text{NaCl}\pm\text{CH}_4$  fluid from Rifle Range Creek samples is similar to the primary, skarn-related end-member fluid observed in high-grade quartz-scheelite veins from the Open Pit orebody at Cantung. It is likely that the  $\text{H}_2\text{O}-\text{CO}_2-\text{NaCl}\pm\text{CH}_4$  fluid in quartz-scheelite veins from Rifle Range Creek has a similar magmatic origin.

The mineralized samples appear to have affinities to a greisen vein-system with a magmatic origin. The fact that mineralized samples have greisen characteristics, and not a skarn, is a function of the chemical composition of the host rocks that ore fluids encountered. If magmatic ore fluids at Rifle Range Creek had encountered a limestone, a skarn might have been deposited.

*Lened:* The Lened showing is approximately 70 km north-northwest of the Cantung mine. At Lened, nodular  $W \pm Cu$  skarn is developed in impure carbonate beds of Cambrian to Cretaceous metasedimentary rocks that were intruded by a Cretaceous granite (Dick, 1979; Marshall et al., 2004).

Two types of veins are present: quartz  $\pm$  carbonate  $\pm$  green beryl (emerald?) veins and skarn-related quartz veins. The relationship of quartz  $\pm$  carbonate  $\pm$  beryl veins to the skarn alteration is not well known. The quartz veins that I sampled are contained within the skarn alteration and have a direct relationship to skarn formation. One idocrase skarn sample, one garnet-pyroxene skarn sample, and one quartz vein sample were collected for fluid inclusion analysis.

Primary (three-phase)  $H_2O-CO_2-NaCl \pm CH_4$  inclusions were observed in one skarn sample, but all three samples examined contained secondary (two-phase) aqueous brine inclusions.  $H_2O-CO_2-NaCl \pm CH_4$  inclusions have  $T_{mCO_2}$  values of  $-91.2^\circ$  to  $-61.4^\circ C$  and  $T_h$  values of  $309^\circ$  to  $337^\circ C$ .

These values are similar to the aplite-related fluid end-member identified in high-grade quartz-scheelite veins from the Open Pit orebody at Cantung.

*Zantung Creek:* The Zantung (Zenchuck?) Creek showing is approximately 20 km north-northeast of the Cantung mine. It is a Au-Ag-base metal quartz vein developed in quartzite. One open-space filling quartz vein was collected for fluid inclusion analysis.

Primary  $\text{H}_2\text{O}-\text{CO}_2-\text{NaCl}\pm\text{CH}_4$  inclusions have  $T_{m\text{CO}_2}$  values of  $-58.8^\circ$  to  $-56.6^\circ\text{C}$ , salinity values of 2.2 to 5.9 wt. % equiv. NaCl, and  $T_h$  values of  $227^\circ$  to  $315^\circ\text{C}$ .

The primary,  $\text{H}_2\text{O}-\text{CO}_2-\text{NaCl}\pm\text{CH}_4$  fluid from Zantung Creek samples is similar to the primary, skarn-related end-member fluid observed in high-grade quartz-scheelite veins from the Open Pit orebody at Cantung, which had a magmatic origin.

*HY Gold Prospect:* The HY gold prospect is approximately 20 km east of the Cantung mine. Steeply dipping north-northwest trending quartz-arsenopyrite and stockwork quartz veins host gold mineralization at the HY prospect. These gold-bearing quartz veins crosscut a Neoproterozoic to Cambrian quartzite (Yusezyu Formation). Quartz veins contain massive, white to gray-blue or ribbon-banded quartz (Hart and Lewis, 2006).

I collected adjacent quartz veins for fluid inclusion analysis. One vein contains massive milky quartz, and the other has ribbon banded quartz with elongated grains of scheelite (Fig. 21).

Both samples contained rare, primary  $\text{H}_2\text{O}-\text{CO}_2-\text{NaCl}\pm\text{CH}_4$  and abundant secondary (two-phase) aqueous brine inclusions.  $\text{H}_2\text{O}-\text{CO}_2-\text{NaCl}\pm\text{CH}_4$  inclusions have  $T_{m\text{CO}_2}$  values of  $-65.5^\circ$  to  $-59.9^\circ\text{C}$  and  $T_h$  values of  $269^\circ$  to  $292^\circ\text{C}$ . These values are similar to the skarn-related end-member fluid found in high-grade quartz-scheelite veins from the Open Pit orebody at Cantung, which had a magmatic origin.

The presence of scheelite and primary  $\text{H}_2\text{O}-\text{CO}_2-\text{NaCl}\pm\text{CH}_4$  inclusions suggests that there may be an intrusion-related component to the gold-bearing quartz veins from

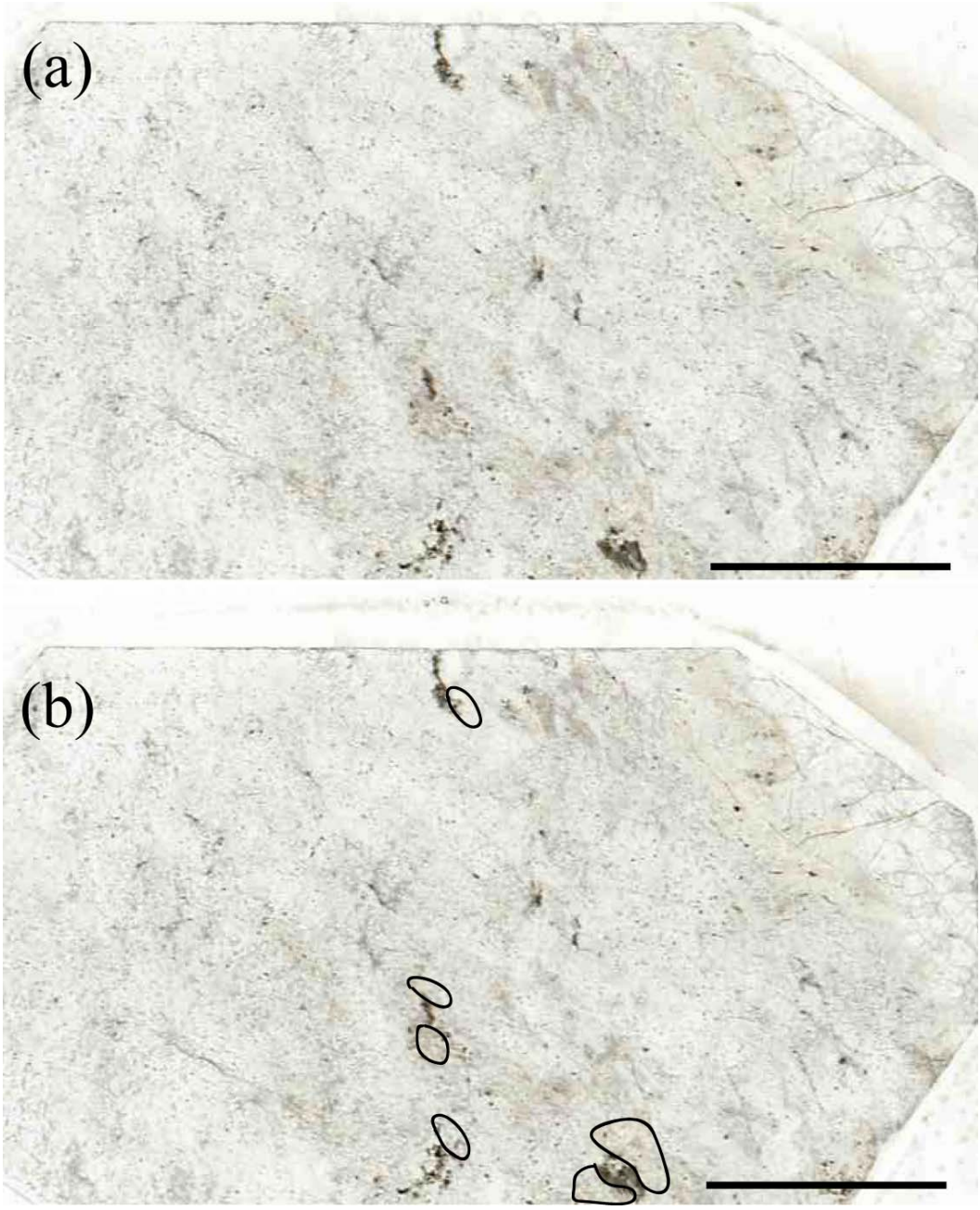


Figure 21. (a) Polished thin section of ribbon-banded quartz vein, KS-05-HY1A, from the HY gold prospect. (b) Same polished thin section with circles around the elongated grains of scheelite. Scale bar is 1 cm.

the HY prospect. At a minimum, there is evidence of W-rich fluids present at the time of deposition of the ribbon banded quartz.

The HY gold prospect was interpreted recently by Hart and Lewis (2006) to be an orogenic gold deposit because of the lack of evidence of an intrusion-related model. The ribbon-banded quartz veins were interpreted to represent numerous fracturing events, distinctive of orogenic gold vein deposits (Sibson et al., 1988).

Although I am unable to speculate on the origin of gold at the HY prospect, a magmatic influence (i.e. scheelite and  $\text{H}_2\text{O}-\text{CO}_2-\text{NaCl}\pm\text{CH}_4$  inclusions) could have formed two different ways. First, the entire vein system could be intrusion-related. The gold and tungsten could both have a magmatic source. Alternatively, the tungsten could have been introduced into the vein system during a later magmatic event. This later event could have overprinted an earlier orogenic system by reactivating faults and other conduits for ore-fluid flow (Bierlein and McKnight, 2005). No matter which scenario occurred, there is a definite magmatic signature associated with gold-bearing quartz vein deposits.

## **Appendix VIII**

### **The Use of Scheelite Fluorescence in the Field**

The optical properties of scheelite are very similar to quartz, making pale colored scheelite difficult to observe in the field. Scheelite fluoresces a light blue color under short wave ultraviolet light, distinguishing it from quartz and other minerals in the Cantung area. Samples collected were routinely examined under ultraviolet light to determine their scheelite content (Fig. 22).

Fluorescence is an interesting mineral property caused by the excitation of electrons under ultraviolet light (Klein, 2002). The invisible short radiation given off by the ultraviolet light excites electrons, making it possible for electrons to ascend to higher energy levels. The electrons, though, may fall back to lower energy levels, and emit a light photon of lower energy (longer wavelength). If the wavelength of the light photon is in the visible light spectrum, it can be seen as fluorescence.

The fluorescent property of scheelite was used for two purposes. First, underground exposures were observed routinely under ultraviolet light and the amount of fluorescence was used to estimate tungsten ore grades. Secondly, the presence and concentration of scheelite can be confirmed using fluorescence.

We routinely used ultraviolet fluorescence to check all samples (in the field and in the lab) for the presence of scheelite. The recognition of scheelite in the HY deposit has important implications for a magmatic versus metamorphic origin of its veins (Fig. 21). Had we not used an ultraviolet lamp in a dark room, we would likely have overlooked the presence of nearly colorless scheelite present in the veins.



Figure 22. Improvised darkroom (underneath a coat) to examine the fluorescent property of scheelite. This was performed routinely in the field to determine the presence and concentration of scheelite in samples.



## References

- Bierlein, F.P., and McKnight, S., 2005, Possible intrusion-related gold systems in the western Lachlan orogen, southeast Australia: *ECONOMIC GEOLOGY*, v. 100, p. 385-398.
- Dick, L.A., 1979, Tungsten and base metal skarns in the northern Cordillera: *in* Current Research, Part A: Geological Survey of Canada, Paper 79-1A, p. 259-266.
- Hart, C.J.R., and Lewis, L.L., 2006, Gold mineralization in the upper Hyland River area: A non-magmatic origin: *in* Emond, D.S., Bradshaw, G.D., Lewis, L.L., and Weston, L.H., eds., Yukon Exploration and Geology 2005: Yukon Geological Survey, Whitehorse, p. 109-125.
- Klein, C., 2002, Mineral Science: John Wiley and Sons, Inc., New York, 639 pp.
- Marshall, D.D., Groat, L.A., Falck, H., Giuliani, G., and Neufeld, H., 2004, The Lened emerald prospect, Northwest Territories, Canada: Insights from fluid inclusions and stable isotopes, with implications for Northern Cordilleran emerald: *Canadian Mineralogist*, v. 42, p. 1523-1539.
- Sibson, R.H., Robert, F., and Poulsen, K.H., 1988, High-angle reverse faults, fluid-pressure cycling, and mesothermal gold-quartz deposits: *Geology*, v. 16, p. 551-555.